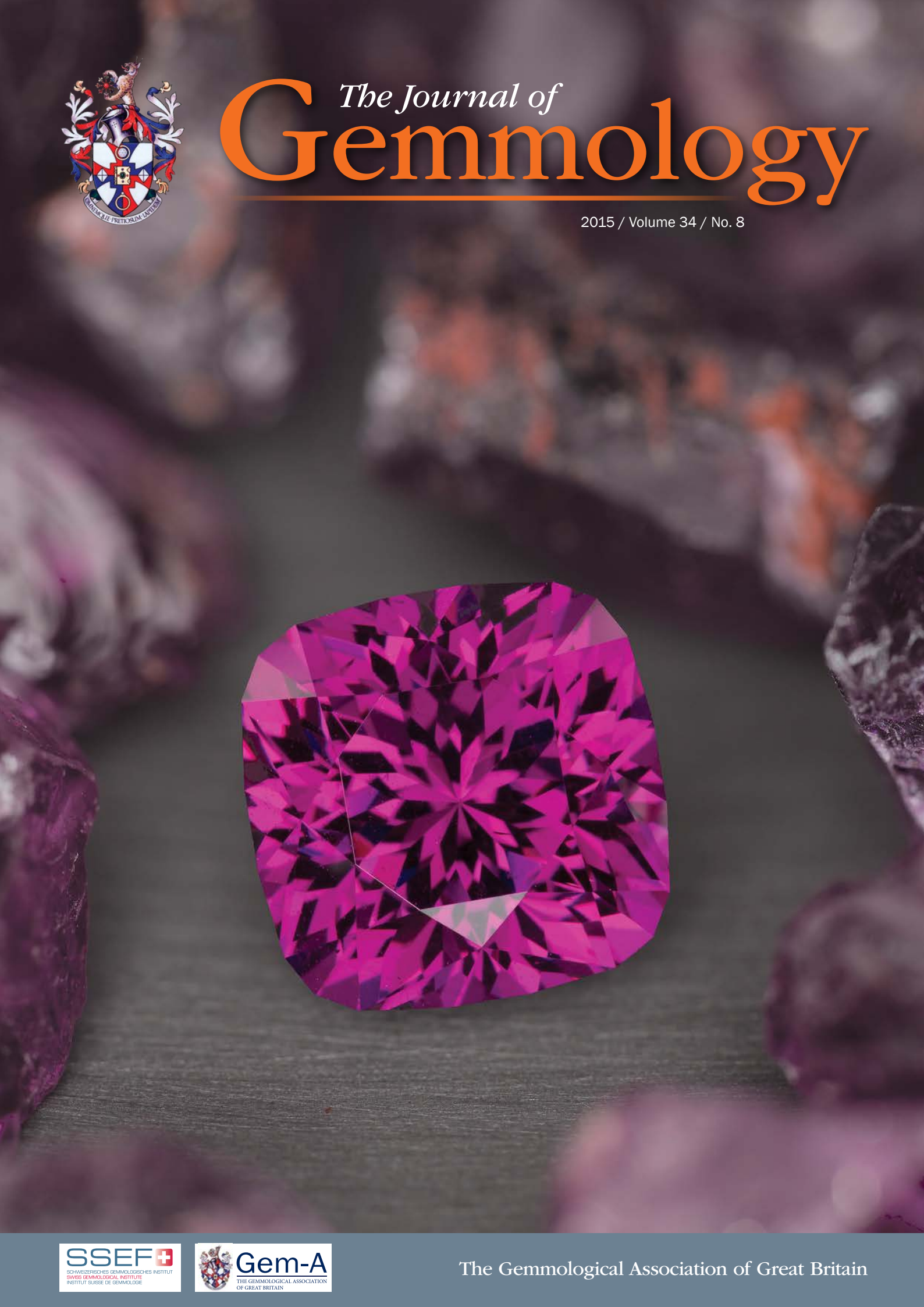

The Journal of Gemmology

2015 / Volume 34 / No. 8

SSEF SCHWEIZERISCHES GEMMOLOGISCHES INSTITUT SWISS GEMMOLOGICAL INSTITUTE INSTITUT SUISSE DE GEMMOLOGIE

Gem-A THE GEMMOLOGICAL ASSOCIATION OF GREAT BRITAIN

The Gemmological Association of Great Britain

Gem-A

THE GEMMOLOGICAL ASSOCIATION
OF GREAT BRITAIN

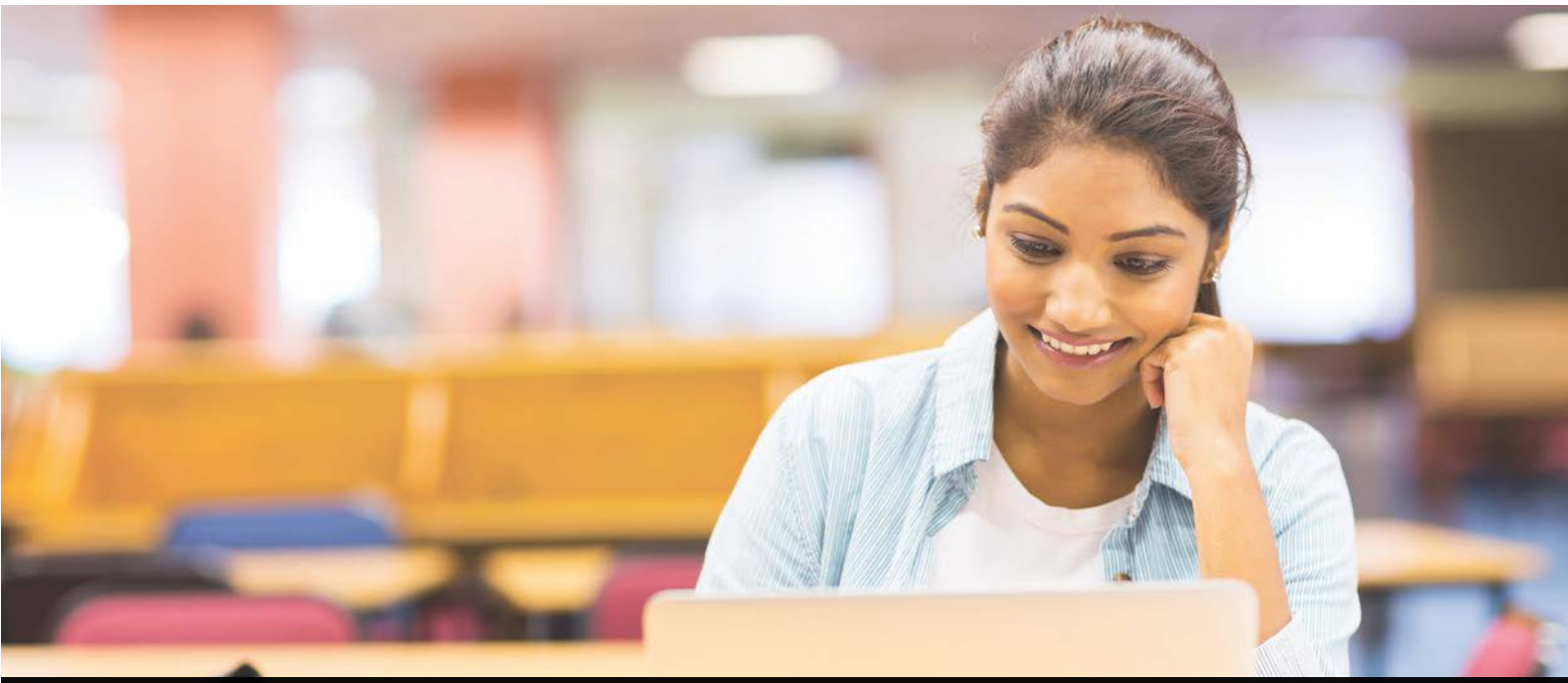

Flexible study to suit you

Our Online Distance Learning (ODL) programmes offer you the chance to study our world-famous Gemmology and Diamond Diplomas from home, work or anywhere else you choose. Graduates of our Gemmology and Diamond Diplomas may apply for Membership, entitling them to use the prestigious FGA and DGA status respectively — recognized symbols of excellence in the trade.

To sign up contact **education@gem-a.com**.

Gemmology Foundation	**Gemmology Diploma**	**Diamond Diploma**
(nine month course)	*(nine month course)*	*(nine month course)*
Starts: 7 March 2016	Starts: 14 March 2016	Starts: 14 March 2016
Price: £2,160	Price: £3,150	Price: £2,625

Understanding Gems

Join us.

The Gemmological Association of Great Britain, 21 Ely Place, London, EC1N 6TD, UK. T: +44 (0)20 7404 3334 F: +44 (0)20 7404 8843. Registered charity no. 1109555. A company limited by guarantee and registered in England No. 1945780. Registered Office: 3rd Floor, 1-4 Argyll Street, London W1F 7LD.

The Journal of Gemmology
2015 / Volume 34 / No. 8

Cover Photo: This 5.86 ct intense reddish purple garnet was cut by Jeff White from rough material that was mined in Mozambique; see Gem Note on pp. 656–658. Photo by Jeff White.

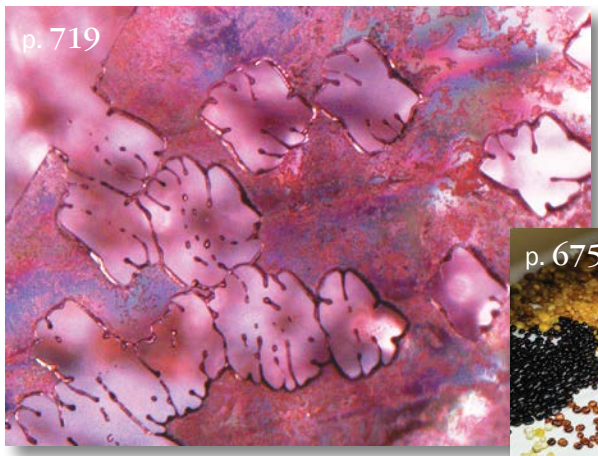
p. 719

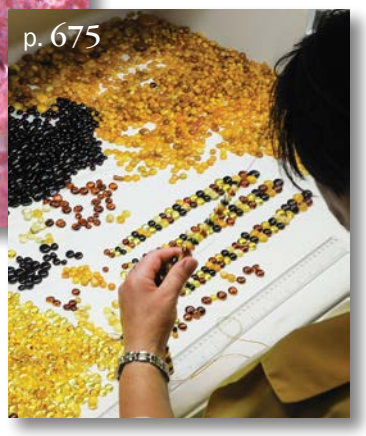
p. 675

The Journal is published by Gem-A in collaboration with SSEF and with the support of AGL.

Gem-A THE GEMMOLOGICAL ASSOCIATION OF GREAT BRITAIN
SSEF SCHWEIZERISCHES GEMMOLOGISCHES INSTITUT SWISS GEMMOLOGICAL INSTITUTE INSTITUT SUISSE DE GEMMOLOGIE
AGL AMERICAN GEMOLOGICAL LABORATORIES

ISSN: 1355-4565, http://dx.doi.org/10.15506/JoG.2015.34.8

The Journal of Gemmology

Content Submission

The Editor-in-Chief is glad to consider original articles, news items, conference/excursion reports, announcements and calendar entries on subjects of gemmological interest for publication in *The Journal of Gemmology*. A guide to the various sections and the preparation of manuscripts is given at www.gem-a.com/publications/journal-of-gemmology.aspx, or contact the Production Editor.

Subscriptions

Gem-A members receive *The Journal* as part of their membership package, full details of which are given at www.gem-a.com/membership.aspx. Laboratories, libraries, museums and similar institutions may become Direct Subscribers to *The Journal* (see www.gem-a.com/publications/subscribe.aspx).

Advertising

Enquiries about advertising in *The Journal* should be directed to the Marketing Consultant. For more information, see www.gem-a.com/publications/journal-of-gemmology/advertising-in-the-journal.aspx.

Database Coverage

The Journal of Gemmology is covered by the following abstracting and indexing services: Australian Research Council academic journal list, British Library Document Supply Service, Chemical Abstracts (CA Plus), Copyright Clearance Center's RightFind application, CrossRef, EBSCO (Academic Search International, Discovery Service and TOC Premier), Gale/Cengage Learning Academic OneFile, GeoRef, Mineralogical Abstracts, ProQuest and the Thomson Reuters' Emerging Sources Citation Index (in the Web of Science).

Copyright and Reprint Permission

Full details of copyright and reprint permission are given on *The Journal*'s website.

The Journal of Gemmology is published quarterly by Gem-A, The Gemmological Association of Great Britain. Any opinions expressed in *The Journal* are understood to be the views of the contributors and not necessarily of the publisher.

Printed by DG3 (Europe) Ltd.

ISSN: 1355-4565

Gem-A
THE GEMMOLOGICAL ASSOCIATION OF GREAT BRITAIN

21 Ely Place
London EC1N 6TD
UK

t: +44 (0)20 7404 3334
f: +44 (0)20 7404 8843
e: information@gem-a.com
w: www.gem-a.com

Registered Charity No. 1109555
Registered office: Palladium House, 1–4 Argyll Street, London W1F 7LD

Good News for *The Journal*!

For more than 60 years, *The Journal of Gemmology* has been one of the top scientific journals in gemmology. Receiving *The Journal* is an important Gem-A membership benefit, and it provides a useful means of continuing education for all gemmologists, in keeping with Gem-A's mission and values. The scientific standing of scholarly publications such as *The Journal* rests heavily on their selection for coverage by the international research platform known as the Web of Science. Formerly known as the ISI (Institute for Scientific Information) Web of Knowledge, this online subscription-based service is maintained by Thomson Reuters and provides comprehensive access to multiple databases covering the sciences, social sciences, arts and humanities.

I am pleased to report that in November 2015, *The Journal* joined the Web of Science (WoS) when it was accepted into Thomson Reuters' new Emerging Sources Citation Index (ESCI) database. Journals in ESCI are indexed like those in other databases within WoS, but they do not receive an impact factor (a measure of how often recent articles are cited in WoS journals). As *The Journal* continues to be evaluated for Thomson Reuters' impact-factor science database (Science Citation Index Expanded), it should benefit greatly from the exposure provided by ESCI. Additional exposure is provided by *The Journal*'s inclusion in databases that are maintained by other indexing services and journal aggregators (e.g. Scopus, EBSCO, ProQuest and GeoRef) that are commonly subscribed to by university libraries and research institutions worldwide.

The Journal's inclusion in WoS is good for our authors, for our readers and for gemmology in general. *The Journal* will now be in a better position to attract articles from researchers at top universities who are required to publish in WoS journals, and our readers will benefit from this cutting-edge research. In addition, *The Journal*'s coverage by WoS will certainly help raise awareness of gemmology in the global scientific community. Being part of WoS will not change the direction or scope of *The Journal*, as gemmology will continue to be the core foundation of its content.

On another subject, thanks to the efforts by consultant Carol Stockton, I am pleased to announce the completion of *The Journal*'s Cumulative Index that covers all issues from 1947 to 2013 (Volumes 1–33). This index is available as a free downloadable PDF file on *The Journal*'s website, and early in 2016 it will be updated to include all issues through 2015.

Coming soon (also scheduled for early 2016), Gem-A will unveil a new website, and this will give Gem-A members free access to the entire archive of *The Journal* as searchable PDF files. In addition, non-members will be able to purchase PDFs of individual articles/sections, as well as complete issues. The availability of the entire *Journal* archive, combined with the Cumulative Index, will provide a comprehensive gemmological reference tool.

Brendan Laurs
Editor-in-Chief

What's New

INSTRUMENTS AND TECHNIQUES

Gemlogis Taupe Diamond Segregator

Gem laboratories are more commonly receiving mixed parcels of natural and synthetic diamonds for identification. At this author's lab, colourless to near-colourless diamonds weighing >0.50 ct are subjected to advanced testing, while smaller stones (i.e. 0.02–0.49 ct) are segregated using a Gemlogis Taupe Diamond Segregator (www.gemlogisusa.com/gemlogis-taupe-diamond-lab-created-tester.htm), which is manufactured by Jubilee Diamond Instrument Ltd., Hong Kong, and was released in May 2014. The instrument is compact and portable, and has a short-wave UV beam that is focused on the sample. Sensors detect the transmission of the UV beam through the sample to identify type II diamonds, thereby flagging potentially CVD- or HPHT-grown synthetics, or natural diamonds that may have been HPHT treated.

The sample is placed table-down on the instrument and the lid is shut for the analysis. Within seconds of pressing the 'test' button, a green light will indicate the diamond is type I (and therefore probably natural), while a yellow-orange light identifies the need for further testing. An advantage of the instrument is that small diamonds down to 0.02 ct can be segregated. For best results, the instrument should be regularly calibrated using known melee-sized CVD- and HPHT-grown synthetic diamonds.

There is an increasing need for such instruments that are affordable and can segregate small potentially synthetic diamonds from natural ones. Although the instrument does not specifically identify synthetic or HPHT-treated diamonds, it is helpful for separating type II gems for further examination.

Jayshree Panjikar (jayshreepanjikar@gmail.com)
Pangem Testing Laboratory (Pangemtech)
Pune, India

M-Screen Automatic Melee Screening Device

In September 2015, HRD Antwerp released the M-Screen device, which rapidly screens melee parcels (0.01–0.20 ct) to separate natural from potentially synthetic/treated diamonds and simulants. The desktop instrument automatically feeds, screens and sorts colourless and near-colourless (D–J) round brilliant diamonds at a rate of 2–5 stones per second (7,200–18,000 per hour). Also, starting in November 2015, HRD Antwerp began offering a rapid (24-hour turnaround time) melee screening service using the M-Screen. Visit www.hrdantwerp.com/en/product/m-screen.

Presidium Synthetic Diamond Screener

In September 2015, Presidium debuted a new device for screening colourless and near-colourless (D–J) diamonds and flagging type IIa stones. The instrument measures 13.0 × 10.0 × 6.5 cm, weighs 210 g and can be operated using AAA batteries or via a USB connection. Samples ranging from 0.1 to 10 ct that are loose or mounted (with an open-back setting) can be tested, and the measurement takes approximately 6 seconds. Visit http://presidium.com.sg/psdproduct/synthetic-diamond-screener-sds.

Spekwin32 Spectroscopy Software

In October 2015, Dr Friedrich Menges released an updated version of the spectroscopy software Spekwin32. New capabilities of interest to gemmologists include 'Spectroscope View'—which renders a spectrum collected using a spectrometer

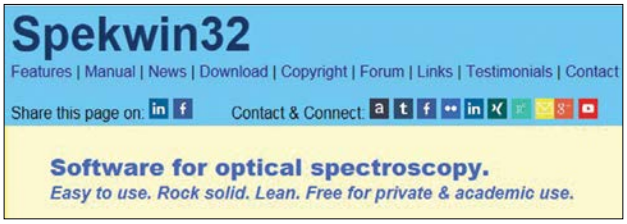

into the visual appearance that would be seen in a hand-held (diffraction grating) spectroscope—and the ability to read file formats from nine additional spectroscopic sources. For more information and to download this free software, visit www.effemm2.de/spekwin/index_en.html.

NEWS AND PUBLICATIONS

CIBJO Coral Book

The newest addition to the line-up of CIBJO Blue Books is *The Coral Book*, released in July 2015. The publication covers the terminology (including definitions) and classification of coral, as well as its treatments and imitations. Various annexes provide a classification flowchart and information on care requirements, normative trade codes, coral species (including those covered in the CITES Appendices), coral sustainability and regulations for harvesting, and a reference list. Download the free publication at www.cibjo.org/download/15-10-01%20official%20Coral%20Book.pdf.

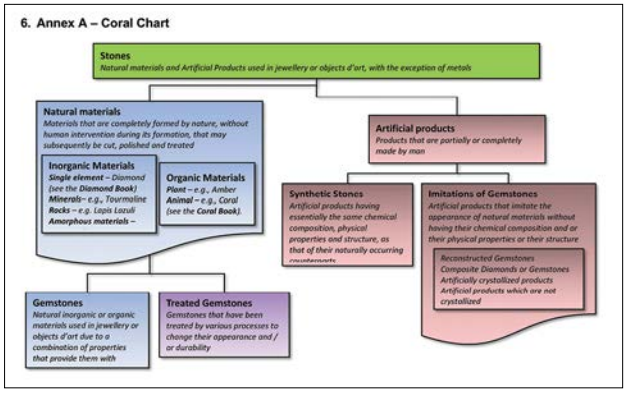

Diamond Industry 2015

The 5th annual report on the global diamond industry prepared by the Antwerp World Diamond Centre and Bain & Company was released in December 2015, titled 'The Global Diamond Industry 2015: Growth Perspectives amid Short-term Challenges'. The paper focuses on long- and short-term drivers of diamond jewellery demand and prices, and concludes by providing an update on the diamond industry outlook through 2030. Download the free report at www.bain.com/Images/FINAL%20bain_diamond_report_2015_01122015.pdf.

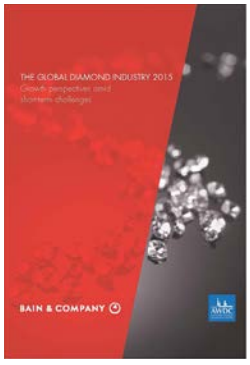

Flux-grown Synthetic Spinel

In September 2015, Gemresearch Swisslab reported on a new line of synthetic spinel manufactured in Russia by Tairus Co. Ltd. The product is available in pinkish red, lavender, colour-change (violet and purplish pink) and violetish blue varieties. Download the report at http://gemresearch.ch/wp/wp-content/uploads/2015/09/2015-09-Spinel_New_Synthetic.pdf.

ICGL Newsletter

The International Consortium of Gem-Testing Laboratories has released the Fall 2015 issue of their newsletter (No. 3/2015), available at http://icglabs.org. It features articles on small HPHT-grown octahedral colourless and blue synthetic diamonds produced using an even-temperature method, heat-treated amber beads, amber in the collection of the Pangem Testing Laboratory (Pune, India) and a proposal to include

certain spectroscopic data on diamond reports to aid in the detection of fraudulent replicas of loose or mounted stones.

ISO Standards for Diamonds

In July 2015, the International Organization for Standardization released a new standard (ISO 18323:2015) for diamond nomenclature: 'Jewellery – Consumer Confidence in the Diamond Industry'. The document is designed to be understood by the consumer, and covers nomenclature and disclosure of diamonds—natural, treated, synthetic, composite and imitation—as well as a glossary. The standard is available for purchase at www.iso.org/iso/catalogue_detail.htm?csnumber=62163.

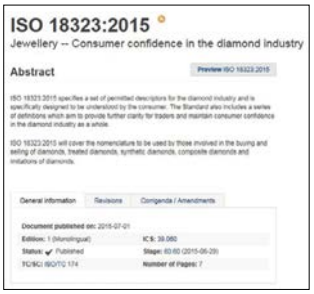

The Journal of Gemmology Cumulative Index

In December 2014, Gem-A released *The Journal*'s Cumulative Index, covering all issues from 1947 to 2013 (Volumes 1–33). In early 2016, it will be updated to include Volume 34 (2014–2015). The contents are listed by subject, and the PDF file is searchable, so entries by specific authors also can be located. The Cumulative Index is available in electronic format only as a free download from *The Journal*'s website at www.gem-a.com/publications/journal-of-gemmology.aspx.

Rare Book Scanning by GIA Library

The Gemological Institute of America's Richard T. Liddicoat Gemological Library and Information Center is in the process of digitizing its collection of rare and historically significant books, and many titles are available for free download at https://archive.org/details/@gia_library. As of 9 December 2015, 101 books had been uploaded, with more being added weekly. Brief descriptions of each item can be seen in list view; most were taken from *Gemology: An Annotated Bibliography* compiled by the late John Sinkankas in 1993.

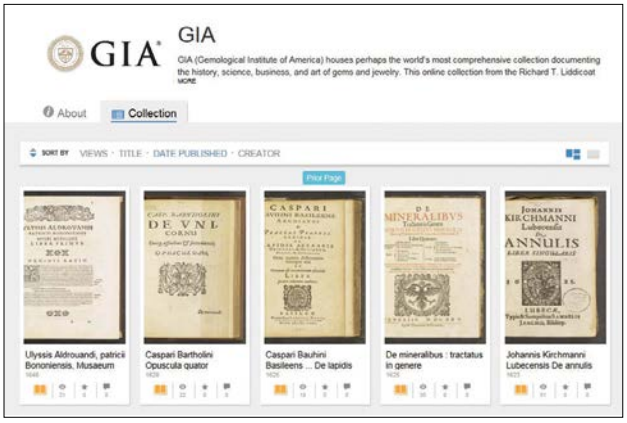

Responsible Business Practices and Jewellery Consumption

A November 2015 presentation delivered at the ESRC Festival of Social Science by Prof. Marylyn Carrigan of Coventry University on preferences by UK jewellery consumers who shop in the Birmingham Jewellery Quarter is available for free download from the National Association of Jewellers' website at http://tinyurl.com/zz6j3qb.

RJC 2015 Progress Report

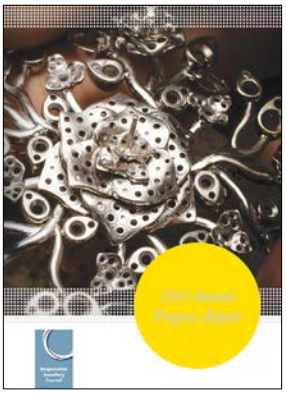

The Responsible Jewellery Council has issued its 2015 annual progress report, which describes the organization's accomplishments in 2014 in areas such as membership growth, certification benchmarks and standards development. Download the free report at www.responsiblejewellery.com/files/RJC-Annual-Report-2015-Web-version.pdf.

What's New provides announcements of new instruments/technology, publications, online resources and more. Inclusion in What's New does not imply recommendation or endorsement by Gem-A. Entries are prepared by Brendan Laurs unless otherwise noted.

The Fire Within

"For in them you shall see the living fire of the ruby, the glorious purple of the amethyst, the sea-green of the emerald, all glittering together in an incredible mixture of light."

– Roman Elder Pliny, 1st Century AD

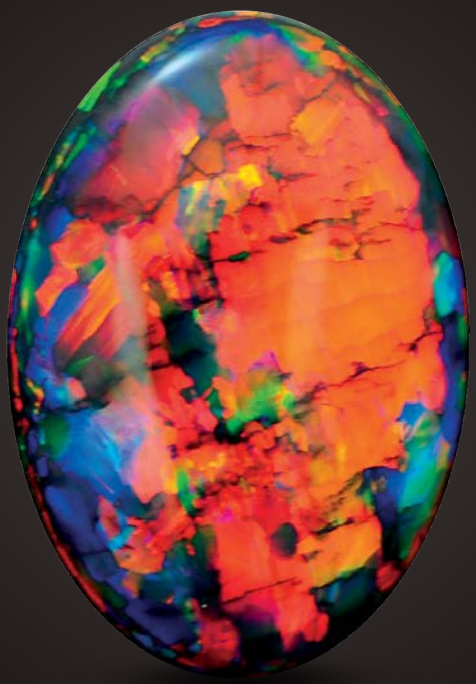

Black Opal 15.7 Carats

Suppliers of Australia's finest opals to the world's gem trade.

CODY OPAL

Level 1 - 119 Swanston Street Melbourne Australia

T. +61 3 9654 5533 E. INFO@CODYOPAL.COM

WWW.CODYOPAL.COM

INTERNATIONAL COLORED GEMSTONE ASSOCIATION MEMBER

JOG

The Kerez Effect in Green Tourmaline

Andrew Fellows

The *Kerez effect* refers to an optical behaviour that is very rarely shown by green tourmaline. Since it is so uncommon, it often goes unreported in gemmology textbooks.

Originally discovered by Dr C. J. Kerez (Read, 1982), this optical effect was apparently first described by Mitchell (1967) in two very unusual Brazilian tourmalines. He wrote: "To all outward appearances they are quite normal stones. Refractometer readings, however, reveal the inexplicable fact that the stones each give four distinct shadow edges…the twin ordinary ray readings remain stationary while the other two move as the stone is rotated." Such additional shadow edges, ranging from two to four pairs (four to eight lines in total), also have been referred to as *satellite readings* (Schiffmann, 1972, 1975). The multiple shadow edges can understandably create confusion for gemmologists.

According to everything that this author has been taught, this optical effect should not happen—and this prompted the author's search for such specimens. Eight years (and many tourmalines) later, an elusive multi-RI stone was found. It consisted of a 1.39 ct oval cut (Figure 1) that produced eight individual shadow edges in the refractometer (Figure 2). The two groups of four edges could easily be differentiated using a polarizing filter, giving the four sets of readings that are shown in Table I (which also gives the results from other visually similar green tourmalines that were studied for comparison). Each set of shadow edges corresponded to the ordinary and extraordinary rays, but interestingly they were not equally spaced, although the birefringence was constant for all four sets.

Figure 1: Of the green tourmalines shown here (0.53–2.74 ct), only one (no. 1) showed the Kerez effect in the refractometer. See Table I for RI data corresponding to each stone. Photo by Henry Mesa.

For stones showing the Kerez effect, the 'true' RI values were shown by Schiffmann (1975) to correspond to the lowest reading of each of the sets of shadow edges. He proved this after repolishing such a stone, which resulted in a single set of readings that were normal for tourmaline. Therefore, the correct RI range for the 1.39 ct stone examined by this author

Table I: RI readings of green tourmalines in this study.

Stone	Weight (ct)	Shape	RI readings	Birefringence
1	1.39	Oval	1.622–1.649 1.627–1.654 1.629–1.656 1.634–1.661	0.027 0.027 0.027 0.027
2	0.67	Emerald cut	1.620–1.640	0.020
3	2.74	Emerald cut	1.621–1.638	0.017
4	0.53	Emerald cut	1.618–1.640	0.022
5	0.53	Oval	1.621–1.640	0.019
6	0.54	Oval	1.622–1.641	0.019
7	2.54	Round	1.624–1.642	0.018

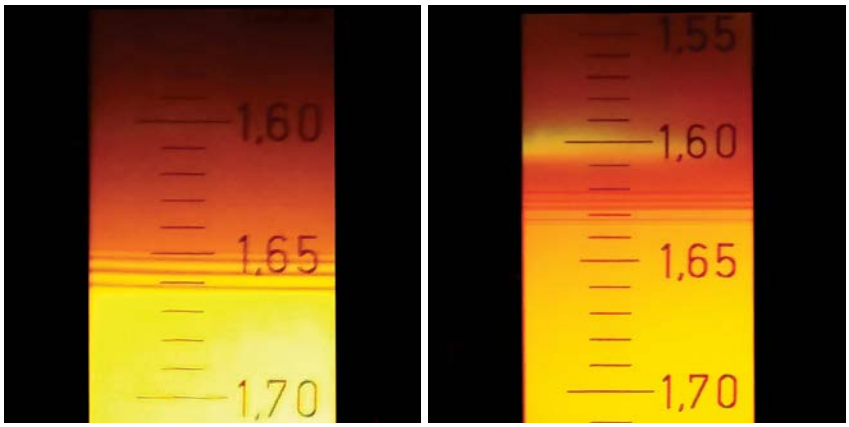

Figure 2: Refractometer readings of the 1.39 ct tourmaline displayed the Kerez effect in four sets of shadow lines corresponding to the ordinary (left) and extraordinary (right) rays. Photos by A. Fellows.

should be inferred as 1.622–1.649.

The Kerez effect is thought to result from the cutting and polishing process, when over-enthusiastic polishing causes a build-up of heat due to friction from the cutting wheel (Schiffmann, 1975). This creates thermal damage that penetrates slightly below the stone's surface.

To check whether the Kerez effect could purposely be created during the cutting process, this author enlisted the help of a fellow gemmologist and local lapidary. Two individual sections of a dark green tourmaline were subjected to heavy polishing, with sufficient speed and pressure used to build up heat within the stones. However, compared to a 'normally' polished section of the same stone, there were no differences seen in the RI readings, and no additional shadow edges were created by the aggressive polishing. It is therefore difficult to see how a lapidary could inadvertently create the Kerez effect, and perhaps there is more than just heat involved.

The exact cause of the Kerez effect, and why it appears restricted to green tourmaline, is still unknown. It is hoped that increasing the awareness of this interesting phenomenon will enable other gemmologists to recognize the effect in tourmalines that they may rarely encounter.

Acknowledgement: The author thanks Sam Lloyd FGA for help with polishing the tourmaline samples, and for independently checking the results.

References

Mitchell R.K., 1967. Refraction anomalies in tourmalines. *Journal of Gemmology*, **10**(6), 194, http://dx.doi.org/10.15506/jog.1967.10.6.194.

Read P.G., 1982. *Dictionary of Gemmology*. Butterworth Scientific, London, 115.

Schiffmann C.A., 1972. Tourmalines: Rare multiple indices on the refractometer. *Journal of Gemmology*, **13**(4), 125–132, http://dx.doi.org/10.15506/jog.1972.13.4.125.

Schiffmann C.A., 1975. Tourmalines: Multiple indices on the refractometer: A further note. *Journal of Gemmology*, **14**(7), 324–329, http://dx.doi.org/10.15506/jog.1975.14.7.324.

Andrew Fellows FGA DGA is the online distance learning tuition manager, and a gemmology and diamond tutor, at Gem-A in London. Email: andrew@gem-a.com

Gem Notes

COLOURED STONES

Apatite from Mozambique

In January 2014, gem dealer Dudley Blauwet (Dudley Blauwet Gems, Louisville, Colorado, USA) obtained a 600 g parcel of rough apatite that his African supplier indicated was from Nhamatanda, Mozambique. In July 2014, cutting of six pieces weighing 236.7 g yielded 55 gemstones with a total weight of 264.44 carats. The largest stones (up to 39 ct) contained parallel arrays of eye-visible platelet inclusions, and some also contained fibrous needles. To decrease the visibility of the platelets, the gems were cut so the inclusions were oriented perpendicular to the table facet. Blauwet loaned two apatites to the American Gemological Laboratories (AGL) for examination, and they were characterized by this author: a 3.88 ct triangle and a 10.61 ct cushion (Figure 1).

Figure 1: These cushion-cut and triangular gemstones (10.61 and 3.88 ct, respectively) consist of apatite from Mozambique. Photo by Kelly Kramer.

The yellowish green colour combined with an excellent polish made these stones quite attractive. Standard gemmological testing of both gems revealed RIs of 1.630–1.635 (birefringence 0.004–0.005) and a hydrostatic SG value of 3.17. These properties confirmed the samples were apatite (cf. O'Donoghue, 2006). They were inert to long-wave UV radiation and exhibited a weak yellow fluorescence to short-wave UV.

Microscopic examination revealed various internal features. Parallel star-like oriented cross-hatch inclusions formed one of the most interesting types (Figure 2a). The stones also contained several high-relief disc-like fissures (Figure 2b). Additionally present were parallel growth tubes with reflective platelets and particles (Figure 2c), as well as minute unidentified crystals with parallel needle-like tubes (Figure 2d).

Semi-quantitative chemical analysis using a Thermo Electron Corp. ARL Quant'X energy-dispersive X-ray fluorescence (EDXRF) spectrometer showed the expected major amounts of Ca and P, as well as minor Mg (~0.7 wt.%) and Mn (~0.2 wt.%), and traces of Fe (~0.07 wt.%).

Gem-quality apatite is known from several localities. It is possible that the inclusion assemblage shown by these Mozambique apatites is unique to their specific locality, but more research would be needed to confirm this.

Monruedee Chaipaksa
(mchaipaksa@aglgemlab.com)
American Gemological Laboratories
New York, New York, USA

Reference

O'Donoghue M., Ed., 2006. *Gems*, 6th edn. Butterworth-Heinemann, Oxford, 382–383.

Figure 2: The Mozambique apatites examined for this report contain an interesting assemblage of internal features, including (a) parallel star-like oriented cross-hatch inclusions, (b) high-relief disc-like fissures associated with stringer particles, (c) fine parallel growth tubes with reflective platelets and particles, and (d) tiny unidentified crystals with parallel needle-like tubes. Photomicrographs by M. Chaipaksa; magnified 70×.

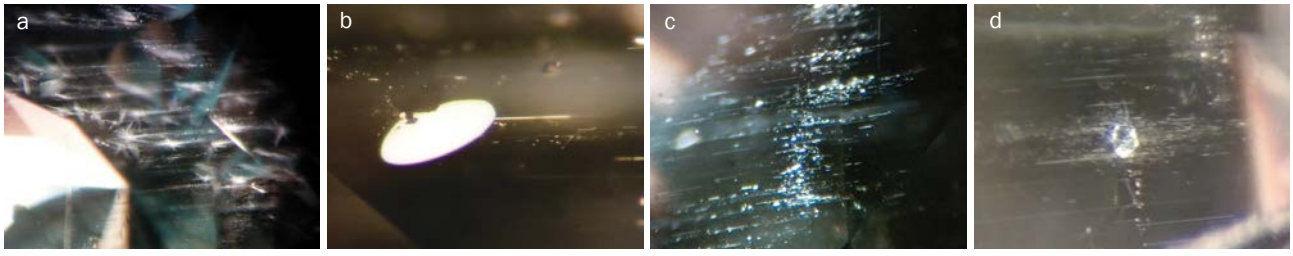

Chondrodite reportedly from Tanga, Tanzania

Chondrodite, $(Mg,Fe^{2+})_5(SiO_4)_2(F,OH)_2$, is an uncommon gem material that is known from various localities, including two places in Tanzania: Sumbawanga in the west-central part of the country (Fritz et al., 2007) and Mahenge in south-central Tanzania (Overton, 2011). A broad range of colour has been documented for Tanzanian chondrodite ('Uncommon minerals as gemstones…', 2007), although the most common colour appears to be 'golden' yellow. In September 2014, gem dealer Dudley Blauwet obtained a parcel of rough from his East African supplier that was represented as chondrodite from a different locality in Tanzania: the Tanga region, in the north-western part of the country. Cutting of 16 pieces of rough weighing 14.78 g yielded 45 gems ranging from 0.15 to 1.96 ct.

Blauwet loaned five of the faceted stones (0.52–1.96 ct; Figure 3) to AGL for examination, and the following gemmological properties were recorded: colour—brownish yellow to yellow, except for one sample that was orangey yellow; no obvious pleochroism; RI—1.592–1.623; birefringence—0.028–0.029; SG—3.12–3.20; fluorescence—inert to long-wave UV and weak-to-moderate yellow to short-wave UV radiation; and no features were visible with the desk-model spectroscope. All of these properties are consistent with data reported for chondrodite by O'Donoghue (2006). Microscopic examination revealed small zones of coarse particles and 'fingerprints' in most of the stones. One sample contained small, parallel needle-like inclusions (Figure 4). EDXRF spectroscopy of the five chondrodite samples showed traces of Al, Mn, Ca, Ti, Na and K, consistent with the results presented by Fritz et al. (2007) for material from Sumbawanga (no chemical data were reported for the chondrodite from Mahenge).

Figure 3: Five chondrodites (0.52–1.96 ct), reportedly from Tanga, Tanzania, were studied for the report. One of them (lower right) was noticeably more orange than the others. Photo by Kelly Kramer.

Figure 4: A parallel array of needle-like inclusions is present within a 'fingerprint' in a chondrodite reportedly from Tanga, Tanzania. Photomicrograph by Christopher P. Smith; magnified 68×.

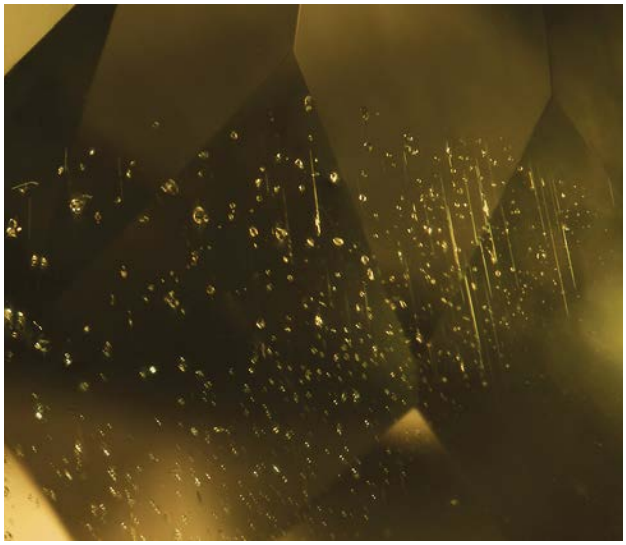

The gemmological properties of these samples are comparable with chondrodite from both Sumbawanga and Mahenge. If the Tanga location can be confirmed, it represents the third location in Tanzania for this unusual gem material.

Bryan Clark (bclark@aglgemlab.com)
American Gemological Laboratories
New York, New York, USA

References

Fritz E.A., Breeding C.M., Rossman G.R., Laurs B.M., Simmons W.B. and Falster A.U., 2007. Gem News International: Yellow-green clinohumite and yellow chondrodite from Tanzania. *Gems & Gemology*, **43**(4), 377–379.

O'Donoghue M., Ed., 2006. *Gems*, 6th edn. Butterworth-Heinemann, Oxford, 399.

Overton T., 2011. Gem News International: Chondrodite from Mahenge, Tanzania. *Gems & Gemology*, **47**(4), 316.

Uncommon minerals as gemstones from Tanzania, 2007. *SSEF Facette*, **14**, 6.

Purple Garnets from East Africa

During the June 2015 JCK gem and jewellery show in Las Vegas, Nevada, USA, news circulated about some attractive new purple garnets from East Africa. Gem dealer Geoffrey Watt (Mayer & Watt, Maysville, Kentucky, USA) had an intense purple 3.87 ct cushion (Figure 5, centre), which was one of two faceted purple garnets that he bought from a Sri Lankan cutter at the 2015 Tucson gem shows. The cutter said he had purchased the rough material in Tanzania. Later, shortly before the JCK show, a 5.86 ct intense purple garnet was faceted by Jeff White (J.L. White Fine Gemstones, Kingsport, Tennessee, USA; see cover of this issue). Subsequently White cut nine more of these garnets, ranging from ~2 ct to 13.31 ct. He purchased the rough from Steve Ulatowski (New Era Gems, Grass Valley, California, USA), who obtained the material in March–April 2015 while on a buying trip to Arusha, Tanzania. His supplier initially told him that the source was Tanzania, but he subsequently confirmed that the material actually came from Catandica, Mozambique. (This also may apply to the origin of Watt's garnet.) Ulatowski noted that the pieces appeared alluvial and were irregularly shaped with a pitted surface texture. After several buying trips to Arusha and Bangkok through October 2015, Ulatowski obtained a total of 1 kg of this garnet (only selecting the better-quality material), commonly in pieces weighing around ½ g each.

Ulatowski also mentioned encountering a different type of purple garnet since December 2014, represented as 'rhodolite' from Salima, Malawi. This material also appeared alluvial but had better shape (like 'gumdrops') and smoother surfaces, and it was available in larger sizes, though stones exceeding 10 g appeared over-dark; he obtained 5–6 kg of this garnet. According to Bill Barker (Barker & Co., Scottsdale, Arizona, USA, the shape of this garnet enables a good cutting yield; he attained 40% from a 1 kg parcel, with individual stones weighing up to 10 ct. Dudley Blauwet also acquired some of the Malawi garnet from an East African supplier, and from 10 pieces of rough weighing 26.4 g, he cut 10 stones (49.96 carats total weight) ranging from 1.47 to 10.60 ct; he loaned two of the more purple gems for examination. They were gemmologically characterized by three of the authors (CW, BW and DH), along with the 3.87 ct cushion from Geoffrey Watt (Figure 5).

Figure 5: Attractive purple garnets were recently produced from East Africa. The cushion-cut gem in the centre (reportedly from Tanzania, but possibly Mozambique) weighs 3.87 ct, and the slightly paler purple stones from Malawi on either side weigh 2.14 ct (left) and 1.47 ct (right). Photo by B. Williams.

The gemmological properties of the three samples are summarized in Table I. They are consistent with those reported for pyralspite garnets by Stockton and Manson (1985), and the RI values of all three samples fall within the ranges expected for both pyrope-almandine (rhodolite) and pyrope-spessartine, with or without some grossular (cf. Jackson, 2006). The magnetic data measured for the 1.47 and 3.87 ct garnets further indicated a pyrope-almandine composition with Pyr>Alm for both gems (cf. Hoover, 2008).

EDXRF spectroscopy using an Amptek X123-SDD instrument with a DP5 preamplifier showed a major amount of Fe, present in approximately equal amounts in all three stones. A small amount of Ca was detected in the three garnets, with slightly more in the 1.47 ct sample; that stone also contained a significant amount of Mn and Cr. (Note: Although Mg was not seen, it is only marginally detectable with this instrumentation.) UV-Vis spectroscopy of the 3.87 and 1.47 ct samples using an Ocean Optics USB4000 instrument showed slightly greater absorption in the ~420 nm region of the 1.47 ct sample. This created a more pronounced transmission window in the violet range for the 3.87 ct stone, corresponding to its more intense purple colour.

Ultraviolet-visible–near infrared (UV-Vis-NIR) absorption spectra also were collected on two

Table I: Properties of the faceted purple garnets from East Africa.[a]

Locality	Tanzania/Mozambique?	Salima, Malawi	
Source	Watt	Blauwet	
Weight (ct)	3.87	2.14	1.47
Colour	Vivid slightly reddish purple	Moderate purplish pink, shifting to a moderate slightly purplish pink in incandescent light	Deep reddish purple, brightening to a vivid reddish purple in incandescent light
RI	1.765	1.749	1.748
SG	3.89[b]	3.75	3.73
Magnetic data[c]	18.01 × 10^{-4} SI	Not determined	11.76 × 10^{-4} SI
Internal features	Many parallel needles, some appearing as broken lines and others corresponding to growth tubes	Clusters of small, colourless, iridescent, crumb-like inclusions and a few short needles	A few fine parallel needles

[a] None of the garnets showed any reaction to the Chelsea filter or UV radiation.

[b] A cavity on the pavilion appeared to be filled with a polishing medium, and it is possible that it may have slightly lowered the SG value.

[c] Volume magnetic susceptibility measurements were performed by author DH using the method described in Hoover (2008).

additional samples by one of us (GRR), merging data from three spectrometers: an OceanOptics UV CCD, a silicon-diode array visible spectrometer and a Nicolet iS50 near-infrared unit (Figure 6). Both samples consisted of doubly-polished slabs. Sample 3237 was prepared from a piece of Mozambique rough material supplied by Jeff White (e.g. see border region of cover photo) that was originally obtained from Steve Ulatowski, and sample 3235 was a slightly less intense purple garnet supplied by Ulatowski from a much earlier find that occurred in Tanga, Tanzania. Both pieces had nearly identical spectra, except 3235 showed greater absorption in the violet range (near 400 nm). The more intense purple sample 3237 had less absorption in that region, producing increased transmission. Manganese (Mn^{2+}) is responsible for absorption in the 400–440 nm region of the spectrum (Manning 1967), and chemical analysis (Table II) showed that sample 3235 had >20% more Mn than 3237. The additional manganese absorption in sample 3235 removed more of the violet light, causing it to appear less purple than 3237. An additional factor contributing to the

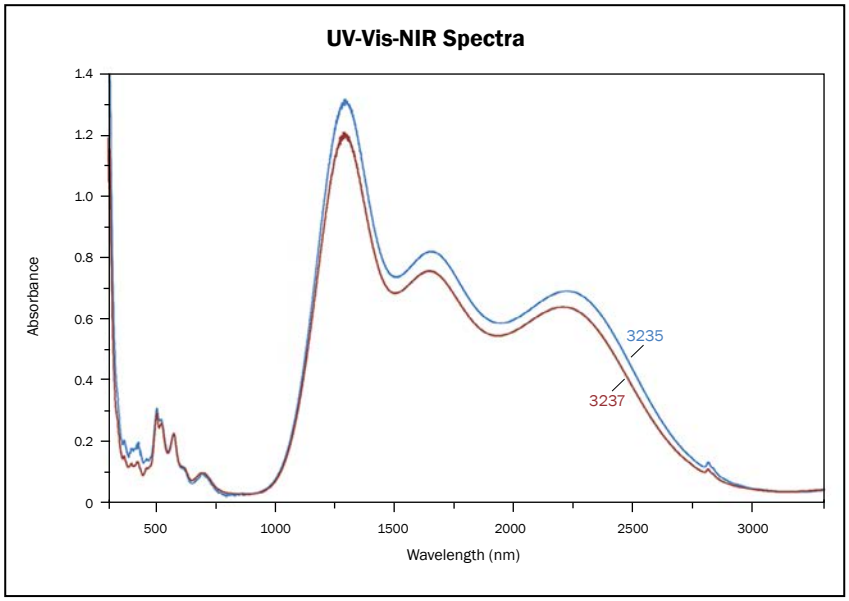

Figure 6: UV-Vis-NIR absorption spectra of two purple garnet slabs from Tanzania (sample 3235) and Mozambique (sample 3237) show nearly identical patterns until the violet range, where 3235 has greater absorption. The more pronounced transmission window in this region for 3237 corresponds to its slightly more intense purple colour. Both samples were scaled to plot as 1.0 mm thick.

colour of 3237 is the absence of Fe^{3+}, that both by itself and through interactions with Fe^{2+} would absorb light in the blue region of the spectrum.

*Table II: Electron microprobe analyses of purple pyrope-almandine garnets from Tanzania and Mozambique.**

Sample no.	3235	3237
Location	Tanga, Tanzania	Catandica, Mozambique
Oxides (wt.%)		
SiO_2	40.40	40.23
Al_2O_3	22.95	23.01
FeO	22.17	24.03
MgO	13.36	12.72
CaO	1.35	0.77
MnO	0.25	0.21
Total	100.48	100.97
Ions per 12 oxygens		
Si	3.002	2.995
Al	2.010	2.019
Fe	1.378	1.496
Mg	1.480	1.412
Ca	0.107	0.061
Mn	0.016	0.013

* Average of five analyses per sample. Cr and Ti were analysed for but not detected. Analyst: Chi Ma. End-member compositions determined by author DH using procedure of Locock (2008): Sample 3235: $Pyr_{49.00}Alm_{44.29}Gro_{5.10}Sps_{0.52}And_{0.48}$ Sample 3237: $Alm_{48.49}Pyr_{46.81}Gro_{3.57}Sps_{0.44}$

Cara and Bear Williams (info@stonegrouplabs.com)
Stone Group Labs, Jefferson City, Missouri, USA

Dr George R. Rossman
California Institute of Technology
Pasadena, California, USA

Brendan M. Laurs

Dr Don Hoover
Springfield, Missouri, USA

References

Hoover D.B., 2008. Magnetic susceptibility, a better approach to defining garnets. *Journal of Gemmology,* **31**(3), 91–103, http://dx.doi.org/10.15506/jog.2008.31.3.91.

Jackson B., 2006. The garnets. In M. O'Donoghue, Ed., *Gems*, 6th edn. Butterworth-Heinemann, Oxford, 195–237.

Locock A.J. (2008) An Excel spreadsheet to recast analyses of garnet into end-member components, and a synopsis of the crystal chemistry of natural silicate garnets. *Computers & Geosciences*, **34**, 1769–1780, http://dx.doi.org/10.1016/j.cageo.2007.12.013.

Manning P.G., 1967. The optical absorption spectra of the garnets almandine-pyrope, pyrope and spessartine and some structural interpretations of mineralogical significance. *Canadian Mineralogist*, **9**, 237–251.

Stockton C.M. and Manson D.V., 1985. A proposed new classification for gem-quality garnets. *Gems & Gemology*, **21**(4), 205–218, http://dx.doi.org/10.5741/gems.21.4.205.

Green Prase Opal from the Kondoa District, Tanzania

A historically important deposit of chrysoprase and prase opal in Tanzania is located at Haneti, situated north of Dodoma in central Tanzania (Shigley et al., 2009). During the 2015 Tucson gem shows, rough and polished material (e.g. Figure 7) from a new deposit in Tanzania was shown by Werner Radl (Mawingu Gems, Niederwörresbach, Germany). He indicated that mining started in early 2014 near Kwa Mtoro village in the Kondoa District; this is also in the Dodoma region of Tanzania, but further north of Haneti. It is likely that several hundred kilograms of rough material have been produced. Radl obtained ~50 kg of rough, some of which he processed into spheres, cabochons and tumbled pieces.

Radl donated two rough pieces (Figure 8) to Gem-A, and they were analysed by this author. Both were largely bluish green and translucent, with portions containing white opaque material (and also some dark brown matrix in one piece). They measured approximately 21.0 × 20.7 × 11.3 mm and 24.3 × 17.0 × 18.0 mm, and weighed 4.44 and 4.46 g, respectively.

A hydrostatic SG of 2.17 was measured on the larger sample. (The SG of the other piece could not be reliably measured, due to the presence of several cracks and voids.) Both samples appeared green through the Chelsea filter. Their reaction to long-wave UV radiation varied from partly inert to a weak chalky blue-

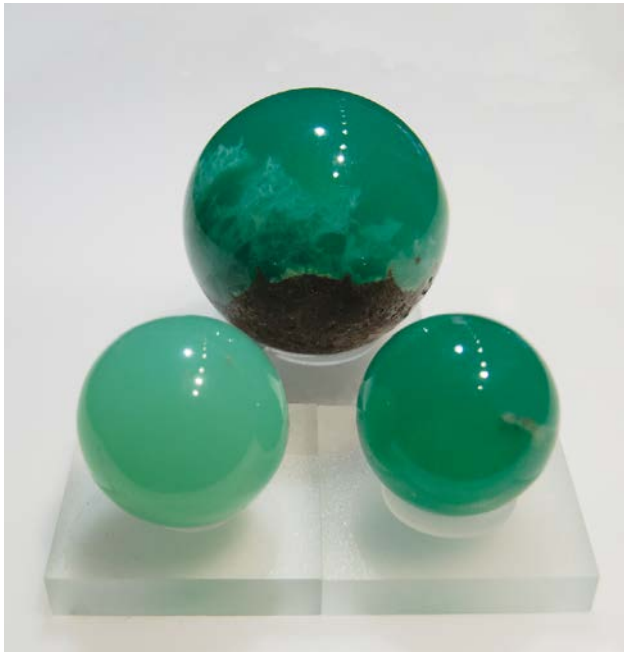

Figure 7: These polished spheres of prase opal (here, ~1.5–2.5 cm in diameter) are from a new deposit in the Kondoa District of Tanzania. Photo by Brendan M. Laurs.

white fluorescence, whereas they showed a weak yellowish green fluorescence to short-wave UV. No phosphorescence was observed.

The SG value was clearly much lower than the ~2.6 expected for chrysoprase, and instead lies in the range of common opal. Both specimens increased in weight after hydrostatic SG weighing, and after one week they still retained a slightly higher weight, indicating some degree of hydrophane character. Infrared spectroscopy of both fragments (using a Thermo Scientific Nicolet iS50 FT-IR spectrometer) showed a pattern characteristic of opal, with a strong absorption band around 5200 cm^{-1} (Figure 9).

Figure 9: This representative Fourier-transform infrared (FTIR) spectrum of the rough material from the Kondoa District shows a strong absorption at ~5200 cm^{-1} that is characteristic of opal.

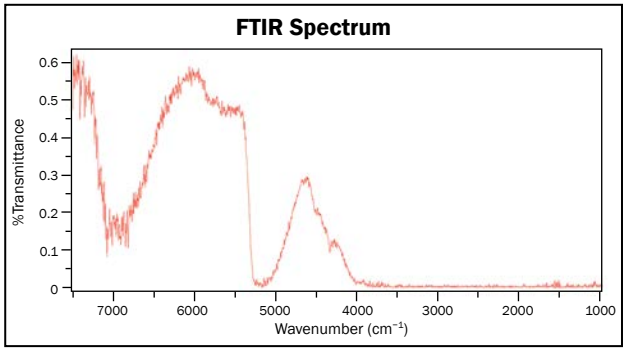

Figure 8: These rough pieces of prase opal (4.44 and 4.46 g) from the Kondoa District were examined for this report. Gift of Mawingu Gems; photo by Dirk van der Marel.

Raman spectroscopy (using a Thermo Scientific DXR Raman microscope with 780 nm laser excitation) produced spectra containing a broad band at ~325 cm^{-1} (the position varied slightly between the two samples), and peaks at 773 and 668 cm^{-1} (Figure 10). The broad band is due to the Raman shift of the O-Si-O bending mode, and its position is characteristic of opal-CT (not totally amorphous, but poorly crystalline cristobalite with some tridymite-like stacking; Fritsch et al., 2012). Moreover, Ilieva et al. (2007) showed that Raman spectra with the most intense (although poorly resolved) band centred near 330–360 cm^{-1} can be considered opal-T, with the proportion of spatial regions containing tridymite-type framework topology being higher than that of cristobalite-type

Figure 10: Raman spectroscopy of the prase opal shows a broad band at 323 cm^{-1}, characterising it as opal-CT or opal-T. A reference spectrum of chrysoprase is shown for comparison; the peak at 465 cm^{-1} indicates the presence of quartz (cryptocrystalline). Both spectra were taken using a 780 nm laser.

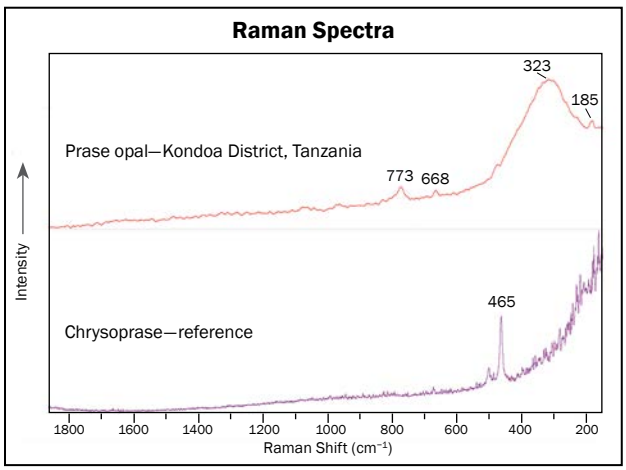

framework typology. The Raman spectra shown in Figure 10 are very similar to the spectra of prase opal presented by Shigley et al. (2009).

EDXRF chemical analyses (with an EDAX Orbis Micro-XRF Analyzer) showed large variations in the Ni content of this prase opal. Analyses of three random spots (300 µm beam diameter) on both samples gave NiO contents of 3.64, 7.36 and 9.72 wt.% for the smaller opal, and 0.73, 3.08 and 5.09 wt.% for the larger piece. On average, the data reflect a relatively high NiO content of slightly below 5 wt.%. Additionally, Fe was not detected, and only traces of Ca were found (0.06–0.26 wt.% CaO).

The high Ni content of this strongly coloured prase opal appears to be consistent with the notion that chrysoprase with a lower degree of crystallinity tends to have greater amounts of Ni and a more intense colour (cf. Gawel et al., 1997), and also with the attribution of the colour to dispersed particles of Ni-containing minerals (cf. Shigley et al., 2009, and references therein).

It is highly likely that this prase opal was found in the same belt of metamorphosed ultramafic rocks that, from Haneti, are aligned in a north-westerly direction along regional shear zones.

J. C. (Hanco) Zwaan (hanco.zwaan@naturalis.nl)
Netherlands Gemmological Laboratory
National Museum of Natural History 'Naturalis'
Leiden, The Netherlands

References

Fritsch E., Rondeau B., Hainschwang T., and Karampelas S., 2012. Chapter 13: Raman spectroscopy applied to gemmology. In J. Dubessy, M.C. Caumon and F. Rull, Eds., *Raman Spectroscopy Applied to Earth Sciences and Cultural Heritage*, EMU Notes in Mineralogy, European Mineralogical Union and the Mineralogical Society of Great Britain and Ireland, **12**, 455–485, http://dx.doi.org/10.1180/emu-notes.12.13.

Gawel A., Olkiewicz S. and Zabinski W., 1997. XRD and IR spectroscopic investigations of some chrysoprases. *Mineralogia Polonica*, **28**(1), 43–51.

Ilieva A., Mihailova B., Tsintsov Z. and Petrov O., 2007. Structural state of microcrystalline opals: A Raman spectroscopic study. *American Mineralogist*, **92**, 1325–1333, http://dx.doi.org/10.2138/am.2007.2482.

Shigley J.E., Laurs B.M. and Renfro N.D., 2009. Chrysoprase and prase opal from Haneti, central Tanzania. *Gems & Gemology*, **45**(4), 271–279, http://dx.doi.org/10.5741/gems.45.4.271.

Flower-shaped Trapiche Ruby from Mong Hsu, Myanmar

Trapiche rubies have been known for years from marble-hosted deposits at Mong Hsu, Myanmar. They have been gemmologically characterized by Schmetzer et al. (1996), and their crystal growth mechanisms were studied by Sunagawa (2003). On three separate trips to Myanmar (Yangon in January 2011 and February 2013, and Mogok in December 2013), this author obtained five interesting flower-shaped trapiche rubies (e.g. Figure 11). They were cut and polished perpendicular to the c-axis, and ranged from ~5 to 7 mm in diameter and were 1.0–1.5 mm thick. At first glance, they showed a similar appearance and structure to ordinary trapiche rubies, with hexagonal cores surrounded by six sectors in a star shape that resembles the cogwheels used in sugar mills.

Microscopic examination revealed that they actually consisted of three separate growth layers (Figure 12), making them different from typical trapiche rubies. All five samples had small hexagonal cores that were overgrown by another hexagonal zone, which in turn was overgrown by radiating petals that originated from each prism face of the intermediate zone. The intermediate zone contained six thin arms extending outward from the corners of the core, producing six trapezoidal ruby sectors. The arms continued outward into the final growth layer to separate the six petals in the outer rim. Both the arms and the boundaries between each layer were delineated by thin white or yellow translucent areas. Carbonate mineral inclusions such as calcite and dolomite were documented in trapiche ruby arms by Schmetzer et al. (1996) and Sunagawa (2003).

When the samples were examined with transmitted light, the deep red cores and the six red

Figure 11: These flower-shaped trapiche rubies from Mong Hsu, Myanmar, contain three growth zones, consisting of a hexagonal core and middle layer, and an outer zone consisting of six heart-shaped (left, 7 × 5 mm) or clothes-pin-shaped (right, 7 × 6 mm) petals. Photos by E. Liu.

sectors in the middle layer appeared transparent, while the six petals of the outer rim appeared translucent pinkish red. In the middle and outer layers, the arms widened into branches toward the outer edges of those zones, forming snowflake-like patterns. The outer layer contained extensive elongate tube-like inclusions that were oriented in three directions, perpendicular to the three sets of hexagonal edges of the middle layer. Depending on the amount of weathering of the arms in the outer layer, the radiating patterns in this layer consisted of either six heart-shaped or six clothes-pin-shaped petals (again, see Figure 11).

Sunagawa's (2003, 2005) diagram of trapiche crystal growth (Figure 13) shows how different kinds of growth mechanisms occurred on either smooth or rough interfaces, with the 'driving force' of crystallization (X-axis) plotted as a function of the growth rate (Y-axis). The dendritic growth of the arms and branches of a trapiche ruby are formed under an 'adhesive-type' multi-phase growth mechanism on a rough interface under high-driving-force conditions. The interstitial sectors are formed by a layer-by-layer growth mechanism on a smooth interface and a later infilling process within the interstices between the previously-formed dendritic arms and branches. Disturbances in the crystal growth by tiny fluid blebs or crystalline

Figure 12: With magnification, this trapiche ruby displays a structure formed by three layers with different growth characteristics: a small deep red core, a middle layer with six arms/branches and an outer petal-shaped zone. Photomicrograph by E. Liu; magnified 15×.

inclusions after multi-phase crystallization in the arms and branches (or on boundaries between each layer) led to the formation of the tube-like inclusions in the outer ruby layer.

Chemical analysis by EDXRF revealed that Cr was higher in the core and middle layers than the rim. The variation of Cr contents and crystal morphology between the different growth layers reflects the complicated growth environment in the Mong Hsu region. The multi-phase and multi-stage formation of these trapiche rubies is due to repeated dendritic growth under high-driving-force conditions, followed by an infilling process within the interstices of the arms through a layer-by-layer growth mechanism.

Edward (Shang-i) Liu (edwardliu@gahk.org)
The Gemmological Association of Hong Kong

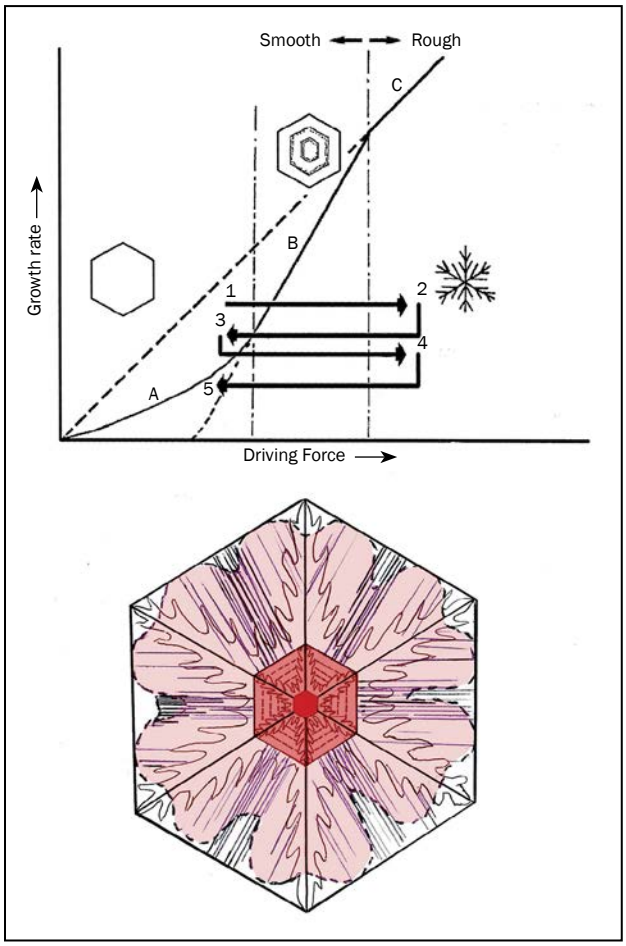

Figure 13: This 'Sunagawa diagram' (top) illustrates the crystal growth mechanisms of a corresponding trapiche specimen (bottom). The favoured growth mechanism is a function of the 'driving force' of crystallization versus the growth rate. The crystal in this example shows a sequence of growth similar to that of the trapiche rubies described in this study. Modified after Sunagawa (2003).

References

Schmetzer K., Hänni H.A., Bernhardt H.-J. and Schwarz D., 1996. Trapiche rubies. *Gems & Gemology*, **32**(4), 242–250, http://dx.doi.org/10.5741/gems.32.4.242.

Sunagawa I., 2003. Growth histories of mineral crystals as seen from their morphological features. In K. Byrappa, T. Ohachi, W. Michaeli, H. Warlimont and E. Weber, Eds., *Crystal Growth Technology*, William Andrew Inc., New York, New York, USA, 1–23, http://dx.doi.org/10.1016/b978-081551453-4.50003-8.

Sunagawa I., 2005. *Crystals: Growth, Morphology, & Perfection*. Cambridge University Press, Cambridge, 253–260.

Sapphires from Kina, Kenya

During the February 2014 Tucson gem and mineral shows, gem dealer Dudley Blauwet obtained from an African supplier a parcel of rough sapphires that reportedly came from Kina in central Kenya, about an hour's drive from Garba Tula. The parcel was particularly notable for its content of bicoloured sapphires, and Blauwet's quick visual comparison with the gem corundum from Kenya's Dusi deposit (near Garba Tula; see, e.g., Simonet et al., 2004) indicated that the present material was somewhat different. From 55 pieces of rough weighing 48.5 g, Blauwet had 57 stones faceted that weighed 83.54 carats and ranged from 0.40 to 2.40 ct. He loaned four samples to AGL for examination (Figure 14).

The three modified cushion cuts and one rectangular emerald cut ranged from 1.03 to 1.94 ct (6.50 × 4.41 × 3.30 mm to 7.85 × 6.36 × 4.23 mm, respectively). Viewed face-up with the naked eye, the stones appeared blue, green, yellow and bicoloured blue-yellow. However, when viewed with diffuse transmitted light in the microscope, they all showed exclusively blue and yellow colour zoning that was both straight and angular.

Visible-range spectroscopy using an S.I. Photonics CCD (charge coupled device)-array

Figure 14: Four sapphires (1.03–1.94 ct) from a relatively new deposit in Kenya were examined for this report: blue, green, yellow (here, appearing greenish yellow due to internal reflections from blue zones) and bicoloured blue-yellow. Photo by Kelly Kramer.

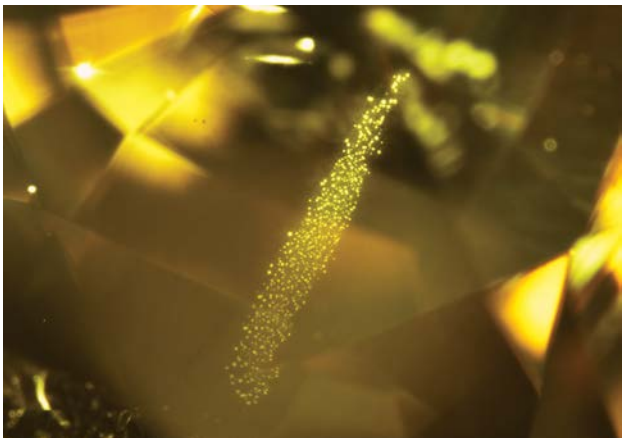

Figure 15: A planar cloud containing whitish, polka dot-like inclusions is seen in the 1.61 ct yellow Kenyan sapphire. Photomicrograph by Christopher P. Smith; magnified 50×.

UV-Vis spectrophotometer showed that all four sapphires were coloured by a combination of Fe^{2+}–Fe^{3+}, Fe^{3+} and Fe^{2+}–Ti^{4+}, and revealed they were of a magmatic-related origin (Smith, 2010), consistent with their overall blue-green-yellow coloration. Mid-infrared spectroscopy of the blue sapphire using a Thermo Scientific Nicolet 6700 FT-IR spectrometer displayed a strong 3309 cm^{-1} series of peaks (strong 3309, 3232 and 3185 cm^{-1}, and nominal 3367 cm^{-1}), while the yellow and green sapphires both showed a nominal 3309 cm^{-1} series (minor 3309 cm^{-1} and extremely small 3232 and 3185 cm^{-1}), while the bicoloured sapphire showed no OH-related features.

Semi-quantitative chemical analysis using a Thermo Scientific ARL Quant'X EDXRF spectrometer showed that all samples contained high amounts of Fe (0.91–1.68 wt.%), which is consistent with their magmatic-related origin. In addition, Ti ranged up to 0.01 wt.%. Neither V nor Cr was detected in any of the stones. Based on their high Fe content, it is not surprising that none of these four sapphires fluoresced to either long- or short-wave UV radiation.

Typical sapphire inclusions were observed in the four stones using a standard gemmological microscope. They consisted of bands of pinpoints (some coarse, some fine), strong straight and angular growth zoning, and a few frosty, whitish, fine-grained 'fingerprints'/healed fissures. Some of the more intriguing inclusion features were found in the yellow sapphire. The largest yellow colour zone in the stone contained an elongate planar cloud consisting of whitish, polka dot-like inclusions, as well as minute spots (Figure 15).

Wendi M. Mayerson (wmayerson@aglgemlab.com)
American Gemological Laboratories
New York, New York, USA

References

Simonet C., Paquette J.L., Pin C., Lasnier B. and Fritsch E., 2004. The Dusi (Garba Tula) sapphire deposit, central Kenya—A unique Pan-African corundum-bearing monzonite. *Journal of African Earth Sciences*, **38**(4), 401–410, http://dx.doi.org/10.1016/s0899-5362(04)00026-0.

Smith C.P., 2010. Inside sapphires. *Rapaport Diamond Report*, **33**(7), 123–132.

Stabilized Shattuckite and Bisbeeite from the Democratic Republic of Congo

During the 2015 Tucson gem shows, stabilized slabs and cabochons represented as shattuckite from the Democratic Republic of Congo (DRC) were sold under the trade name *Lunazul* by Brett and Allyce Kosnar (Kosnar Gem Co., Black Hawk, Colorado, USA). The Kosnars obtained approximately 40 kg of the rough material in October 2013 that reportedly came from the Tantara mine in Katanga District. They processed 11 kg of the rough into slabs and 2 kg into

Figure 16: These samples from the DRC, consisting of a mixture of shattuckite and bisbeeite, were examined for this report. The slab weighs 19.91 ct, the flat cabochons are 3.14 and 3.61 ct, and the rough piece weighs 2.58 g. Gift of Kosnar Gem Co.; photo by Dirk van der Marel.

cabochons. Prior to cutting, they stabilized the material with resin at a pressure of 5,000 psi for nearly three weeks. The Kosnars kindly donated to Gem-A one slab (19.91 ct) and two flat cabochons (3.14 and 3.61 ct) along with a piece of unstabilized rough material (2.58 g), and these samples were examined by this author for this report (Figure 16).

All of the stones were opaque and showed pleasing light- and dark-blue colours, with the polished pieces having a slightly darker tone than the rough material. The rough consisted of sprays of radiating fibrous crystals. This same fibrous texture was exhibited by the two cabochons, combined with a locally more granular texture. The slab showed the same textures (Figure 17, left), combined with circular fibrous areas similar to patterns often seen in malachite (Figure 17, right).

Spot RI readings of the polished pieces were ~1.65, and hydrostatic SG values varied between 3.05 (for a cabochon) and 3.16 (for the slab). The stones were mostly inert to long- and short-wave UV radiation, except that the lighter blue parts showed a weak blue fluorescence to long-wave UV.

These properties did not match the known values of shattuckite, $Cu_5(Si_2O_6)_2(OH)_2$, which has RIs of 1.752–1.815 and SG values of 3.80–4.11 (Dedeyne and Quintens, 2007), so further testing was required. Raman analysis (with a Thermo Scientific DXR Raman microscope) identified areas of shattuckite, but also revealed the presence of another mineral showing a close match with reference spectra of bisbeeite ($CuSiO_3 \cdot nH_2O$) in the RRUFF database (Figure 18). The granular areas in the slab consistently gave Raman spectra for shattuckite, regardless of tone (light or dark), and an associated small green-stained area was identified as calcite (Figure 17, right). However, the areas of the slab showing fibrous structure were bisbeeite. The 3.61 ct cabochon also contained a fibrous area of bisbeeite, and an intermediate region with a fibrous/granular structure that showed mixed Raman peaks relating to bisbeeite and shattuckite. For the 3.14 ct sample, shattuckite

Figure 17: Microscopic examination of the slab showed areas of a radiating fibrous texture that were identified as bisbeeite and a more massive, granular structure corresponding to shattuckite (left image). Within the granular areas, small circular fibrous areas showing a malachite-like texture also were identified as shattuckite. Additionally present was a small mass of green-stained calcite (right). Photomicrographs by J. C. Zwaan; image width 15 mm (left) and 8.2 mm (right).

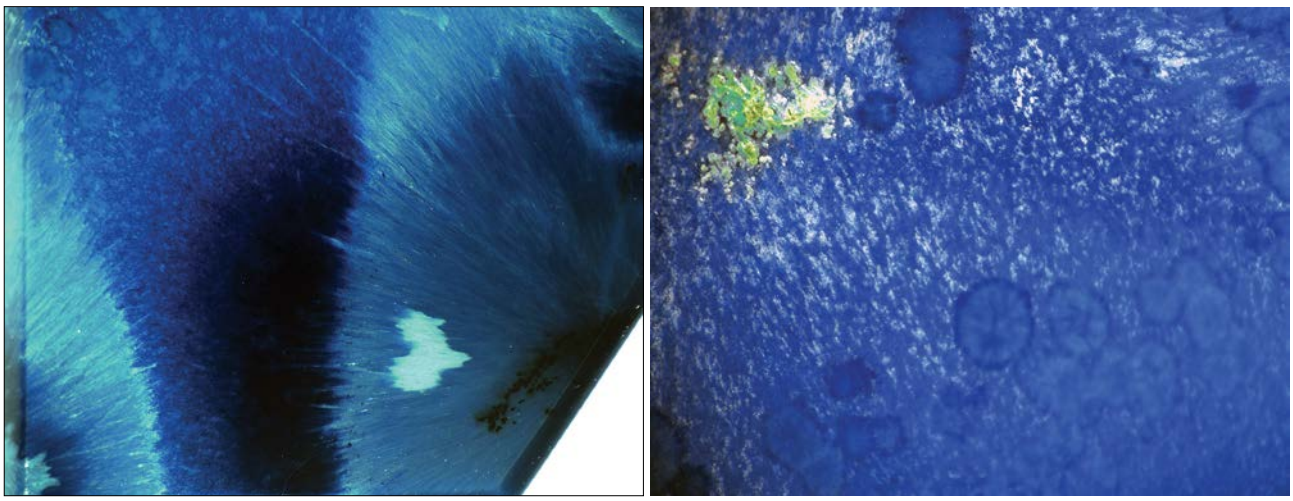

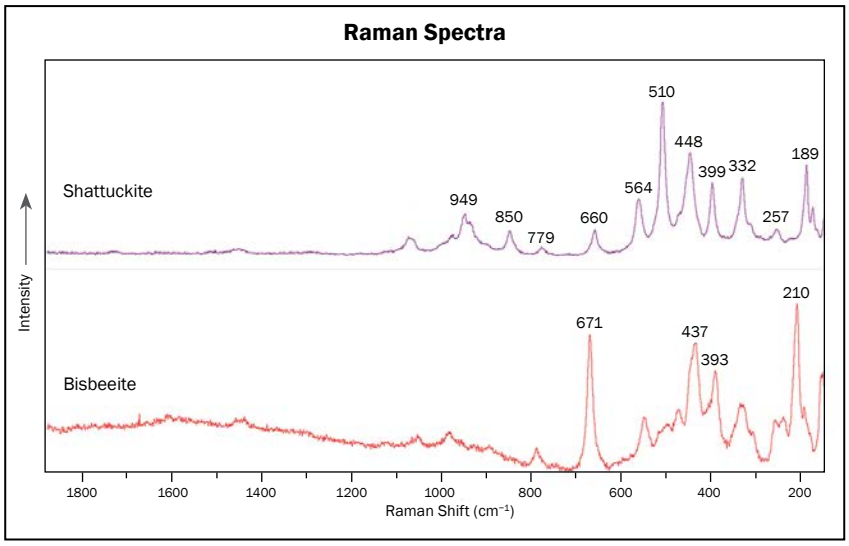

Figure 18: Both shattuckite and bisbeeite were identified by Raman spectroscopy in all three cabochons. Shown here are spectra from the 3.14 ct sample.

was only identified in a small dark spot showing granular texture on one side of the cabochon, while the fibrous areas analysed were bisbeeite. Granular areas on the other side of the stone matched shattuckite, regardless of colour (dark or light blue). A flat fibrous area on the rough sample showed only bisbeeite. Thus it appeared that the fibrous portions of the material consisted of bisbeeite and the more granular parts correlated to shattuckite.

Shattuckite was discovered in Bisbee, Arizona, USA (Shattuck mine) as a pseudomorph after malachite (Schaller, 1915). Bisbeeite is another rare, but poorly defined, secondary copper mineral, which was confirmed by Laurent and Pierrot (1962) as a distinct species. However, Van Oosterwyck-Gastuche (1968) concluded that the validity of bisbeeite was doubtful, and the mineral was discredited by the International Mineralogical Association's Commission of New Minerals and Mineral Names in 1977, when it was considered as a synonym for chrysocolla, $(Cu,Al)_2H_2Si_2O_5(OH)_4 \cdot nH_2O$ (www.mindat.org/min-26553.html). Interestingly, the measured Raman spectra of bisbeeite in the samples we examined showed the best match with RRUFF reference spectra of bisbeeite from Shangulume, Katanga Province, DRC, which showed features significantly different from the spectra of chrysocolla (typically lacking a prominent peak at 211–210 cm^{-1}, and showing a broad band in the 410 cm^{-1} range). Additionally, EDXRF chemical analyses (with an EDAX Orbis Micro-XRF Analyzer) revealed Cu and Si as the main elements in the samples, and did not detect any Al. Fleischer (1972) suggested that bisbeeite could be part chrysocolla and part plancheite, $Cu_8Si_8O_{22}(OH)_4 \cdot H_2O$, but Raman spectra do not support this possibility (cf. Frost and Xi, 2012).

From these preliminary data, as well as the radiating fibrous texture and deep blue colour seen in our samples, it appears that bisbeeite indeed differs from chrysocolla and needs to be better defined. Laurent and Pierrot (1962) gave RIs of 1.613–1.710 for bisbeeite, which explains the spot RI readings of ~1.65. Those values are significantly higher than the RI range for chrysocolla (1.46–1.57). Also, Laurent and Pierrot (1962) reported an SG value for bisbeeite of 3.45 ± 0.05, also higher than the SG of chrysocolla (1.93–2.45), and slightly higher than the SGs of 3.05–3.16 measured for the present samples. These low measured values are apparently due to the stabilized nature of the material.

As expected for the polished samples, which reportedly had been stabilized, Raman spectra showed features in the 3400–1200 cm^{-1} region that are typical of a polymer: main peaks in the 3100–2800 cm^{-1} region due to C-H stretching, a peak at 1725 cm^{-1} due to C=O stretching and a peak at 1457 cm^{-1} (Figure 19; cf. Johnson et al., 1999; Moe et al., 2007). The latter two peaks are similar to those at ~1730 and 1453 cm^{-1} that are characteristic of Norland Optical Adhesive 65, a colourless UV-hardened polymer that is used to stabilize turquoise (Moe et al., 2007). No such polymer-related features were recorded from the rough sample (reportedly untreated), which

also did not show any other visible signs of the presence of a polymer such as filled cavities.

J. C. (Hanco) Zwaan

References

Dedeyne R. and Quintens I., 2007. *Tables of Gemstone Identification*, Glirico, Gent, Belgium, 309 pp.

Fleischer M., 1972. New mineral names. *American Mineralogist*, **57**, 1003–1006.

Frost R.L. and Xi Y., 2012. A vibrational spectroscopic study of planchéite $Cu_8Si_8O_{22}(OH)_4 \cdot H_2O$. *Spectrochimica Acta Part A: Molecular and Biomolecular Spectroscopy*, **91**, 314–318, http://dx.doi.org/10.1016/j.saa.2012.01.051.

Johnson M.L., Elen S. and Muhlmeister S., 1999. On the identification of various emerald filling substances. *Gems & Gemology*, **35**(2), 82–107, http://dx.doi.org/10.5741/gems.35.2.82.

Laurent Y. and Pierrot R., 1962. Nouvelles données sur la bisbeeite. *Bulletin de la Société Française de Minéralogie et de Cristallographie*, **85**, 177–180.

Moe K.S., Johnson P. and Moses T.M., 2007. Polymer-impregnated turquoise. *Gems & Gemology*, **43**(2), 149–151, http://dx.doi.org/10.5741/gems.43.2.149.

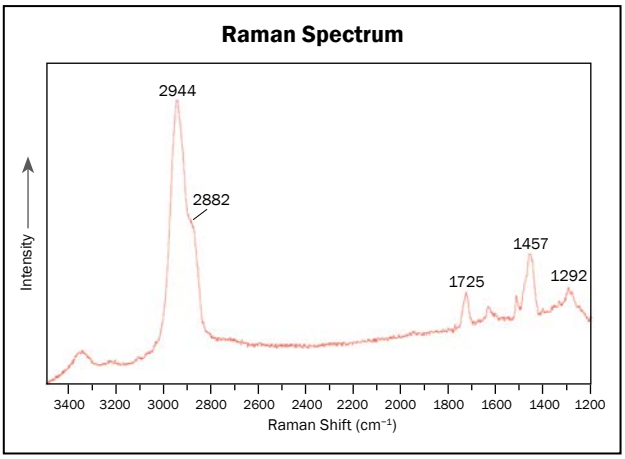

Figure 19: The polished samples of shattuckite/bisbeeite showed features in the 3400–1200 cm^{-1} region of the Raman spectrum that indicate the presence of a stabilizing polymer.

Schaller W.T., 1915. Four new minerals. *Journal of the Washington Academy of Sciences*, **5**, 7.

Van Oosterwyck-Gastuche M.C., 1968. Nomenclature of some Katangan copper silicates. Plancheite-shattuckite-bisbeeite-katangite minerals. *Annales de la Société Géologique de Belgique*, **91**, 401–422 (in French).

Purple Tourmaline from Maraca, Mozambique

In the past few years, a relatively new alluvial deposit of tourmaline was found at Maraca, Mozambique. This area is located only ~20 km from the well-known Cu-bearing tourmaline deposits of Mavuco in the Nampula area (e.g. Laurs et al., 2008a). The Maraca area reportedly also has produced Cu-bearing tourmaline, although the stones are smaller and more included.

Two water-worn pebbles from Maraca were loaned for examination by Michael Puerta and Farooq Hashmi (Intimate Gems, Glen Cove, New York, USA). Puerta obtained them during a visit to the nearby village of Iulùti (or Lulùti) in June 2014. The samples were medium purple and dark purple, and weighed 1.73 and 1.75 g, respectively (Figure 20). Their colours resembled those seen in some Cu-bearing tourmaline from Mavuco that is commonly heat-treated to a Paraíba-like blue appearance. The samples showed distinct pleochroism, in orangey yellow and purple, and in slightly greenish yellow and dark purple, respectively. The hydrostatic SG of both pebbles was 3.03. Viewed with a desk-model spectroscope, they showed a doublet at about 450 and 455 nm (with the first line being darker), a broad absorption band between 480 and 560 nm, and gradually decreasing absorption from ~530 to 560 nm; these features are common for purple tourmaline when viewed with a

Figure 20: These two transparent waterworn tourmaline pebbles (1.73 and 1.75 g) are from a new mine at Maraca, Mozambique, which is situated near the Mavuco Cu-bearing elbaite deposit. However, they were found to contain significant Fe and no Cu. Photo by Dirk van der Marel.

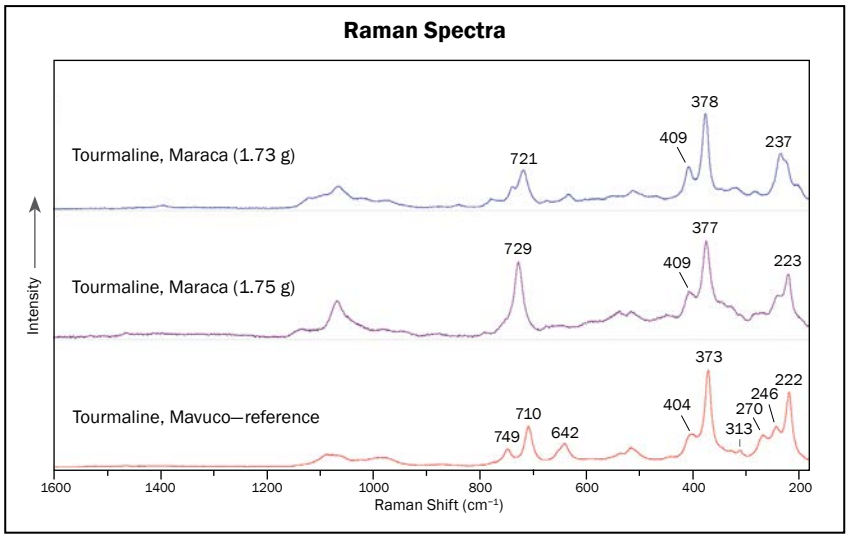

Figure 21: Raman spectra of the tourmaline pebbles from Maraca showed best matches with reference spectra of liddicoatite (for the 1.73 g sample) and liddicoatite/elbaite (for the 1.75 g sample). Shown for comparison is a reference spectrum of Cu-bearing tourmaline (elbaite) from Mavuco.

spectroscope (e.g. GIA, 1995). The stones were inert to long- and short-wave UV radiation.

The Raman spectrum (obtained with a Thermo Scientific DXR Raman microscope) of the 1.73 g sample showed a good fit with spectra of liddicoatite in the RRUFF database, while the 1.75 g piece also showed a best match—although less convincing—with the reference spectra of liddicoatite (in addition, it roughly matched spectra for elbaite). Both samples had Raman spectra that were quite different from that of a slightly reddish purple Cu-bearing tourmaline from Mavuco (no. 510-10, characterized by Laurs et al., 2008a), which best matched elbaite in the RRUFF database (Figure 21).

Semi-quantitative EDXRF chemical analyses (Table III) were obtained from five random spots on each pebble using an EDAX Orbis Micro-XRF Analyzer. The instrument did not detect Cu in either sample, but showed significant amounts of Fe. This is unlike purple Cu-bearing elbaite from Mavuco, which consistently shows extremely low Fe content (again, cf. Laurs et al., 2008a).

Table III. EDXRF analyses (wt.%) of minor and trace elements in Maraca tourmaline.

Sample	1.73 g	1.75 g
Na_2O	0.94–1.0	1.6–2.6
K_2O	0.04–0.13	0.07–0.19
CaO	3.4–3.9	1.0–1.3
MnO	0.07–0.08	0.51–0.66
FeO	0.03–0.96	0.04–0.73
PbO	0.75–1.0	Not detected

The 1.73 g sample showed relative amounts of Ca and Na that would be expected for liddicoatite (although EDXRF spectroscopy is only marginally sensitive to Na). It also contained significant Pb, which is not typical for tourmaline from the Nampula region (cf. Krzemnicki, 2007; Laurs et al., 2008a,b), but has been documented in tourmaline from elsewhere (e.g. Madagascar: Lussier et al., 2006).

The 1.75 g pebble contained Na>Ca, which is not unusual for dark rubellite (cf. Deer et al., 1986). However, the calcium content was still much higher than in purple Cu-bearing elbaite from Mavuco, which typically has very low Ca.

As we analysed only two samples, this study can hardly be seen as representative for tourmaline from Maraca. The alluvial deposit could contain gem rough originating from various sources, and it would not be surprising for Cu-bearing tourmaline to be included among the production of stones from this new locality that is relatively close to Mavuco.

J. C. (Hanco) Zwaan

References

Deer W.A., Howie R.A. and Zussman J., 1986. *Rock-Forming Minerals–Disilicates and Ring Silicates*, Vol. 1B, 2nd edn. Longman Scientific and Technical, Harlow, Essex, 629 pp.

GIA, 1995. *Gem Reference Guide*. Gemological Institute of America, Santa Monica, California, USA, 270 pp.

Krzemnicki M.S., 2007. "Paraiba" tourmalines from Brazil and Africa—Origin determination based on LA-ICP-MS analysis of trace elements. *SSEF Facette*, **14**, 8.

Laurs B.M., Zwaan J.C., Breeding C.M., Simmons W.B., Beaton D., Rijsdijk K.F., Befi R. and Falster A.U., 2008a. Copper-bearing (Paraíba-type) tourmaline from Mozambique. *Gems & Gemology*, **44**(1), 4–30, http://dx.doi.org/10.5741/gems.44.1.4.

Laurs B.M., Zwaan J.C., Simmons W.B. and Falster A.U., 2008b. Gem News International: Tourmaline from Muva, Mozambique. *Gems & Gemology*, **44**(3), 273–275.

Lussier A.J., Hawthorne F.C., Aguiar P.M. and Kroeker S., 2006. Zoning in a single crystal of liddicoatite (tourmaline) from Madagascar: Crystal structure refinement, infrared spectroscopy, and ^{11}B, ^{27}Al, ^{29}Si magic-angle-spinning nuclear magnetic resonance spectroscopy. *Geological Society of America Abstracts with Programs,* **38**(7), 167.

Tourmaline Slices from Myanmar

Large, colourful tourmaline slices displaying intricate patterns are well-known for liddicoatite from Madagascar (e.g. Dirlam et al., 2002). Recently, this author was surprised to see similar slices that reportedly came from Myanmar, in the collection of Bill Larson (Palagems.com, Fallbrook, California, USA). Larson obtained the two slices from Mark Smith (Thai Lanka Trading Ltd. Part., Bangkok, Thailand), who takes frequent buying trips to Myanmar. In February 2015, Smith encountered these colourful slices with a Burmese dealer who had six pieces that were all cut from the same piece of alluvial rough. The dealer reported that they came from Möng Long (or Maing Lon), which is located about 20 km south of Mogok. Smith purchased the three most attractive slices (Figure 22). In a subsequent trip in October 2015, the same dealer had some additional Möng Long slices, but they displayed an ordinary 'watermelon' concentric pattern with pale coloration. Smith reported that in the past, Möng Long has produced some cabochon- and facet-grade red and green tourmaline, but this is the first time he has seen slices from this locality. The patterns seen in the Möng Long tourmaline are typical of liddicoatite, although these samples have not been chemically analysed to determine the species present. Similar patterns were displayed in a tourmaline slice from Vietnam that proved to consist of Ca-rich elbaite and liddicoatite (Laurs et al., 2002).

Tourmaline slices also have been recently produced from an additional location in Myanmar: Khetchel (or Khetchey, Kat Chay) in the Molo area, Momeik Township, located 75 km north-east of Mogok. The so-called mushroom

Figure 22: These three slices (5.7 × 4.6 cm each) were cut perpendicular to the c-axis from the same tourmaline crystal, which reportedly came from Möng Long, Myanmar. The pair on the left (101.76 and 112.42 ct) is in the collection of Bill Larson; photo by Orasa Weldon. The slice on the right (132.70 ct) is owned by Wing Chiu Li; photo by Mark Smith.

Figure 23: These three slices (11.04, 23.95 and 37.96 ct, from left to right) were cut perpendicular to the c-axis from different crystals of mushroom tourmaline originating from the Molo area of Myanmar. Specimens and photo courtesy of Mark Smith.

tourmalines from this area commonly have a black core and a bulbous triangular top consisting of pink-to-red fibrous elbaite (e.g. Lussier et al., 2008). When sliced perpendicular to the c-axis, they show various concentric patterns in pink-to-red, dark blue/green and black (Figures 23 and 24). They are frequently oiled due to their limited transparency. According to gem and mineral dealer Federico Bärlocher (Como, Italy), who specializes in Burmese stones, the size range of such slices is typically restricted by the relatively small size of the mushroom tourmaline crystals, as compared to the large liddicoatite specimens from Madagascar.

Brendan M. Laurs

References

Dirlam D.M., Laurs B.M., Pezzotta F. and Simmons W.B., 2002. Liddicoatite tourmaline from Anjanabonoina, Madagascar. *Gems & Gemology*, **38**(1), 28–53, http://dx.doi.org/10.5741/GEMS.38.1.28.

Laurs B.M., Simmons W. and Falster A, 2002. Gem News International: Elbaite-liddicoatite tourmaline from Vietnam. *Gems & Gemology*, **38**(2), 181–182.

Lussier A.J., Hawthorne F.C., Herwig S., Abdu Y., Aguiar P.M., Michaelis V.K. and Kroeker S., 2008. Mushroom elbaite from the Kat Chay mine, Momeik, near Mogok, Myanmar: II. Zoning and crystal growth. *Mineralogical Magazine*, **72**(5), 999–1010, http://dx.doi.org/10.1180/minmag.2008.072.5.999.

Figure 24: A single tourmaline crystal from Molo, Myanmar, was cut perpendicular to the c-axis into this series of slices (up to ~6.7 cm in diameter). Specimens and photo courtesy of Federico Bärlocher.

Gem-quality Wurtzite from Tanzania

An interesting discovery of orange-brown gem-quality wurtzite took place in 2012 at the famous tanzanite deposits in the Merelani Hills of northern Tanzania (Hyršl, 2013). The wurtzite came from Block D of the mining area, and was associated with tanzanite or alabandite (a manganese sulphide, MnS). Wurtzite is the hexagonal polymorph of zinc sulphide (ZnS), and was named by the French chemist and mineralogist Charles Friedel (1832–1899) after his

Figure 25: This wurtzite crystal (1.7 × 2.5 cm) from Merelani, Tanzania, shows a typical hexagonal habit. J. Hyršl collection and photo.

Figure 26: Wurtzite from Merelani is rarely facetable and typically suitable for cutting only small gemstones, such as the 0.91 and 0.83 ct samples shown at the bottom of this photo. By contrast, the exceptionally large specimen shown above weighs 76.42 ct. J. Hyršl collection and photo.

tutor Charles Adolphe Wurtz (1817–1884). Well-known occurrences of relatively large crystals are Oruro and Animas in Bolivia, Huanzala in Peru and Talnakh in Russia (Bernard and Hyršl, 2015).

In nature, zinc sulfide generally occurs in the form of the cubic polymorph sphalerite (α-ZnS), which crystallizes under a wide pressure-temperature range. Sphalerite deposits are the most important source of zinc. The crystallization of wurtzite (β-ZnS) is less common, and is typically linked to relatively high temperatures of about 1,020°C (Palache et al., 1944). Metastable formations may occur under lower-temperature conditions (e.g. in acidic solutions or favoured by the presence of cadmium; Okrusch and Matthes, 2014).

The partly translucent to transparent wurtzite crystals from Merelani are generally 2–3 cm in size (e.g. Figure 25), and faceted stones have been documented that weigh 0.30–1.74 ct (Hyršl, 2013) and 3.97 ct (Cooper and Renfro, 2014). More recently, a much larger wurtzite from Merelani was faceted: 76.42 ct (Figure 26).

The two smaller gems in Figure 26 (0.83 and 0.91 ct) were investigated for this report. Viewed with the polariscope, these distinctly fissured stones appeared streaky and exhibited tabby extinction. The high RI of wurtzite cannot be measured on a standard gemmological refractometer, but an approximate value of 2.36 was determined using a so-called digital refractometer (a lustre meter measuring reflectivity). An SG of 3.81 was measured with a hydrostatic balance. These values correspond to reference data for wurtzite (e.g. Phillips and Griffin, 1981).

Quantitative chemical analyses by electron microprobe (Jeol JXA 8200 at the Institute for Geosciences, Johannes Gutenberg-University Mainz, Germany) were obtained for these faceted wurtzite samples (Table IV). The significant Mn and low Cd contents of the two gems characterize

Table IV: Chemical composition of wurtzite from Tanzania (wt.%).

Sample	0.83 ct	0.91 ct
Zn	56.60	56.84
S	33.03	33.27
Mn	9.26	9.19
Cd	0.43	0.41
Fe	0.04	0.10
Cu	0.14	0.10
Ni	0.01	0.01
Total	99.51	99.92

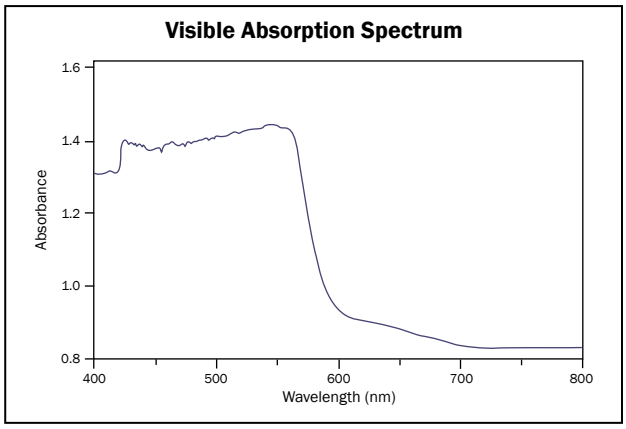

Figure 27: This absorption spectrum of the wurtzite from Merelani shows a flat-topped pattern due to strong reflections, but a broad band in the violet-to-orange spectral range (~400–600 nm) is apparent.

them as the zinc-rich member (wurtzite) of the wurtzite-rambergite-greenockite series (ZnS-MnS-CdS).

Visible absorption spectra (e.g. Figure 27) of the gems were recorded with a PerkinElmer Lambda 12 spectrometer. The spectra were heavily distorted because of strong reflection effects. A broad band in the violet-to-orange spectral range is thought to be caused by an electron transition between a Mn^{2+} *d*-electron level and an unoccupied ZnS energy band (Prof. Dr A. N. Platonov, pers. comm., 2015).

Dr Ulrich Henn FGA (ulihenn@dgemg.com)
and Fabian Schmitz
German Gemmological Association
Idar-Oberstein, Germany

Dr Jaroslav Hyršl (hyrsl@hotmail.com)
Prague, Czech Republic

References

Bernard J.H. and Hyršl J., 2015. *Minerals and Their Localities*, 3rd edn. Prague, Czech Republic.

Cooper A. and Renfro N., 2014. Lab Notes: Rare faceted wurtzite. *Gems & Gemology*, **50**(2), 156.

Hyršl J., 2013. Gem News International: Faceted wurtzite from Tanzania. *Gems & Gemology*, **49**(4), 261–262.

Okrusch M. and Matthes S., 2014. *Mineralogie*, 9th edn. Springer Spektrum, Berlin, Germany (in German).

Palache C., Berman H. and Frondel C., 1944. *The System of Mineralogy of James Dwight Dana and Edward Salisbury Dana: Yale University 1837–1892. Vol. I: Elements, Sulfides, Sulfosalts, Oxides*, 7th edn. John Wiley & Sons Inc., New York, New York, USA.

Phillips W.R. and Griffin D.T., 1981. *Optical Mineralogy: The Nonopaque Minerals*. W.H. Freeman and Co., San Francisco, California, USA.

Zircon Showing Asterism

Zircon ($ZrSiO_4$) is an interesting mineral in gemmology, not only because it is found in attractive colours such as yellow, red, brown, green and even blue (due to heat treatment) combined with a high lustre, but also because it is important as a solid inclusion in numerous other gems. It may be useful for detecting heat treatment of corundum, and also for revealing information about the formation conditions/age and geographical origin of a gemstone.

Gem-quality zircon is typically transparent and cut into faceted gems. Rarely, zircon shows chatoyancy, and such gems have been documented from Sri Lanka (Fryer 1983, 1985; Hänni and Weibel, 1988). Hänni and Weibel described heated zircons containing two sets of tiny cleavage fissures, each responsible for a cat's-eye reflection. However, due to the geometric orientation of these tiny features, they did not produce a star effect.

During the early 2000s, one of the authors (MPS) obtained an attractive asteriated zircon in Ratnapura, Sri Lanka. After years of searching, he has been unable to find any publications mentioning star zircon. He recently loaned the gem to the Swiss Gemmological Institute SSEF for examination, and it was characterized by author MSK. The oval cabochon weighed 13.60 ct, and was light yellowish brown with reduced transparency due to the presence of multiple tiny inclusions. It showed no reaction to long-wave UV radiation, and a weak yellowish fluorescence to short-wave UV. The most notable characteristic of this zircon was the presence of moderate

Figure 28: This 13.60 ct zircon cabochon shows moderate asterism and a bright reflection at the centre of the star. The vertical branch of the star is most prominent, followed by two weaker branches inclined 45° on each side of the vertical band. Additionally there is a very weak and short horizontal branch, thus resulting in a star with a total of eight rays when observed in optimum lighting conditions. Photo © V. Lanzafame, SSEF.

asterism (Figure 28). Two branches of the star were rather weak and by visual observation oriented perpendicular to each other, with a third and more prominent bright band intersecting them with an angle of 45°. Close examination revealed an additional but very weak and short branch that was oriented perpendicular to the most intense band (horizontal in Figure 28). Depending on the observation conditions, this zircon thus revealed a star effect with six or maximum of eight rays. In addition to this, the centre of the star was further pronounced by a bright reflection from the overhead light source.

Microscopic observation of the asteriated zircon revealed three sets of oriented planar features (Figure 29, left), each perpendicular to the weaker branches of the star, combined with a set of very fine short tubes or fissures that were responsible for the distinctly more intense branch (vertical in Figure 28). The bright area at the centre of the star resulted from another set of micro-features (Figure 29, right) that was oriented perpendicular to the inclusions producing the star effect. Due to the highly included nature of

Figure 29: Microscopic observation showed that various micro-features are responsible for the star effect (left) and the central bright reflection (right) in the zircon. Photomicrographs © M. S. Krzemnicki, SSEF; magnified 75×.

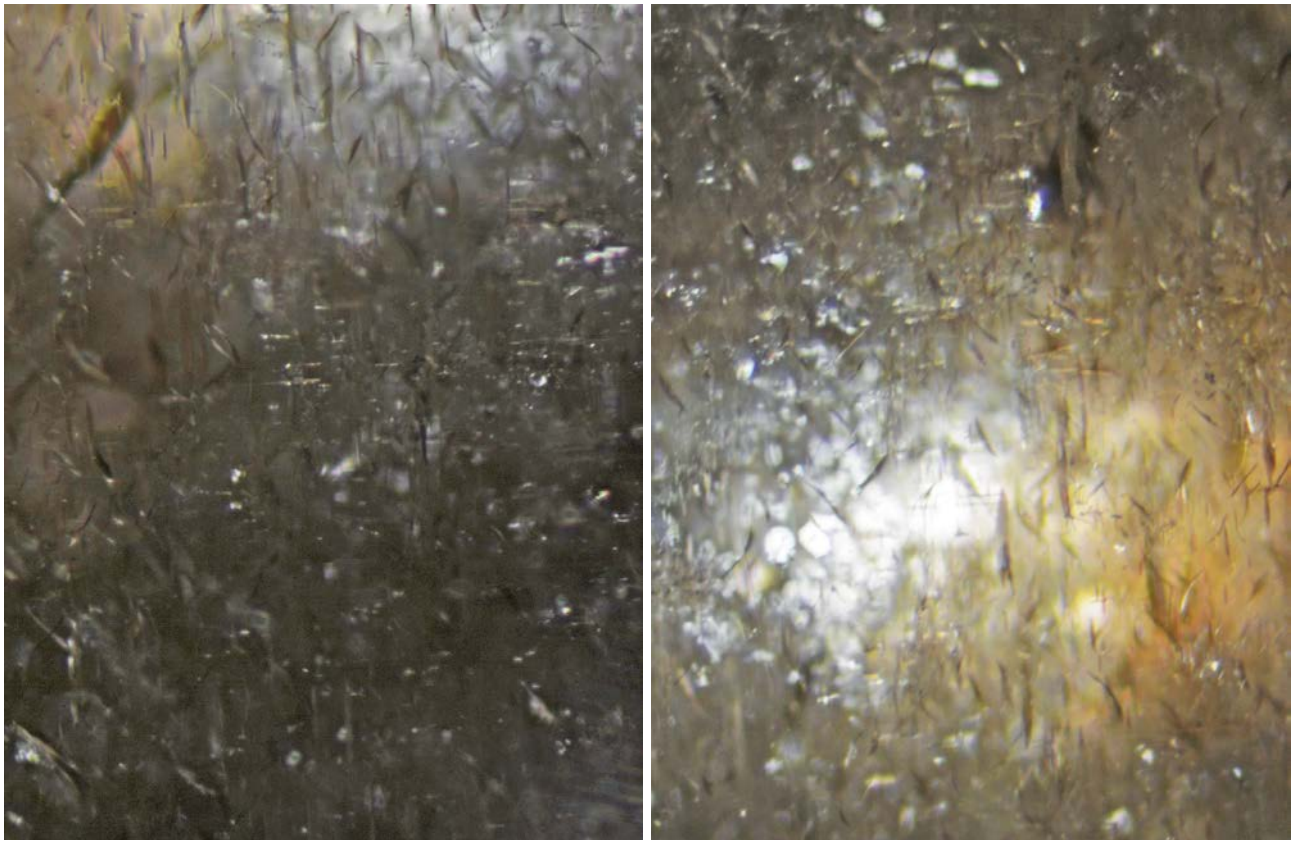

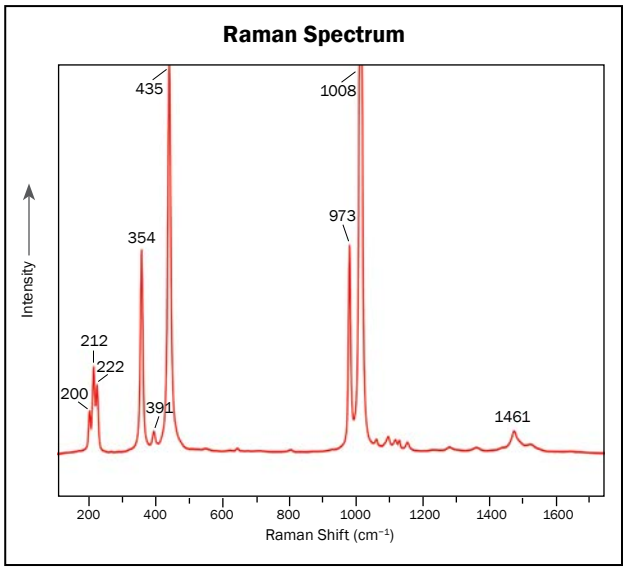

Figure 30: The Raman spectrum of the asteriated zircon shows sharp and pronounced vibrational peaks, characteristic of heat treatment.

the specimen, the crystallographic orientations of the observed micro-structures could not be determined.

Raman micro-spectroscopy of the inclusion features revealed only Raman peaks of zircon, so they are interpreted as micro-fissures along cleavage directions, or another type of micro-structure. Based on the similarity of these complex micro-features to those described by Hänni and Weibel (1988) for heated cat's-eye zircon, it seems probable that the star effect in this specimen is also the result of a heating process. This is supported by the Raman spectrum of this zircon (Figure 30), which is characterised by very sharp and pronounced vibrational peaks, as would be expected in metamict and translucent zircon only after heat treatment (Zhang et al., 2000; Nasdala et al., 2002; Wang et al., 2006; Krzemnicki, 2010) or in well-crystallized (non-metamict) and commonly transparent zircon.

Dr Michael S. Krzemnicki (gemlab@ssef.ch)
Swiss Gemmological Institute SSEF
Basel, Switzerland

Martin P. Steinbach
Steinbach – Gems with a Star
Idar-Oberstein, Germany

References

Fryer C., 1983. Gem Trade Lab Notes: Zircon, a rare cat's-eye. *Gems & Gemology*, **19**(4), 237.

Fryer C., 1985. Gem Trade Lab Notes: Zircon, cat's-eye. *Gems & Gemology*, **21**(2), 113–144.

Hänni H.A. and Weibel M., 1988. Origin of the cat's-eye effect in heat-treated zircons from Sri Lanka. *Australian Gemmologist*, **16**, 363–366.

Krzemnicki M.S., 2010. How to get the blues out of the pink: Detection of low-temperature treatment of pink sapphires. Presentation to Gemmological Association of Hong Kong, March, www.ssef.ch/fileadmin/Documents/PDF/650_Presentations/HK2010March_PinkSapphire.pdf.

Nasdala L., Hanchar J., Wirth R., Blanc P., Kennedy A. and Seydoux-Guillaume A., 2002. Annealing radiation damage and the recovery of cathodoluminescence. *Chemical Geology*, **191**(1–3), 121–140, http://dx.doi.org/10.1016/s0009-2541(02)00152-3.

Wang W., Scarratt K., Emmett J.L., Breeding C.M. and Douthit T.R., 2006. The effects of heat treatments on zircon inclusions in Madagascar sapphires. *Gems & Gemology*, **42**(2), 134–150, http://dx.doi.org/10.5741/gems.42.2.134.

Zhang M., Salje E.K.H., Capitani G.C., Leroux H., Clark A.M., Schlüter J. and Ewing R.C., 2000. Annealing of α-decay damage in zircon: A Raman spectroscopic study. *Journal Physics: Condensed Matter*, **12**, 3131–3148, http://dx.doi.org/10.1088/0953-8984/12/13/321.

ORGANIC MATERIALS

Amber Processing in Lithuania

On 1 September 2015, a group of participants from the International Gemmological Conference visited the Amber Queen processing facility in Klaipėda, Lithuania, as part of the post-conference field trip. The tour was led by Sigita Pevceviciute (Figure 31), who explained the various stages of amber processing and acted as an interpreter for our group's questions. The factory employs 150 workers and processes 1.5 tonnes of Baltic amber per month.

The raw amber is initially sorted into transparent material (and rarely, amber containing interesting

Figure 31: At the Amber Queen processing facility, autoclaves (left, with tour leader Sigita Pevceviciute) are used to clarify the raw amber (right). Photos by B. M. Laurs.

inclusions) versus that which needs to be clarified with treatment in an autoclave (Figure 31). We were told that, in general, approximately 20% of the raw amber is of jewellery quality, and the rest undergoes autoclave treatment. To remove bubbles and fractures, the amber is heated to 150–200°C at a pressure of 30 atmospheres in nitrogen gas.

The amber is then worked into pieces of various shapes followed by initial polishing using buffing wheels. Most of the pieces are drilled, either by hand (Figure 32, left) or by machine. Traditionally, drilling is done by men, while polishing is done by women. The beads are drilled from both sides to help prevent breakage and so they slide more smoothly during stringing.

Approximately 90% of raw Baltic amber is pale yellow, and it commonly undergoes a simple heat treatment procedure to darken its colour. The heating is done in air using conventional ovens at various temperatures and durations to create six colour categories ranging from yellow to orange, orangey brown and black. To obtain an attractive yellow colour, the amber is baked at 140°C for three hours, while 'black' amber (actually a black 'skin' on yellow amber) is produced by heating to 200°C for eight hours. Heating at lower temperatures for longer periods (e.g. 100°C for two weeks) is also done to give the amber an 'aged' appearance, to resemble that seen in vintage jewellery (e.g. Figure 32, right).

Figure 32: Hand drilling of amber pieces from both sides requires experience and concentration (left). Either before or after drilling, much of the amber undergoes heat treatment to darken its colour or create an 'aged' appearance (right). Photos by B. M. Laurs.

Figure 33: Amber beads of various colours are strung into necklaces that display repeating patterns. Photo by B. M. Laurs.

Final polishing is done using a two-step process. First the amber pieces are placed into vibra-polishers for 2–3 days together with various mixtures consisting of water, dish soap, ceramic pieces, fine quartz sand and glass balls. Then the amber pieces are put into rotating wooden drums with small pieces of beech wood and polishing powder (for 14 hours) or polishing liquid (for another 14 hours).

The beads are incorporated into a variety of jewellery pieces (necklaces, bracelets, earrings, etc.), and the various colours are often strung into attractive repeating patterns (e.g. Figure 33). Another product made by the factory consists of heat-treated amber cabochons from which the black 'skin' has been polished off the domes and the bases carved to create intricate patterns (Figure 34).

The various amber by-products from the factory (drill filings, powder, dust, etc.) are collected and sold for use in the electronics industry as well as in incense, facial creams and soap, so none of the amber that enters the facility for processing is wasted. No pressed amber products are made at the Amber Queen facility.

The jewellery is sold along with amber souvenirs and *objets d'art* in Amber Queen's shops in Klaipėda and Vilnius (Lithuania) and in Riga, Latvia. Our group visited the main store in Klaipėda, which also hosts an amber museum that displays an impressive private collection of Baltic amber.

Brendan M. Laurs

Figure 34: These amber cabochons (approximately 1.5–2.5 cm long) have been carved on their bases to remove the black 'skin' created by heat treatment. Intricate patterns are seen through the polished domes of the cabochons. Photo by B. M. Laurs.

Shungite for Jewellery Use

Recently a client submitted some pieces of a black gem material they called shungite. Initially we thought they were jet, but the gemmological properties were different. According to the literature, shungite is a mineraloid consisting of more than 98% carbon (Mastarlez et al., 2000). A mineraloid is a mineral-like substance that does not have a crystalline structure and possesses

Figure 35: This 4.32 ct piece of shungite has been cut in a freeform shape, and the top surface has been left unpolished to show its conchoidal fracture patterns. Photo by Pangemtech staff.

chemical compositions that vary beyond the generally accepted ranges for specific minerals. Shungite was first described from a deposit near Shunga village, in Karelia, Russia, and it has been reported to contain fullerenes (molecules of carbon in the form of hollow spheres, tubes and other shapes; Reznikov and Polekhovskii, 2000).

The samples submitted by the client consisted of assorted broken fragments and some flat-backed pieces that were cut into various shapes for mounting in jewellery; we tested a 4.32 ct sample (Figure 35). It was opaque black with a vitreous lustre and a surface that showed conchoidal fracture patterns. It was inert to UV radiation and gave a black streak. The sample showed a spot RI value of 1.62 and a hydrostatic SG of 1.86. FTIR spectroscopy recorded an absorption band at ~1578 cm^{-1}. According to information given in Reznikov and Polekhovskii (2000), shungite has an RI of 1.6, SG values between 1.83 and 1.96, and IR absorption between 1580 and 1575 cm^{-1}. The properties we determined for the 4.32 ct sample fell within the range for shungite and not jet (which has SG = 1.20–1.30).

The client explained that shungite is commonly used by crystal healers, and is also being mounted into some unusual designer jewellery (e.g. Figure 36).

Jayshree Panjikar (jayshreepanjikar@gmail.com)
Pangem Testing Laboratory & Pangemtech
Pune, India

References

Mastarlez M., Glikson M., Stankiewicz B.A., Volkova I.B. and Bustin R.M., 2000. Organic and mineral matter in a Precambrian shungite from Karelia, Russia. In M. Glikson and M. Mastarlez, Eds., *Organic Matter and Mineralisation: Thermal Alteration, Hydrocarbon Generation, and Role in Metallogenesis*, Springer Science+Business Media, Dordrecht, The Netherlands, 102–116, http://dx.doi.org/10.1007/978-94-015-9474-5_6.

Reznikov V.A. and Polekhovskii Yu.S., 2000. Amorphous shungite carbon: A natural medium for the formation of fullerenes. *Technical Physics Letters*, **26**(8), 689–693, http://dx.doi.org/10.1134/1.1307814.

Figure 36: This unusual pendant features a rectangular shungite (upper right, 2.50 × 1.01 cm), a cabochon of spotted coral (4.50 × 2.80 cm) and pear-shaped treated grey-green quartz (1.30 × 0.80 cm). Photo by Pangemtech staff.

PEARLS

Gem-set Cultured Pearls

The past several years have witnessed many creative innovations in modifying cultured pearls for use in jewellery, including carving their surfaces to create interesting patterns or expose an underlying bead made of various materials; embedding them with tags and other devices that can be used to include identifying information or custom-recorded audio, video or image files; and setting them with faceted gemstones (e.g. Hänni and Cartier, 2013; http://galateausa.com). Some new variations in setting gem materials into cultured pearls were recently developed, starting in March 2014, by Hisano Shepherd (little h, Los Angeles, California, USA).

Several cultured pearl varieties are used as starting materials, including both freshwater (soufflé and drop) and saltwater (Tahitian baroque, drop and keshi; golden and white South Sea baroque, drop and keshi; Sea of Cortez keshi; and Vietnamese blue akoya). These are carefully processed using three different methods. For the 'Pearl Geode Collection', they are sliced in half and each side is hollowed out, while for the 'Finestrino Collection' a concave opening is made into the interior of whole cultured pearls, and for the 'Grotto Collection' the cultured pearls are carved to create an opening that goes all the way through them (Figure 37). The interior surfaces of the cultured pearls are polished and then lined with a variety of different melee-sized gem materials (faceted stones or beads), including white and black diamonds, amethyst, ruby, emerald, sapphire and peridot, among others; cultured seed pearls also are used. The rubies and emeralds are commonly 'reclaimed' from old jewellery pieces, and the stone size and shape varies. The gemstones or seed pearls are affixed to the inner walls of the cultured pearls using resin.

The completed gem-set cultured pearls range from 9–10 mm up to 30+ mm, and are set into pendant, earring, ring and necklace designs. Shepherd has made over 300 of these items in her studio and office in Los Angeles. Her inspiration for creating them came from seeing quartz geodes at the Tucson gem shows, and she desired to recreate their geode-like appearance using cultured pearls.

Brendan M. Laurs

Reference

Hänni H.A. and Cartier L.E., 2013. Tracing cultured pearls from farm to consumer: A review of potential methods and solutions. *Journal of Gemmology*, **33**(7), 239–245, http://dx.doi.org/10.15506/jog.2013.33.7.239.

Figure 37: The earrings on the left are part of the 'little h' Pearl Geode Collection, and feature a pink soufflé cultured freshwater pearl measuring 13 × 20 mm that has been sliced in half and lined with light-to-dark pink sapphires (2.86 carats total weight) and set in 14-carat yellow gold. The Finestrino pendant in the centre is made from a pink soufflé cultured freshwater pearl measuring 30 × 33 mm that has been filled with ruby beads (40+ carats total weight) and set in a 14-carat rose gold necklace. The Grotto pendant on the right features a white soufflé cultured freshwater pearl measuring 20 × 31 mm containing ruby pieces (17.06 carats total weight) with a diamond-set bail in 14-carat white gold. Photos by Katja Bresch (left and right) and Angela Peterman (centre).

From Exsolution to 'Gold Sheen': A New Variety of Corundum

Thanh Nhan Bui, Katerina Deliousi, Tanzim Khan Malik and Katrien De Corte

Sapphires displaying an attractive golden sheen reportedly were discovered in eastern Kenya in late 2009, and were recently brought to market in commercial quantities. The basic gemmological properties of the so-called Gold Sheen sapphires are consistent with typical corundum. Microscopic examination and Raman micro-spectroscopy showed that Fe-Ti oxides (hematite, ilmenite and magnetite) are the main solid inclusions, and they are oriented parallel to crystallographic directions in the basal pinacoid of corundum characterized by a six-fold rotational symmetry. Hematite and ilmenite are present in the form of exsolution intergrowths within platelets or needles. Magnetite typically appears as larger and thicker black platelets. The sheen effect in these sapphires originates from the simultaneous reflection of light from the oriented network of exsolved hematite-ilmenite inclusions.

The Journal of Gemmology, 34(8), 2015, pp. 678–691, http://dx.doi.org/10.15506/JoG.2015.34.8.678

Introduction

At the end of 2009, African gem brokers brought a new type of sapphire to the Bangkok gem market. While the rough material appeared dark and opaque overall, it displayed a peculiar weak golden shimmering effect on basal pinacoid surfaces. Author TKM, a gem cutter and dealer for over 25 years, identified a potential business opportunity in this sapphire, and entered into an exclusive selling agreement with the mine owner. The material reportedly was produced from pits measuring a few metres deep in eastern Kenya near the border with Somalia. From 2010 to 2014, the rough material was exported to Thailand. The deposit was subsequently exhausted, with only non-commercial-quality gems extracted during the past two years. About 25 tonnes of rough have been stockpiled in Bangkok, where experiments on cutting and polishing are being conducted to best emphasize the distinctive golden shimmer of this corundum. Its appearance led author TKM to name the stone 'Gold Sheen' sapphire; the gems also have been presented as 'Zawadi' sapphire by some suppliers (e.g. Laurs, 2015).

In this article, we present a detailed gemmological study of the Gold Sheen sapphires and their inclusions, and compare their properties to those of other sheen-displaying gems to further understand their distinctive optical effect.

Samples and Methods

For this study, author TKM supplied 105 samples of Gold Sheen sapphire with a total weight of 675 carats. The stones ranged from 1 to 30 ct.

Figure 1: These Gold Sheen sapphires, faceted into checkerboard cuts or polished as cabochons, weigh up to 30 ct each. The golden sheen, colour zoning and fracture patterns are present in various combinations. Photo by T. K. Malik.

Except for one rough sample, they were cut and polished as cabochons and faceted gemstones of various qualities with regard to the golden sheen effect (e.g. Figure 1). Most of the cabochons were double-sided and displayed a light yellow to golden six-rayed star under a point light source (e.g. Figure 2). The faceted gems were cut into various common and fancy shapes. Due to a lack of transparency in the material, the proportions of the crown and pavilion were optimized for weight rather than for brilliance. Some of the crowns displayed a modified brilliant style, but the majority were fashioned into checkerboard cuts. The cutting and polishing of the rough material was the only processing imposed on the stones. Therefore, the Gold Sheen sapphires and their visual effect are completely natural.

Figure 2: A golden six-rayed star is shown by this 25.06 ct cabochon of Gold Sheen sapphire. Photo by T. K. Malik.

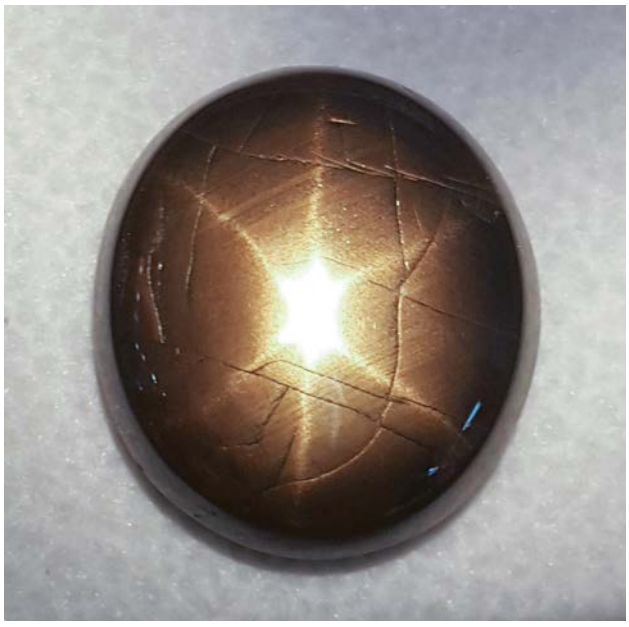

Basic gemmological characterization was performed on 46 samples at HRD Antwerp, and included visual observations, RI and hydrostatic SG measurements, polariscope and dichroscope reactions, hand-held spectroscope absorption spectra, and long- and short-wave UV fluorescence observations. In addition, the samples were studied with the D-Scope gemmological microscope from HRD Antwerp.

Energy-dispersive X-ray fluorescence (EDXRF) spectroscopy was achieved with a PANalytical Epsilon 5 instrument on 29 samples. For primary excitation, the Gd tube anode was operated with a current of 6–24 mA, a voltage of 25–100 kV and a power of 600 W, depending on the nine

secondary targets used for the emission of the different characteristic X-ray lines. The samples were analysed for 10–300 sec, focusing on the analytical X-ray line of each target according to the elements of interest. We used the *Kα* emission lines for most of the light trace elements and the *Lα* emission lines for elements with *Kα* lines greater than 20 keV.

Inclusions were identified in 20 samples using a Horiba LabRAM 800HR micro-Raman spectrometer at the Catholic University of Louvain (Louvain-la-Neuve, Belgium). Calibration was performed on a silicon substrate with a first-order Raman peak located at 520.7 cm^{-1}. A green laser (514 nm) was used to excite the samples, and its power was modulated to between 50% and 100%. The acquisition time for each spectrum ranged from 10 sec to 2 min, and each spectral acquisition was performed twice. Due to the very small size of the inclusions, we used magnifications of 500× and 1,000×. Raman spectra were normalized according to the most intense Raman peak, so as to plot several curves in the same graph. The background was not subtracted from the spectra.

The microstructure of the inclusions in one sample was investigated by a Zeiss Ultra55 field emission scanning electron microscope (SEM). We used a low accelerating voltage (2 keV) and the In-Lens secondary-electron detector with an optimized working distance (~2 mm) to obtain clear micrographs of the girdle profile of the sample where there was a high probability of surface-reaching needles and platelets. These parameters allowed us to resolve the cross-sections of the platelet inclusions to assess their thickness in SEM micrographs. The micrographs were horizontally aligned with the basal pinacoid and vertically aligned parallel to the c-axis of the corundum host.

All of the measurements were performed at ambient pressure and temperature, and none required any sample preparation.

Results

Visual Observations: Colour and Transparency

The body colour of the host sapphires was blue, green and/or yellow, with the latter being the most frequently encountered. The metallic sheen was characterized by a (golden) bronze colour that shimmered when the cabochons and faceted gems were illuminated. As demonstrated below, the shimmer was due to inclusions within the sapphires.

The c-axis of the corundum was oriented perpendicular to the crown/dome of the polished stones. Some samples displayed colour zoning in three orientations at 60°/120°, typical of the six-fold rotational symmetry in the basal plane of the rhombohedral system. Colour zoning in parallel lamellar patterns was created by layers containing various concentrations of inclusions that mechanically coloured those areas. Due to the reflection of light from the inclusions, those bands containing abundant particles appeared light, while the interstitial areas containing few inclusions showed the body colour of the sapphire, which generally appeared dark (especially for sapphires with blue body colour). Intermediate concentrations of inclusions exhibited a mixture of golden sheen and the body colour from the host sapphire.

Within areas showing the golden sheen, we typically observed dark surface-reaching cracks showing random paths. Their full extension was more visible when we observed the samples at an oblique angle to the surface of the stone.

In general, the diaphaneity of the sapphires varied according to the amount of sheen that they displayed. Samples showing less sheen were nearly transparent. Where the sheen was present over a larger area of a gemstone, the diaphaneity was translucent. In areas of darker bronze sheen, the stone could be completely opaque. This suggests that the inclusions responsible for the sheen also cause diminished transparency of the host sapphire.

Physical Properties

As the gemstones were heavily fractured, full of inclusions, typically translucent and not perfectly polished, routine gemmological testing was challenging. The overall results from the 46 samples were: RI—1.76–1.77 (spot reading), birefringence—0.01, SG—3.95–4.05, UV fluorescence—inert to long- and short-wave UV radiation, and spectroscope spectrum—absorption at 450 nm and in some samples a cutoff at ~500 nm. These are typical readings for corundum.

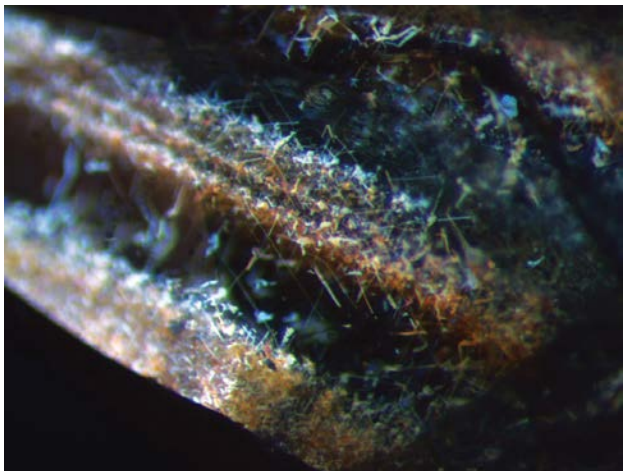

Figure 3: In areas of the sapphires showing sheen, networks of oriented inclusions consisting of needles and platelets lie within the basal pinacoid. Photomicrograph by T. N. Bui using brightfield illumination; magnified 60×, field of view 1.87 × 1.45 mm.

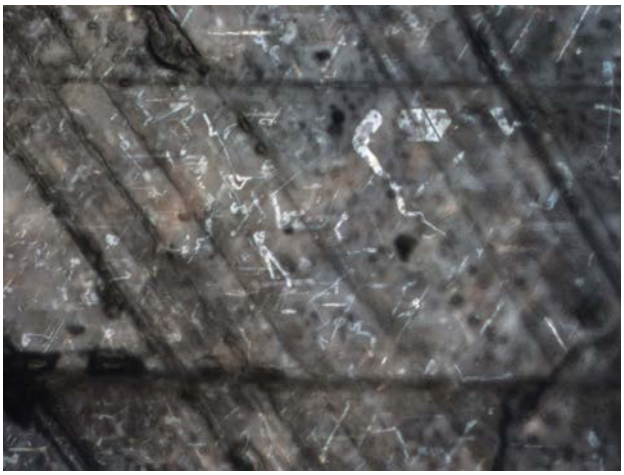

Figure 4: The surface of the basal pinacoid in this particular rough sapphire exhibits growth lines in three directions, parallel to {10$\bar{1}$0}. The needle inclusions below the surface are parallel to these growth lines. Photomicrograph by T. N. Bui using brightfield illumination; magnified 100×, field of view 860 × 635 µm.

Microscopic Characteristics

Under the gemmological range of magnification (10×–80×), we clearly observed hexagonal growth patterns and colour zoning in the sapphires. Furthermore, areas showing the sheen correlated to networks of numerous tiny straight needles and flakes lying within the corundum basal plane (Figure 3). In reflected light, the inclusions were golden metallic, and thus reflections from the inclusion networks created the golden sheen. In transmitted light, the inclusions appeared more orangy brown, and under oblique illumination they exhibited various colours due to thin-film interference (see Figure DD-1 in the Data Depository). The latter observation indicates an inclusion thickness in the nanometre range.

As mentioned above, the inclusions were present in three different orientations intersecting at 60°/120°, typical of the six-fold rotational symmetry in the basal plane of the rhombohedral system. These orientations also were parallel to the corundum growth lines (Figure 4), which are aligned along the first-order hexagonal prism {10$\bar{1}$0} (Hughes, 1997, p. 446). Also present in some samples were larger platelets that contained small dark areas (Figure 5).

Zones in the sapphires consisted of alternating bands of needles and platelets of different concentrations, at various positions along the c-axis (Figure 6). The bands containing inclusions of higher density and closer to the surface produced a golden bronze colour, while those of lower density and deeper inside the host produced a brownish bronze sheen, which resulted from a combination of reflections from the inclusions and the dark body colour of the host sapphire. This is well illustrated by comparing the appearance of a thin sample in reflected vs. transmitted light (again, see Figure 6).

Less abundant, but always present within the inclusion networks in the golden sheen areas, were black plates that were a similar size or larger than the platelets described above (Figure

Figure 5: The platelets in this sapphire contain dark areas and appear to be composed of different minerals. Photomicrograph by T. N. Bui using brightfield illumination; magnified 50×, field of view 1.3 × 1.0 mm.

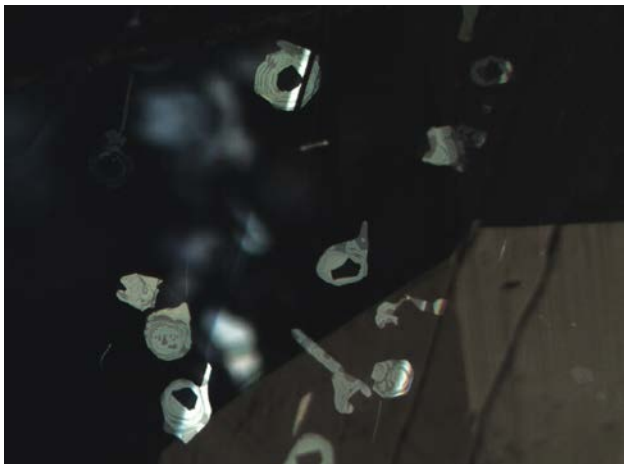

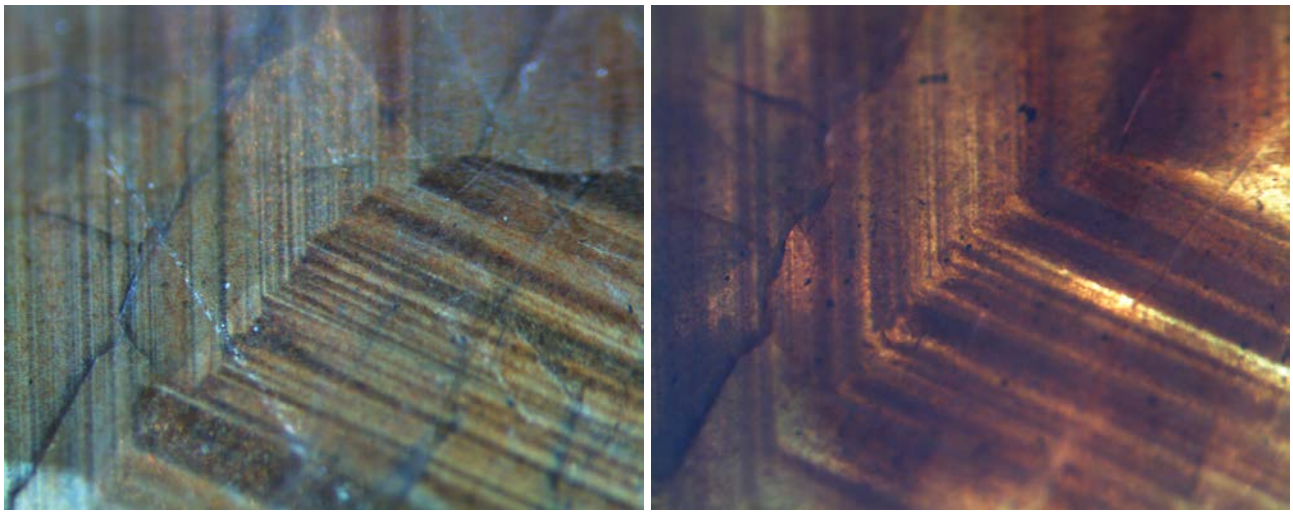

Figure 6: Colour zoning in this sapphire is characterized by different bronze colorations along the crystallographic directions of the corundum host (left, brightfield illumination). With transmitted light, the golden bronze-coloured bands appear dark and the brownish bronze-coloured bands are bright (right). This highlights variations in the concentration of needle and platelet inclusions along the c-axis. Photomicrographs by T. N. Bui; magnified 30×, field of view 4.76 × 3.81 mm.

7). Some of them were so large that they were visible to the naked eye, negatively affecting the appearance of the gemstone. The edges of these hexagonal-shaped inclusions were clearly parallel to the other inclusions and to the colour zoning.

The characteristics of the fractures within the sheen areas became more obvious when viewed with magnification. Their macroscopic 'dark vein' appearance correlated to the absence of inclusions around them. This indicates that these cracks were not created during the cutting of the stones. The absence of inclusions was evident only on one side of the fractures, characterized by a gradual increase in inclusion density away from the fractures. This asymmetry induced a colour gradient on one side leading up to the sharp boundary line of the fracture (Figure 8). This was easily observed with the naked eye in samples containing larger veins. Further microscopic investigations, combining brightfield and darkfield illuminations, showed a correlation between the asymmetry of the dark veins and the pattern of the associated fractures. The side of the dark vein presenting a concentration gradient of inclusions corresponded to the curvature direction

Figure 7: Black plates are present along with the network of needles and platelets in the Gold Sheen sapphires. These plates do not contribute to the sheen. Some of their borders are parallel to the orientation of the needles. Photomicrograph by K. Deliousi using transmitted light; magnified 80×, field of view 1.64 × 1.31 mm.

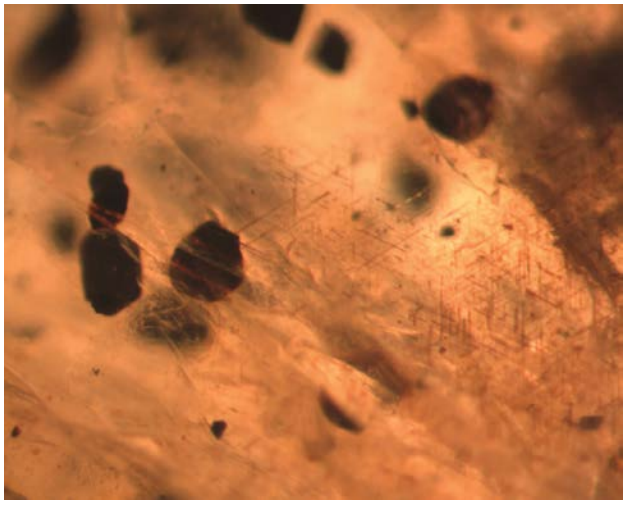

Figure 8: Surface-reaching fractures in the sheen area of the sapphires are characterized by asymmetric dark veins. Photomicrograph by K. Deliousi using brightfield illumination; magnified 25×, field of view 5.67 × 3.85 mm.

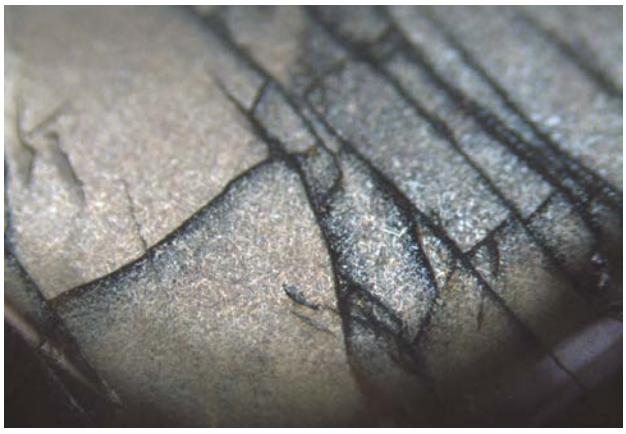

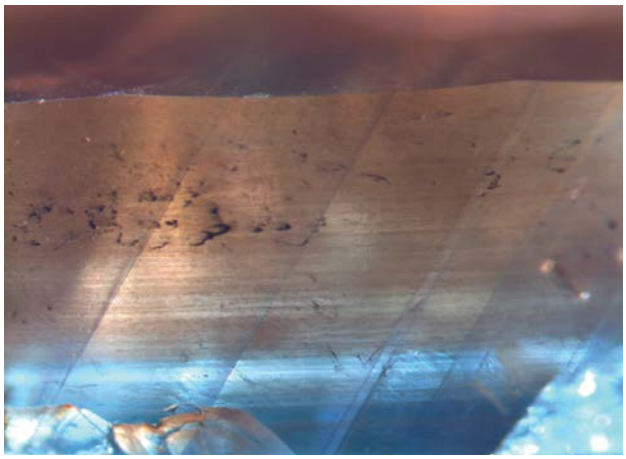

Figure 9: This view of the girdle of a Gold Sheen sapphire shows parallel brownish lines representing networks of needle and platelet inclusions along the basal pinacoid, and also a set of parallel lines (polysynthetic twin planes) oriented at about 58° and 32° to the basal pinacoid and the c-axis, respectively. Photomicrograph by T. N. Bui using darkfield illumination; magnified 30×, field of view 4.76 × 3.35 mm.

of the fracture. The distance along which the gradient extended was proportional to the slope of the fracture curvature. The asymmetric dark veins thus constituted an indirect mapping of the cracks underneath, shadowed by the inclusions.

Some samples showed a series of parallel lines when viewed at certain angles along the girdle profile (in a direction perpendicular to the c-axis). The angle between the lines and the basal pinacoid was 58° and that between the lines and the c-axis was 32° (Figure 9). These parallel lines are attributed to polysynthetic twin planes corresponding to the rhombohedral $\{10\bar{1}1\}$ faces of corundum. We observed parallel long white needles coincident with these twin planes when we looked through the table of the gemstones in a direction close to the c-axis (see Figure DD-2).

Due to the limited transparency of the gems, other solid inclusions were difficult to locate and identify. However, some surface-reaching inclusions in the lower-quality samples are described further below. In addition, planar assemblages of negative crystals corresponding to healed fractures were seen in some samples (e.g. Figures DD-3 and DD-4).

Chemical Composition

Qualitative EDXRF spectroscopy revealed the presence of the following trace elements in all 29 samples analysed: Fe, Ti, V, Cr, Ga, Nb and Ta. A relatively large amount of Fe suggested that this element was probably the main ingredient of the inclusions, especially in the networks of needles and platelets.

There was no obvious correlation between the blue body colour of some of the sapphires and the presence of Ti, as peaks of a similar intensity were also present in samples showing yellow and green body colours. Therefore, Ti could mainly be attributed to the inclusions. Other trace elements that are usually encountered as impurities in corundum include Ga, Nb and Ta; their concentrations varied in our samples.

Some of the sapphires, particularly those of low quality, contained additional trace elements including Zr, S, Ba, Cu, K, Na and Si. These may be attributed to various inclusions other than the metallic-appearing needles and platelets.

Inclusion Observations under High Magnification, and Raman Identification

Raman micro-spectroscopy is a powerful tool for identifying microscopic inclusions that are located at or near the surface of a gemstone (Bersani and Lottici, 2010; Kiefert and Karampelas, 2011). Since some inclusions had lateral dimensions of only a few microns, we used an optical magnification of 1,000× in order to obtain a laser spot of 1 µm. All of the analysed inclusions could be successfully identified by comparing their Raman spectra to those in the RRUFF database.

The high density of the inclusions responsible for the golden sheen makes them suitable for investigation through Raman spectroscopy. In most cases, the networks of needles and platelets reached the surface of the gems, or were less than 5 µm from the surface. Individual needles/platelets had such narrow thicknesses (less than 100 nm) that their surface-reaching cross-sections were extremely small to analyse, so it worked better to look for those that were located just under the surface. The particles selected for analysis had no intervening inclusions between them and the surface, nor ones situated directly below them. Therefore, the Raman spectra consisted exclusively of the superimposition of signals from both the sapphire and the inclusion. Figure 10a shows the spectrum of a host sapphire (α-Al_2O_3

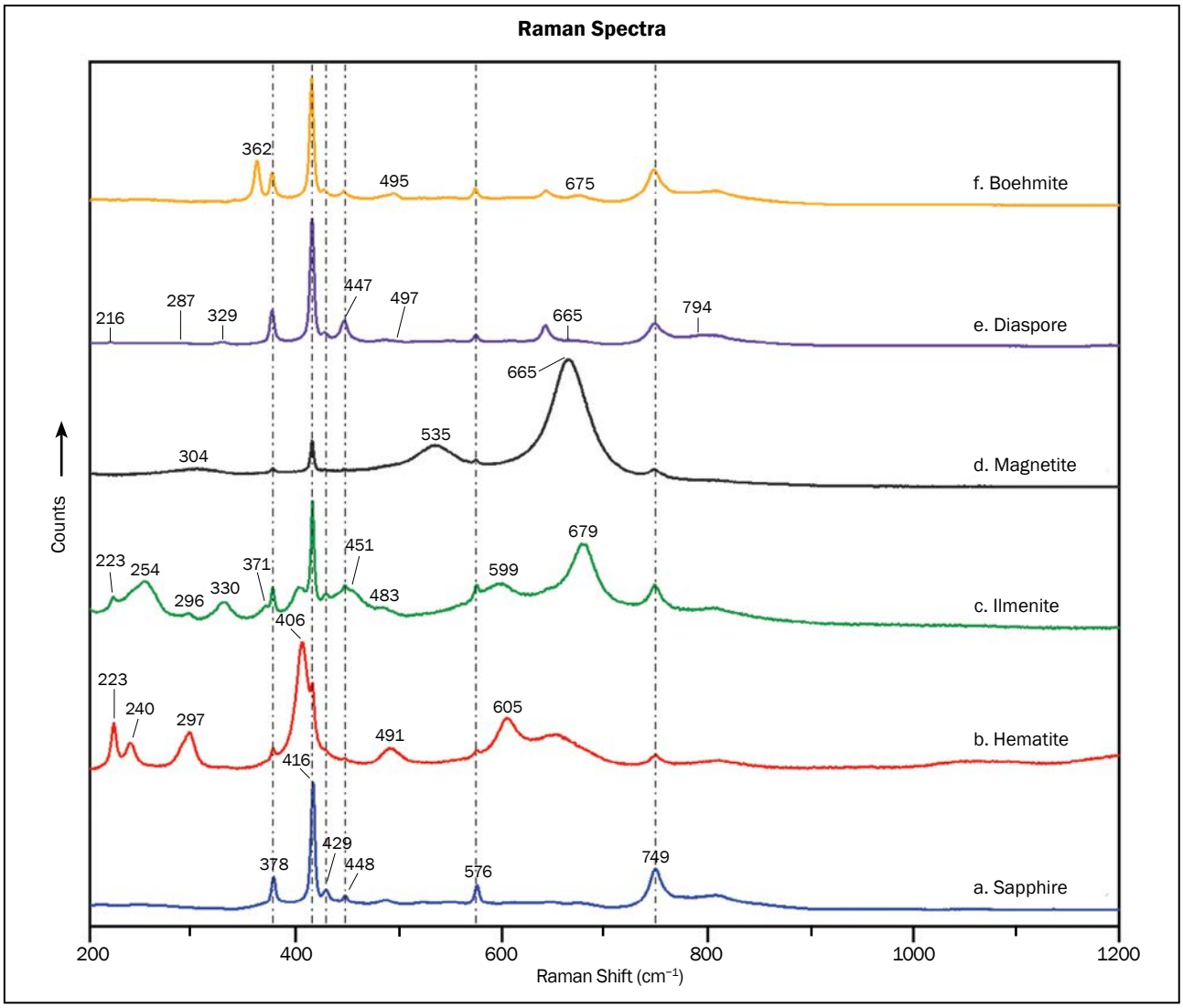

Figure 10: Raman spectra are shown for a host sapphire (a) and for various inclusions (b–f). The vertical dashed lines indicate the Raman peaks of corundum superimposed on those of the analysed inclusions. The two minerals present in the exsolved needles and platelets are hematite and ilmenite. Larger and thicker black plates were identified as magnetite. Diaspore and boehmite are the two polymorphs of AlO(OH) present in long white needles formed along the polysynthetic twin planes. (A peak that is present at 642 cm^{-1} in the spectra of both diaspore and boehmite is due to the A1g vibrational mode of the host corundum. These were the only spectra taken with the laser beam not perpendicular to the basal plane of the corundum.)

corundum), free of inclusions. In agreement with earlier studies (e.g. Xu et al., 1995), it includes peaks at 378, 416, 429, 448, 576 and 749 cm^{-1}.

The built-in optical microscope of the Raman micro-spectrometer, with magnifications from 200× to 1,000×, permitted us to identify some features that were barely distinguishable even when using the highest magnification of a typical gemmological microscope. Examples are provided by the needles and platelets illustrated in Figure 11. Several dark areas of various size and abundance were seen on many of the platelet inclusions. The duality of the colours within each inclusion suggested the presence of two different materials in the platelets. By contrast, in most cases the needles were of uniform colour, so they probably consisted of just one mineral. However, as the thickness of the needles increased, the probability was higher of observing colour inhomogeneities that may correspond to different minerals.

The platelets showed polygonal shapes with some of their edges parallel to the needles and other edges perpendicular to them. These edges were in turn parallel to the faces of the first- and second-order hexagonal prisms, {10$\bar{1}$0} and {11$\bar{2}$0},

Figure 11: The platelets and larger needles in the Gold Sheen sapphire consist of hematite and ilmenite (light and dark, respectively, in reflected light). The lighter areas (hematite) of the inclusions may display various colours due to thin-film interference from the nanometre-scale thickness of the inclusions. Two or more colours may be seen on the same platelet, indicating a variation in thickness (top right and bottom left). The darker areas (ilmenite) may also exhibit colour variations depending on thickness, but they are not as evident. Photomicrographs by T. N. Bui using brightfield illumination; magnified 1,000×, field of view 80 × 60 µm.

of the rhombohedral corundum host. The angles between two edges of the same polygon thus have the following possible values: 30°/150°, 60°/120° and 90°. Depending on the sample, the lateral dimensions of the platelets ranged from just a few to hundreds of micrometres. In SEM images, we observed a series of short white lines parallel to the basal pinacoid, corresponding to the needle-like and platelet inclusions. High magnification (100,000×) revealed the thickness of these inclusions was around 100 nm (Figure 12).

Raman micro-spectroscopy identified the smaller needles and the light-coloured areas of the platelets as hematite (α-Fe_2O_3), with the largest Raman peak at 406 cm^{-1} located near to that of sapphire, and other peaks recorded at 223, 240, 297, 491 and 605 cm^{-1} (Figure 10b). This is in good agreement with previous work on hematite (e.g. de Faria et al., 1997). Raman spectra of the dark areas of the platelets, characterized by a strong band at 679 cm^{-1}, were assigned to ilmenite ($FeTiO_3$); the other vibration modes describing this mineral were 223, 254, 296, 330, 371, 451, 483 and 599 cm^{-1} (Figure 10c). The obtained spectra are in good agreement with natural ilmenite for the main Raman peaks (e.g. Rull et al., 2004, 2007) and with pure synthesized ilmenite for the weaker Raman peaks (e.g. Sharma et al., 2009; Guan et al., 2013).

As mentioned previously, some black plates also were present in the golden sheen areas. The deep boundaries and terraces on the surfaces of these inclusions indicated that they are relatively thick (at the micron scale). Their

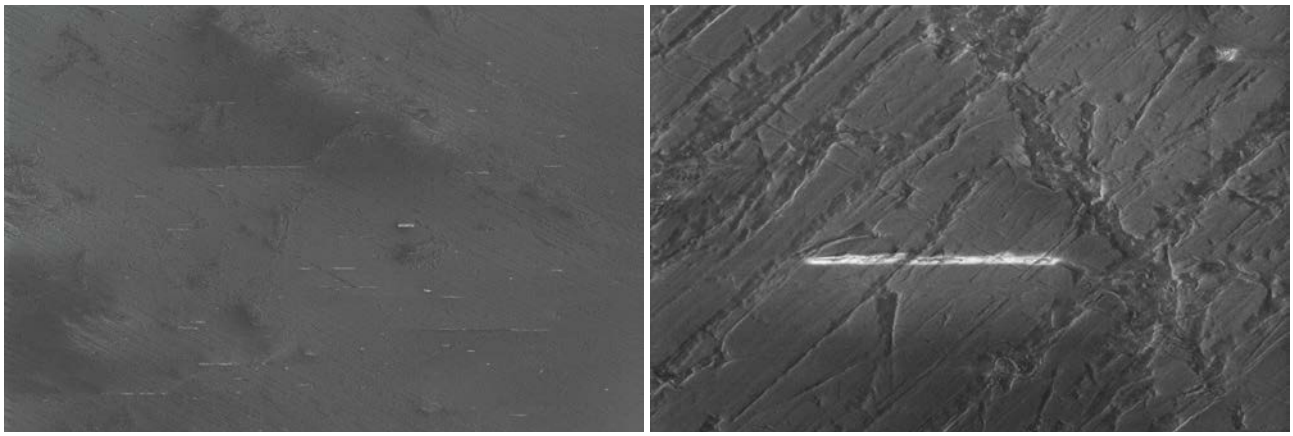

Figure 12: Cross-sections of platelet inclusions are observed in these SEM images taken from the girdle of a Gold Sheen sapphire. They appear as light grey thin parallel lines of various lengths at several levels along the c-axis (left). Closer examination of a single platelet inclusion (right) with the SEM shows that its thickness is 83 nm. Electron micrographs by T. N. Bui; magnified 2,000× (field of view 150 × 100 µm, left side), 20,000× (15 × 10 µm, right side).

lateral dimensions were generally greater than the hematite-ilmenite platelets. Observations with the Raman microscope confirmed their polygonal shape, with edges showing the same orientations as the platelets (Figure 13). Raman micro-spectroscopy identified these black inclusions as magnetite (Fe_3O_4), with three characteristic peaks at 304, 535 and 665 cm^{-1}, the latter being the strongest (Figure 10d). The obtained Raman spectra compared well to previous investigations on magnetite (de Faria et al., 1997).

The long needles lying along the polysynthetic twin planes were seen at high magnification to consist of tiny particles rather than a monocrystalline mineral. The concentration of these particles was higher toward the central core of the needle (Figure 14). Raman spectra obtained from different locations of several needles showed that the particles consisted of two polymorphs of aluminium oxide hydroxide. Most common was diaspore [α-AlO(OH)], with peaks at 216, 287, 329, 447 (strongest), 497, 665, 794 and 1191 cm^{-1} (Figure 10e). Occasionally, we found boehmite [γ-AlO(OH)], characterized by three Raman peaks at 362, 495 and 675 cm^{-1}, the first being the most intense (Figure 10f). All of these Raman features are in good agreement, for example, with a study on naturally occurring diaspore and synthesized boehmite (Ruan et al., 2001).

Several additional surface-reaching minerals were identified that did not contribute to the golden sheen: pyrite, baryte, covellite, zircon, muscovite, albite and K-feldspar. Photomicrographs and/or Raman spectra of these inclusions are provided in the Data Depository (Figures DD-5 to DD-7).

Discussion

Inclusions in the Gold Sheen Sapphires

The physical properties measured for the sapphires were not affected by the presence of their abundant inclusions. The concentration or weight of the inclusions was negligible in regard to the sapphire host, and the SG, RI and birefringence remained consistent with corundum. Optical microscopy highlighted the presence of a network of metallic-appearing needles and platelets and some larger black plates. Raman spectroscopy identified those inclusions as the Fe-Ti oxides hematite, ilmenite and magnetite. The presence of these inclusions in areas showing the golden sheen is consistent with the overall relatively high concentration of Fe (and Ti) in these sapphires.

The alignment of the colour zoning and the networks of hematite-ilmenite needles along the second- and first-order hexagonal prisms, $\{11\bar{2}0\}$ and $\{10\bar{1}0\}$ respectively, is consistent with previous studies of similar inclusions in black sapphires from Australia (Moon and Phillips, 1984). In that article, it was estimated from energy-dispersive spectroscopy that the exsolved inclusions consisted ~50% each of hematite and ilmenite. This is in reasonable agreement with high-magnification observations of the inclusions in our samples, although we noted a slightly higher amount of hematite (e.g. Figure 11).

Figure 13: Black plates in the Gold Sheen sapphires were identified as magnetite. The edges of the inclusions are aligned along the first- and second-order hexagonal prisms. Photomicrographs by T. N. Bui using brightfield illumination; magnified 500× or field of view 175 × 130 µm (top left, top right and bottom left) and 1,000× or 80 × 60 µm (bottom right).

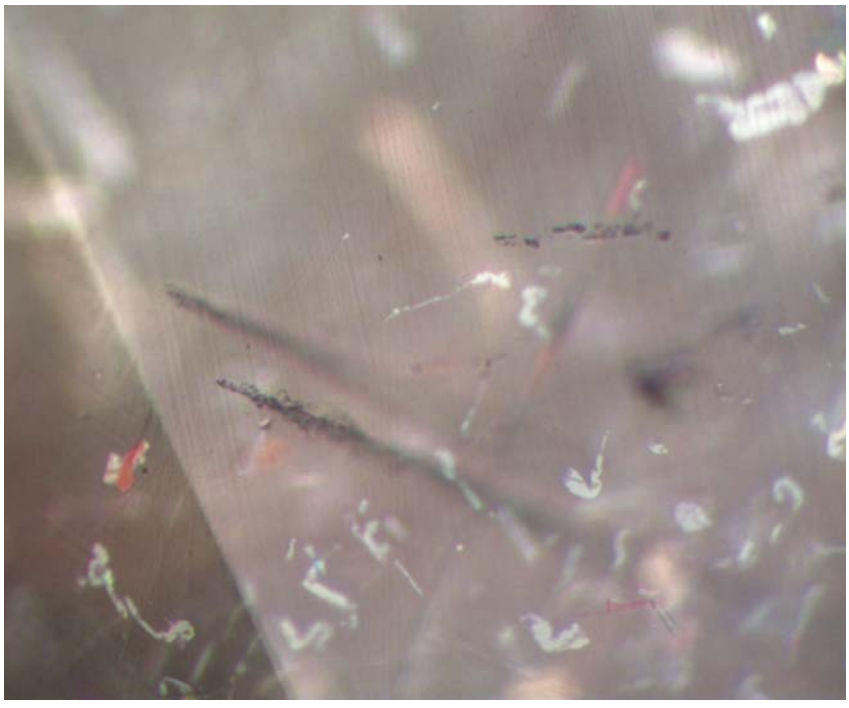

Figure 14: Needle-like inclusions consisting of diaspore and boehmite particles (appearing dark in brightfield illumination) lie along polysynthetic twin planes in the Gold Sheen sapphire. Photomicrograph by T. N. Bui; magnified 200×, field of view 360 × 300 µm.

As observed previously, in contrast to the needles, the edges of the platelets showing polygonal shapes were mostly parallel to both the first- and second-order hexagonal prisms of the host corundum. This difference highlights the preferential growth of the needles along the <10$\bar{1}$0> direction, probably due to the structural mismatch between the Fe-Ti oxides and corundum. The in-plane orientation of the hematite-ilmenite needles and platelets, and the similar crystal structure of hematite and ilmenite to corundum, suggest that the basal pinacoid direction of the inclusions and the host are parallel.

The edges of the magnetite plates had the same orientation as the hematite-ilmenite platelets. As shown in Figure 13, the magnetite plates commonly had triangular and hexagonal shapes. Since magnetite belongs to the spinel group, which crystallizes in the isometric crystal system, these shapes indicate a tetrahedral crystal habit.

Magnetite is known to be the most magnetic naturally occurring mineral. We tested the magnetism of the sapphires with neodymium-iron-boron magnets, and those containing large plates of magnetite were attracted to the magnets when the samples were floated in water (cf. Gumpesberger, 2006). A few low-quality sapphires possessing eye-visible magnetite inclusions were attracted to the magnets even without flotation (see Figure DD-8).

The Fe-Ti oxides and the diaspore-boehmite needles all formed in the sapphire as a result of epigenetic solid exsolution (cf. Hughes, 1997, pp. 93–94). Hematite, ilmenite and magnetite all have different chemical compositions, but they grew according to the crystallographic directions in the basal pinacoid of the host corundum. Such epigenetic inclusions crystallize due to the presence of defects and impurities of Fe and Ti in the host crystal as it cools after its formation (Hughes, 1997, pp. 93–94), forming microscopic needles and plate(let)s. The network of hematite-ilmenite inclusions in these sapphires is responsible for the asterism as well as the golden sheen.

As demonstrated above and verified through optical microscopy, the colour zoning in the sapphires is a consequence of the presence of hematite-ilmenite inclusions grouped into bands parallel to the second-order hexagonal prism {11$\bar{2}$0}. The resulting mechanical colour zoning is therefore linked to exsolution of these particles and also is epigenetic.

The dark-appearing veins following fractures in the Gold Sheen sapphires appear to have formed after the exsolution of Fe-Ti oxides. The exsolved inclusion particles evidently were not stable adjacent to (and on one side of) the fractures.

The presence of the long parallel white needles, identified as diaspore and boehmite, is correlated to the polysynthetic twin planes oriented in rhombohedral {10$\bar{1}$1} directions in the sapphire. In the literature, such inclusions are generally described as boehmite rather than diaspore (White, 1979; Hänni, 1987). Both diaspore and boehmite polymorphs of AlO(OH) were identified in our Raman spectra. They formed by the alteration of corundum at the intersections of two twin planes. Polysynthetic twin planes in corundum are created by mechanical stress after crystallization and are also known as slip twins (Hughes, 1997, p. 97). The angle of 58° between these twin planes and the basal pinacoid and 32° between the twin planes and the c-axis is consistent with the {10$\bar{1}$1} faces of the rhombohedral corundum.

Fe-Ti Oxide Inclusions in Other Gemstones

Plate-like inclusions of hematite and/or ilmenite also exist in other gem minerals. Their highly reflective surfaces produce optical effects such as aventurescence in oligoclase, often called *sunstone* (Gübelin and Koivula, 1986, pp. 165, 279; 2005, pp. 126, 413–415), and in cordierite (Gübelin and Koivula, 1986, pp. 163–164, 269; 2008, pp. 520–521). As in the Gold Sheen sapphires, the plate-like inclusions are parallel to the basal pinacoid. The cutting of the stones is such that the plates are oriented parallel to the girdle profile to highlight the optical effect. The abundance of the inclusions in the host also contributes to the body colour of the stones.

The aventurescence effect produces a kind of iridescence under oblique illumination, inducing various colours due to thin-film interference from the very thin plate-like inclusions. In oligoclase, beryl and cordierite, the inclusions are eye-visible, whereas in the Gold Sheen sapphires they are distinguishable

only with magnification. In the gems displaying aventurescence, the tiny reflective inclusions produce minute sparkles when the stone or the light source is moved. Gold Sheen sapphires display a golden shimmering effect originating from the specular reflections of light from the hematite-ilmenite inclusions. Instead of metallic single glitters, the microscopic network of oriented inclusions reflects light simultaneously, defining the golden sheen area. The smaller dimensions of the inclusions (below 100 µm) and their high concentration in the Gold Sheen sapphires account for the different appearances of the golden sheen and the aventurescence.

Comparison with Black Star Sapphires

Most cabochons of Gold Sheen sapphire display six-rayed asterism, similar to other star corundum. The presence of the asterism is dependent on the presence of oriented networks of hematite-ilmenite needles rather than platelets, and the sharpness of the star is determined by the aspect ratio of those needles. Since the hematite-ilmenite needles are perpendicular to the colour zoning, each ray of the star is, as a result, parallel to the colour zoning and to the second-order hexagonal prism $\{11\bar{2}0\}$. This optical characteristic is the same as that displayed by black star sapphires (Moon and Phillips, 1984; Hughes, 1997, p. 446). Those from Thailand, Australia and Laos are known to have inclusions caused by exsolution of hematite and ilmenite (Hughes, 1997, pp. 297, 380, 447).

In black 12-rayed star sapphires from Thailand, a less intense white six-rayed star is perpendicularly superimposed over a yellow/golden six-rayed star that originates from long, thin rutile needles aligned along the first-order hexagonal prism $\{10\bar{1}0\}$ (Hughes, 1997, p. 447). In our samples of Gold Sheen sapphire, no rutile needles perpendicular to the hematite-ilmenite needles were found by optical microscopy, and so far we have not encountered any 12-rayed stars in these cabochons.

Due to the high concentration of hematite-ilmenite inclusions in black star sapphires, some of these gems show basal parting on their flat base, characterized by a step-like appearance. Fractures due to this basal parting may be filled by residue from the dopping process during cutting (Hughes, 1997, pp. 125, 447). In Gold Sheen sapphires, no basal parting was seen in any of the cabochons. In a few faceted samples showing basal parting, the stones were completely opaque due to the high concentration of inclusions. As most Gold Sheen sapphires are translucent and not opaque, basal parting is not common.

Geological Inferences

Little information is available on the Gold Sheen sapphire deposit. According to the mine owner, it is located in eastern Kenya, near the border with Somalia. This area belongs to Kenya's North Eastern Province and has a low relief with an elevation less than 500 m. The climate is semi-arid, with desert scrub vegetation being most common. The geology of north-east and eastern Kenya is characterized by Mesozoic (Karoo) and Quaternary sedimentary rocks. The former includes Jurassic limestone, shale and gypsum, as well as Cretaceous siltstone, mudstone, limestone and sandstone. The Quaternary sediments are composed of lacustrine and fluvial deposits and gypsum. This entire region of East Africa is located on the Somali Plate, adjacent to the East African Rift and the Nubian Plate. Linear trends in the sedimentary rocks are orientated in relation to the Kenyan Dome (Mathu and Davies, 1996).

Kenya's previously known gem corundum deposits include the John Saul ruby mine located in Mangari (far south) and various other ruby and sapphire localities in the Mangari area, and the Turkana area in the north-western part of the country (Hughes, 1997, pp. 374–379; Shor and Weldon, 2009). To our knowledge, no corundum deposits have been reported in areas near Somalia.

The blue, green and yellow body colours of Gold Sheen sapphires are typical of magmatic-type corundum. Other magmatic deposits containing corundum with similar exsolved inclusions of Fe-Ti oxides are known from Australia (Anakie), Laos (Ban Huai Sai) and Thailand (Chanthaburi). The gemmological properties of black star sapphires from Australia and Thailand most closely resemble those of the Gold Sheen sapphire, including the high Fe content, lack of UV fluorescence, healed fractures and polysynthetic twinning. As there are no volcanic source rocks in the reported mining area for the Gold Sheen sapphires, their geological origin remains enigmatic.

Figure 15: Gold Sheen sapphires may create bold expressions in jewellery. The cabochon in this gold-plated silver pendant weighs 40–50 ct. Photo by T. K. Malik.

Conclusion

This article investigates the recently discovered Gold Sheen sapphires from East Africa, focusing on their peculiar golden sheen effect (e.g. Figure 15). Optical microscopy verified that the sheen is due to the reflection of light from an oriented network of exsolved needles and platelets of Fe-Ti oxides (hematite and ilmenite). The oriented needles also cause asterism (i.e. a six-rayed star) to be seen in cabochons cut from this sapphire.

Black star sapphires may contain similar oriented assemblages of exsolved Fe-Ti oxides. The main difference is the absence of rutile needles from the Gold Sheen sapphires, which explains the lack of 12-rayed asterism. Despite the presence of similar hematite-ilmenite inclusions in both types of sapphire, the large difference in their appearances suggests the need for further investigations into their optical phenomena.

An already-exhausted mine is the only known source of the Gold Sheen sapphires. Cutting of the existing stock of rough material is expected to fulfil market demand for the near future.

References

Bersani D. and Lottici P.P., 2010. Applications of Raman spectroscopy to gemology. *Analytical and Bioanalytical Chemistry*, **397**(7), 2631–2646, http://dx.doi.org/10.1007/s00216-010-3700-1.

de Faria D.L.A., Venâncio Silva S. and de Oliveira M.T., 1997. Raman microspectroscopy of some iron oxides and oxyhydroxides. *Journal of Raman Spectroscopy*, **28**(11), 873–878, http://dx.doi.org/10.1002/(sici)1097-4555(199711)28:11<873::aid-jrs177>3.3.co;2-2.

Guan X.-F., Zheng J., Zhao M.-L., Lia L.-P. and Li G.-S., 2013. Synthesis of $FeTiO_3$ nanosheets with {0001} facets exposed: Enhanced electrochemical performance and catalytic activity. *RSC Advances*, **3**(33), 13635–13641, http://dx.doi.org/10.1039/c3ra22125c.

Gübelin E.J. and Koivula J.I., 1986. *Photoatlas of Inclusions in Gemstones*. ABC Edition, Zurich, Switzerland, 532 pp.

Gübelin E.J. and Koivula J.I., 2005. *Photoatlas of Inclusions in Gemstones*, Vol. 2. Opinio Publishers, Basel, Switzerland, 829 pp.

Gübelin E.J. and Koivula J.I., 2008. *Photoatlas of Inclusions in Gemstones*, Vol. 3. Opinio Publishers, Basel, Switzerland, 672 pp.

Gumpesberger S.M., 2006. Magnetic separation of gemstones. *Gems & Gemology*, **42**(3), 124.

Hänni H.A., 1987. On corundums from Umba Valley, Tanzania. *Journal of Gemmology*, **20**(5), 278–284, http://dx.doi.org/10.15506/jog.1987.20.5.278.

Hughes R.W., 1997. *Ruby & Sapphire*. RWH Publishing, Boulder, Colorado, USA, 512 pp.

Kiefert L. and Karampelas S., 2011. Use of the Raman spectrometer in gemmological laboratories: Review. *Spectrochimica Acta Part A: Molecular and Biomolecular Spectroscopy*, **80**(1), 119–124, http://dx.doi.org/10.1016/j.saa.2011.03.004.

Laurs B.M., 2015. Gem Notes: 'Zawadi' sapphires. *Journal of Gemmology*, **34**(5), 393.

Mathu E.M. and Davies T.C., 1996. Geology and the environment of Kenya. *Journal of African Earth Sciences*, **23**(4), 511–539, http://dx.doi.org/10.1016/s0899-5362(97)00016-x.

Moon A.R. and Phillips M.R., 1984. An electron microscopy study of exsolved phases in natural black Australian sapphire. *Micron and Microscopica Acta*, **15**(3), 143–146, http://dx.doi.org/10.1016/0739-6260(84)90044-3.

Ruan H.D., Frost R.L. and Kloprogge J.T., 2001. Comparison of Raman spectra in characterizing gibbsite, bayerite, diaspore and boehmite. *Journal*

of Raman Spectroscopy, **32**(9), 745–750, http://dx.doi.org/10.1002/jrs.736.

Rull F., Martinez-Frias J., Sansano A., Medina J. and Edwards H.G.M., 2004. Comparative micro-Raman study of the Nakhla and Vaca Muerta meteorites. *Journal of Raman Spectroscopy*, **35**(6), 497–503, http://dx.doi.org/10.1002/jrs.1177.

Rull F., Martinez-Frias J. and Rodríguez-Losada J.A., 2007. Micro-Raman spectroscopic study of El Gasco pumice, western Spain. *Journal of Raman Spectroscopy*, **38**(2), 239–244, http://dx.doi.org/10.1002/jrs.1628.

Sharma Y.K., Kharkwal M., Uma S. and Nagarajan R., 2009. Synthesis and characterization of titanates of the formula $MTiO_3$ (M = Mn, Fe, Co, Ni and Cd) by co-precipitation of mixed metal oxalates. *Polyhedron*, **28**(3), 579–585, http://dx.doi.org/10.1016/j.poly.2008.11.056.

Shor R. and Weldon R., 2009. Ruby and sapphire production and distribution: A quarter century of change. *Gems & Gemology*, **45**(4), 236–259, http://dx.doi.org/10.5741/gems.45.4.236.

White J.S., 1979. Boehmite exsolution in corundum. *American Mineralogist*, **64**(11–12), 1300–1302.

Xu J.-A., Huang E., Lin J.-F. and Xu L.Y., 1995. Raman study at high pressure and the thermodynamic properties of corundum: Application of Kieffer's model. *American Mineralogist*, **80**(11–12), 1157–1165.

The Authors

Thanh Nhan Bui
Boulevard Edmond Machtens 180
1080 Brussels, Belgium
Email: tnhan93@gmail.com

Katerina Deliousi and Dr Katrien De Corte
HRD Antwerp, Institute of Gemmology
Hoveniersstraat 22, 2018 Antwerp, Belgium

Tanzim Khan Malik
Genuine Gems & Jewellery Co. Ltd.
316/9 Silom Road, Bangkok 10500, Thailand

Acknowledgements

The authors thank Dr Ellen Biermans and Ellen Barrie for EDXRF spectroscopy data. They are also grateful to Dr Ferran Ureña from the Catholic University of Louvain (Louvain-la-Neuve, Belgium) for the micro-Raman spectroscopy data. They express their sincere gratitude to Yiannis Karvelis for proofreading the English text.

Age Determination of Zircon Inclusions in Faceted Sapphires

Klemens Link

The age determination of zircon inclusions in faceted sapphires by LA-ICP-MS may provide a valuable tool to support geographical origin determination. In this initial study, U-Pb dating of a zircon inclusion in a pink sapphire from Madagascar yielded an age of 650 million years (Ma), suggesting a syngenetic origin (i.e. formed at the same time as the host sapphire) of the zircon. In a greenish blue sapphire from Madagascar, an included zircon yielded a U-Pb age of 1,750 Ma, pre-dating the host sapphire, and therefore indicating the zircon is an inherited inclusion (i.e. it originated from rocks that existed before the host sapphire crystallized). These results are supported by indications provided from conventional methods of geographical origin determination. This article also discusses the potential influence on U-Pb age dating of post-formation metamorphic events, laboratory heat treatment and the possibility of complex zoning in the zircon inclusions.

The Journal of Gemmology, 34(8), 2015, pp. 692–700, http://dx.doi.org/10.15506/JoG.2015.34.8.692

Introduction

Laser ablation–inductively coupled plasma–mass spectrometry (LA-ICP-MS) has become an established tool in the past decade for use by prominent well-equipped gemmological laboratories (Breeding et al., 2010). Standard routines have been developed to measure trace-element concentrations in various gem materials to detect treatments and/or determine a stone's geographical origin (e.g. Günther and Kane, 1999; Guillong and Günther, 2001; Abduriyim and Kitawaki, 2006). The geographical origin of high-end coloured stones is seen by the trade as a key value driver, and has developed into one of the main tasks for gem-testing laboratories. Initially LA-ICP-MS was mainly applied to research samples, but with increasing experience and confidence, as well as improved instrumentation, this technique is now routinely used for analysing client-submitted stones. The biggest challenge and the highest priority are to gain meaningful data without damaging or affecting the quality of the stone (i.e. to work quasi-non-destructively).

LA-ICP-MS is a well-established and frequently used method in the geosciences for measuring *in situ* uranium-lead (U-Pb) ages of zircon (e.g. Jackson et al., 2004). Microscopic crystals or grains of zircon can be dated regardless of their host matrix, provided that they reach the surface of the stone and thus can be sampled by the instrument's laser beam.

Zircon inclusions in rough gem-quality corundum have been investigated by numerous researchers using LA-ICP-MS (e.g. Coenraads

Figure 1: These Sri Lanka and Madagascar sapphires are typical candidates for hosting zircon inclusions that could be used for age determination to better characterize their origins. The stones range between 1.4 and 29.7 ct, and are unheated with the exception of the yellow sapphire on the left. Photo by K. Link.

et al., 1990; Sutherland et al., 2008; 2015), and recently the technique was used to perform U-Pb age dating of blue sapphires from Myanmar, Madagascar and Sri Lanka that were sawn and polished to expose zircon inclusions on their surface (Elmaleh et al., 2015). However, determining the age of zircon inclusions in high-quality faceted gemstones such as those commonly submitted to gem labs (e.g. Figure 1) has not been reported until now. Since July 2015, this procedure has been routinely applied to client stones at the Gübelin Gem Lab (GGL) when zircon inclusions are exposed on the surface and age data is particularly helpful for origin determination (e.g. for separating some blue sapphires from Myanmar and Madagascar). It can also provide indications of heat treatment.

Age data for zircon inclusions in sapphires can shed light on the genetic conditions under which the sapphire formed, as well as point to the original host rocks. The latter is particularly important for sedimentary deposits without any connection to their primary host rocks, such as the economically important Ilakaka mining region in south-western Madagascar (Rakotondrazafy et al., 2008).

Materials and Methods

The samples comprised two faceted fancy-colour sapphires (pink and greenish blue; see Figure 2), each weighing ~12 ct, that were submitted to the Gübelin Gem Lab in Lucerne by professional gem traders. Both samples contained zircon inclusions that reached the surface at the girdles, and routine origin determination procedures performed in our laboratory clearly indicated that both stones were from metamorphic-type deposits in Madagascar. The pink sapphire had clusters of small, colourless, rounded anhedral zircon that each measured a maximum 60 µm long and 30 µm wide (Figure 3a). Although heat treatment at relatively low temperatures could not be excluded, the stone clearly had not been exposed to high-temperature heating. The greenish blue sapphire, which was found to be untreated, contained randomly scattered zircon inclusions with subhedral elongated shapes (e.g. Figure 3b,c). The investigated zircon crystal in the greenish blue sapphire was ~90 µm long and 35 µm wide.

To avoid leaving eye-visible traces from LA-ICP-MS analysis, client stones are typically sampled

Figure 2: These pink and greenish blue sapphires (each ~12 ct) were submitted to the Gübelin Gem Lab in 2015. Both sapphires had surface-reaching zircon inclusions on their girdles, so age determination could be conducted. Photos by Janine Meyer, GGL.

Figure 3: (a) In this cluster of zircon inclusions within the pink sapphire, the surface-reaching zircons that were analysed for age determination are circled. (b) Internal features in the greenish blue sapphire consist of isolated zircon crystals (top-centre and top-right), among other inclusions. (c) This zircon inclusion in the greenish blue sapphire was used for in situ *age determination; the circle marks the position and size of the applied laser pit. Photomicrographs (a) and (c) by Klaus Schollenbruch, GGL; (b) is courtesy of Bulgari, image width ~2 mm.*

with the laser only on their girdle (with some exceptions). The pit diameter must not exceed 50–70 µm, and the depth of the pit usually does not exceed its diameter. The resulting pits are not eye visible and have no significant effect on the weight of the stone.

For the U-Pb age dating of zircon inclusions in sapphires, to avoid sampling the corundum host, the LA-ICP-MS signal is carefully controlled for any sudden change in indicative elements such as Si or Zr. Although corundum usually does not contain significant U or Pb, and slightly ablating the host sapphire therefore should not disturb the results, we are sure to avoid any such possible contamination. For both samples described here, the spot diameter of the laser was limited to 30 µm by the size of the outcropping zircon inclusions (Figure 3), and this limited the depth of the pits to ~30 µm as well. The weight loss of the samples after analysis was calculated to be only approximately 0.000004 ct.

The analytical conditions used for this study are listed in Table I. The LA-ICP-MS system at the Gübelin Gem Lab consists of an ESI NWR193^{UC} ArF excimer-based UV laser ablation system with a large-format sample chamber and a flexible cup that collects the ablated material, which is coupled with a PerkinElmer ELAN DRC-e quadrupole ICP mass spectrometer (Figure 4). The laser has a wavelength of 193 nm, which allows precise ablation at the micrometre scale without cracking or splintering the sample. The ablated

Table I: LA-ICP-MS analytical parameters.

Laser	**NWR193^{UC} from ESI**
System	193 nm ArF excimer laser
Sample cell	High-performance two-volume chamber system
Sample carrier gas	1,000 ml/min He
Laser pulse rate	14 Hz
Laser energy	6.3 J/cm^2
ICP-MS	**PerkinElmer ELAN DRC-e quadrupole ICP-MS**
Auxiliary gas	0.66 l/min Ar
Nebulizer gas	0.675 l/min Ar
Plasma gas	16.5 l/min Ar
RF power	1,350 W

Figure 4: The instrumentation at the Gübelin Gem Lab used for this study consists of an ICP-MS (left side) and a laser ablation unit (right side). Photo by K. Link.

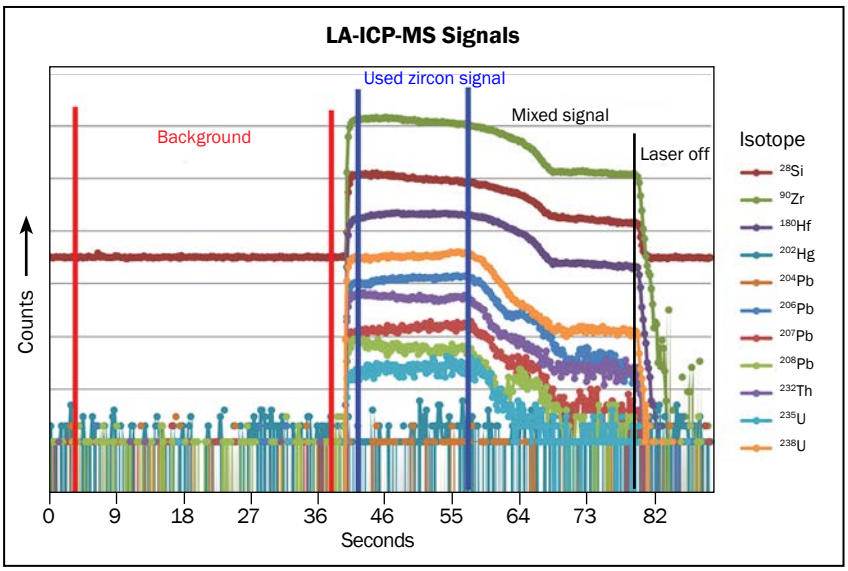

Figure 5: This diagram shows the raw signals for various isotopes obtained during the ablation of the zircon inclusion in the greenish blue sapphire. The portions used for data reduction are marked in red and blue.

material is transported in a flow of He carrier gas to the Ar plasma of the mass spectrometer. Within the plasma, the 60–150 nm-sized particles are disintegrated at ~7,000°C into ions that are selectively detected by the mass spectrometer.

The optimal laser conditions were found by monitoring the U-Pb ratios and searching for the minimum deviation to reduce the errors in age calculations. The dwell times for individual mass scans were 10 milliseconds for all measured isotopes (^{28}Si, ^{90}Zr, ^{180}Hf, ^{202}Hg, ^{204}Pb, ^{206}Pb, ^{207}Pb, ^{208}Pb, ^{232}Th, ^{235}U and ^{238}U). The background was analysed for 40 seconds, and the ablation signal from the zircon was measured until it became unstable after around 15 seconds (Figure 5). Only the area of the signal showing a flat plateau was used for integration. A Plesovice zircon (Sláma et al., 2008) was used for standardization; a GJ zircon (Jackson et al., 2004) and an in-house reference zircon were used for quality control.

For age determination (see Box A and Table II), ^{207}Pb/^{235}U ratios were calculated from the measured ^{206}Pb/^{238}U and ^{207}Pb/^{206}Pb ratios using a constant value for present-day ^{235}U/^{238}U. The ICP-MS was optimized on a daily basis for a maximum sensitivity to heavy elements with minimum (<0.5%) oxide generation (monitored using Th/ThO). Data reduction and the time-dependent laser- and mass spectrometer-induced inter-element mass fractionation (Pb/U) corrections were applied using in-house Microsoft Excel worksheets. Ages, errors (2σ) and concordia diagrams were produced using Isoplot3 macros for Excel (Ludwig, 2003).

Common lead was monitored via non-radiogenic ^{204}Pb, and ^{202}Hg was checked to estimate the interference of ^{204}Hg on ^{204}Pb. For both samples, ^{204}Pb was below the detection limit, so we assumed that no common lead was present.

Results and Discussion

The results of U-Pb age dating of the zircon inclusions are presented in Table II and shown in Figure 6.

Pink Sapphire

The analysed zircon from the inclusion clusters in the pink sapphire yielded a concordant U-Pb age of 652 ± 41 Ma (Figure 6a). From the appearance of the zircon inclusions, they are interpreted as syngenetic with the host sapphire, and are considered to be in equilibrium with the corundum. Thus, the age we obtained should correspond to the formational age of this sapphire. The crystallization ages of the sapphires from Madagascar are not yet well known, but published work (e.g. Rakotondrazafy et al., 2008, and references therein) indicates ages around 560 Ma. Associated granulite- and amphibolite-facies rocks and linked felsic intrusives cluster between 560 and 650 Ma (Kröner et al., 1999). The basement rocks of Madagascar were affected by the Pan-African tectono-metamorphic event (730–550 Ma; Black and Liegeois, 1993), which extended across a broad region that included other sapphire-bearing areas such as East Africa

Box A: Zircon Geochronology

Zircon ($ZrSiO_4$) is a mineral of great benefit for geochronologists. It occurs in nearly all rock types and is very resistant to physical abrasion as well as thermal alteration. In addition, zircon has no or only limited susceptibility to chemical diffusion with its environment under most conditions in the earth's crust. The zirconium cations (Zr^{4+}) in the crystal lattice have an ionic radius that is only about 15% less than uranium ions (U^{4+}), so uranium is somewhat compatible in zircon and can be incorporated up to a few hundred parts per million. Lead cations (Pb^{2+}) are around 50% larger, so that they are far too big for zircon's crystal structure and therefore highly incompatible. Any Pb that may have been incorporated during zircon formation is ideally below the detection limit of LA-ICP-MS.

Starting at the time the zircon is formed, U isotopes undergo radioactive decay to form Pb daughter isotopes ($^{235}U \rightarrow {}^{207}Pb$ and $^{238}U \rightarrow {}^{206}Pb$) according to their decay constants. Measuring the radiogenic Pb allows one to precisely calculate the formation age of the zircon. The two measurable radioactive U isotopes provide two independent radioactive systems ('clocks'). This gives valuable information for determining the plausibility of the calculated ages. If both systems yield the same ages within their errors, the age can be considered as robust or concordant (i.e. it can be assumed that the isotopic system was not disturbed by any chemical or physical process after zircon formation). A good way to visualize and validate U-Pb ages is with a *concordia* diagram, as introduced by Wetherill (1956; see Figure 6 in the text of this article). The concordia diagram plots the isotopic ratios of the two radioactive systems $^{206}Pb/^{238}U$ versus $^{207}Pb/^{235}U$. All possible concordant ages plot along a concordia curve in the centre of the plot. Samples with older ages (higher radiogenic lead and lower radioactive uranium, leading to higher Pb/U ratios) plot further to the top and right on the curve, and younger samples plot toward the bottom left. The different decay constants for the two radioactive systems cause the curved shape. The age including the errors (typically 2σ) is presented as an ellipse in the diagram. The ratios and the sizes of the individual errors define the form, size and orientation of the ellipse. Disturbances of the isotopic system in the zircon corresponding to episodic or continuous Pb diffusion out of the system will cause a sample to plot on a straight *discordia* line. Such values plot below the concordia curve, between the original formational age of the zircon and a younger age-disturbing event.

Using the ratio in the decay constants between ^{238}U and ^{235}U, and assuming that a zircon did not incorporate any common lead during its formation, it is possible to combine the two isotopic U-Pb systems by simply taking the ratio of the two daughter isotopes $^{207}Pb/^{206}Pb$, as this ratio is only a function of time. The Pb-Pb ages can be quite useful since they do not depend on measuring the ratios of two different elements (U and Pb). Besides requiring fewer fractionation corrections, this method allows one to validate the concordance of U-Pb ages and to obtain ages even for disturbed systems, as such processes would affect only the element ratios (U/Pb) and not the isotopic ratios (Pb/Pb). The Pb-Pb ages are particularly important for very old time scales. For extra assurance, Pb-Pb ages are commonly considered minimum ages.

and Sri Lanka, and led to the formation of the so-called Mozambique Belt. More research is needed on Madagascar and other Pan-African-related sapphire age populations before using them as hard criteria for origin determination.

Greenish Blue Sapphire

The zircon analysed in the greenish blue sapphire gave a concordant age of 1,742 ± 70 Ma (Figure 6b). The individual ages given in Table II for the various isotopic pairs ($^{207}Pb/^{235}U$, $^{206}Pb/^{238}U$

Table II: Geochronological results for zircon inclusions in the two sapphires.

Data	$^{207}Pb/^{235}U$	± 1σ	$^{206}Pb/^{238}U$	± 1σ	$^{207}Pb/^{206}Pb$	± 1σ	roh[a]
Pink sapphire	0.9003	0.045	0.1064	0.0056	0.0617	0.0019	0.94
Greenish blue sapphire	4.5779	0.212	0.3144	0.0202	0.1074	0.0051	0.72
Age (Ma)	$^{207}Pb/^{235}U$	± 2σ	$^{206}Pb/^{238}U$	± 2σ	$^{207}Pb/^{206}Pb$	± 2σ	prob[a]
Pink sapphire	651	32	651	34	663	20	0.99
Greenish blue sapphire	1745	80	1762	112	1755	86	0.82

[a] Abbreviations: roh = error correlation between $^{207}Pb/^{235}U$ and $^{206}Pb/^{238}U$ ratios; prob = probability of concordance (taken from Isoplot).

and $^{207}Pb/^{206}Pb$) show a slightly greater variance than those from the pink sapphire, but within their errors they provide good matches with the integrated concordia age, and correspond to an 82% probability of concordance. The reasons for the slightly varying individual ages may be related to post-formation diffusion processes, elemental zoning (see below), or slight differences in the accuracy or precision of measuring the various isotopes.

The ~1,740 Ma age does not coincide with the assumed Pan-African-associated formation of this Madagascar sapphire. Hence, this subhedral zircon is more complicated to interpret (see below).

Influence of Post-Formation Metamorphism on Zircon

Once a zircon has crystallized, very high pressure-temperature conditions are required to destroy it (Watson, 1996). The closure temperature of zircon, which is above 900°C at most geologically relevant time scales (Cherniak and Watson, 2003), marks the condition at which diffusion becomes sufficient to exchange U and/or Pb, and therefore disturb the U-Pb system and thus the age determination. In most cases, temperatures during metamorphism are less than 1,000°C (i.e. combined with high pressures, as with upper granulite facies conditions). Since the Pb content of zircon is preserved through all but the most extreme conditions of metamorphism, its original formation age is usually not disturbed by such events (Watson, 1996). However, depending on the duration of a high-temperature metamorphic event, there may be a severe impact on the zircon (Blackburn et al., 2011). Uranium is rather compatible in the zircon structure, whereas Pb is not (Cherniak and Watson, 2003). Increasing temperatures drive recrystallization processes as well as diffusion rates (Nasdala et al., 2001). This leads to enhanced Pb diffusion toward the outer rim or completely out of the zircon. The loss of

Figure 6: Concordia plots made with Isoplot software (Ludwig, 2003) are shown for the zircon inclusions in the pink sapphire (a) and the greenish blue sapphire (b).

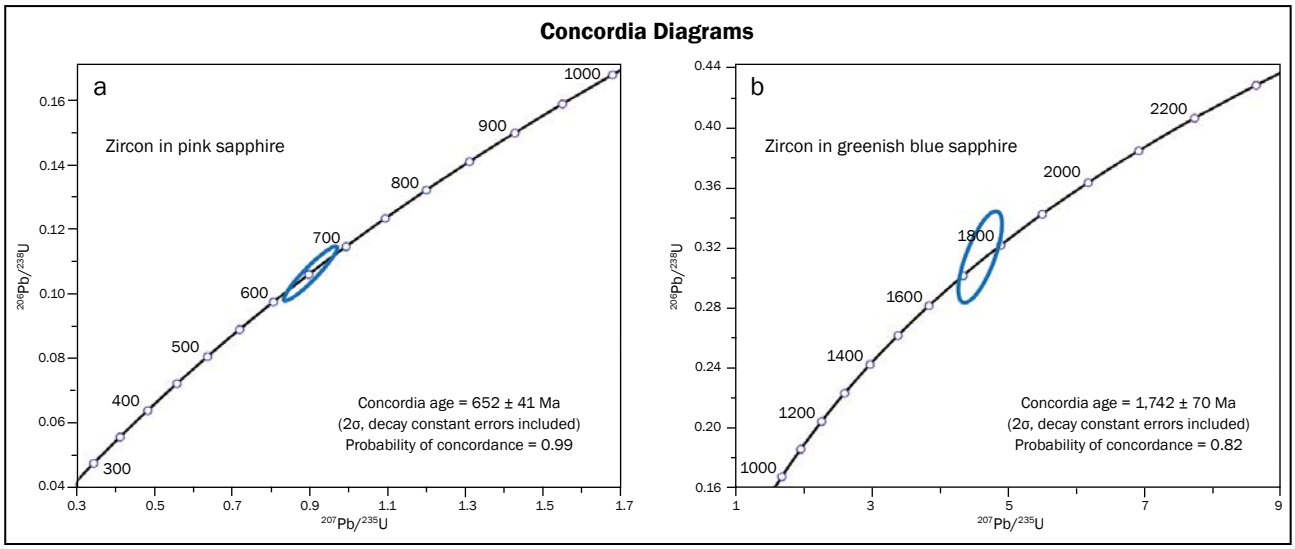

(radiogenic) Pb changes the U/Pb ratio and resets the 'radiogenic clock'. This may be visualized in a concordia diagram (described in Box A), in which the so-called concordia line in the centre of the plot shows the U-Pb ratios for undisturbed, 'closed' systems where all the Pb originates from U decay. Disturbed U-Pb ratios result in combined ratios lying below the concordia on a line called the discordia which leads toward younger ages. In an ideal case, the discordia points to the age of the event that 'opened' the U-Pb system (Dickin, 2005). If the measured U-Pb data plot nicely on the concordia, it can be assumed that the U/Pb ratios were undisturbed by later events such as metamorphism.

Rocks affected by the Pan-African event were tectonically overprinted under amphibolite- to granulite-facies pressure/temperature conditions. Nevertheless, old inherited zircons that preserve the age of the rocks before the intense deformation are well known in the literature (e.g. Kröner et al., 1999). The 1,742 Ma age we obtained for the zircon inclusion in the greenish blue sapphire coincides with the age of zircons possibly derived from granulites found, for example, in southern Madagascar (Kröner et al., 1999). These granulites are interpreted to have formed at 1,740 Ma and to have been later tectonically overprinted during the Pan-African event. The somewhat rounded, resorbed-appearing morphology of the zircon inclusions in this sapphire supports an inherited (protogenetic) origin for these crystals (cf. Corfu et al., 2003). If this is correct, then these zircon inclusions must have been derived from the host rock and trapped in the corundum during its crystallization. Although proving such a scenario is beyond the scope of this article, it does fit well with the Madagascar origin of this sapphire. This is further supported by zircon inclusions in sapphires from Madagascar that have been previously described as ranging around 1,500 Ma (Elmaleh et al., 2015). In addition, the author is not aware of a similar published age for the other potential areas of origin such as Sri Lanka and East Africa.

Potential Effect of Heat Treatment

It is well known that sapphires are commonly heat treated to enhance their appearance. What is the effect of heat treatment on the calculated U-Pb age of their zircon inclusions?

Previous experiments indicate that sapphire heat treatment has an effect on the crystallinity of zircon inclusions — depending on temperature and time — although the extent of this effect is a matter for debate (Nasdala et al., 2001; Wang et al., 2006). Furthermore, it is not clear if or to what extent Pb loss in a diffusive process is measurable for these heated stones. Zircon heating experiments have been done to investigate the amount of Pb loss due to diffusion. Cherniak and Watson (2003) claimed that below 1,200°C, the time to reach 1% Pb loss in an effective 10 µm zone exceeds one year. More relevant is the temperature range between 1,200°C and 1,450°C. At these temperatures, measurable Pb loss can be assumed for heating periods of less than one day (Cherniak and Watson, 2003). Also, the diffusion rate may increase due to strong radiation damage in metamict zircon. Above 1,400°C, zircon ($ZrSiO_4$) becomes unstable and partially melts to form baddeleyite (ZrO_2) and silicate-rich phases (Wang et al., 2006; Váczi et al., 2009). More experiments in the range of 1,200–1,400°C are required to better quantify the diffusive effect on Pb in zircon.

Therefore, sapphire heat treatment may to some extent lead to Pb loss from zircon inclusions. As this does not consider the lifetime of the various U-Pb decay systems, the decay loss must result in an effect similar to natural Pb loss from high-temperature metamorphism. Thus the U-Pb ages of zircon inclusions in heated sapphires would be expected to plot beneath the concordia curve and follow linear trends towards younger ages. Conversely, this implies that concordant-plotting zircons most probably were not exposed to high-temperature heat treatment. U-Pb data that plot discordantly could be the result of exposure to either intense laboratory heat treatment or natural high-temperature metamorphism. Even apparently concordant-plotting zircons may to a minor extent be affected by Pb loss (their error ellipses plot on the concordia line, but the true ages within the ellipses can be slightly discordant). In such cases, the calculated ages represent minimum ages.

With a calculated probability of concordance of 99% (Table II), the zircon in the pink sapphire clearly yielded a concordant age. The age obtained from the zircon in the greenish blue sapphire was 82% concordant, so despite the

high level of confidence there is some possibility of slight discordance. As heat treatment of that sapphire could be excluded, this may be due to tectono-metamorphic events that the zircon was exposed to after its formation and before being trapped in the sapphire.

Highly Zoned Zircons

A potential complication for age dating could be caused by complexly zoned zircons, in which the varying zones represent different times of formation. If the zones with different ages are smaller than the spatial resolution of the laser spot, then mixed ages would result. In the concordia diagram, such results may plot similarly to zircons that have experienced Pb loss. In some cases, different growth zones might be indicated by sudden trace-element concentration changes in the mass spectrum during ablation. If available, cathodoluminescence (CL) imaging is the most powerful tool to identify these zones. The minimum spot size of the LA-ICP-MS instrument (and ion probes such as SIMS or SHRIMP) is around 10–15 µm in diameter, depending on the amount of U and Pb in the zircons, thus dictating the minimum homogeneous zone in a zircon that is required for a 'good' age determination. The zircon inclusions analysed for this article showed no evidence of multiphase mineral formation (i.e. there were no sudden variations in trace-element composition during the analyses).

Conclusions

LA-ICP-MS is effective for determining the age of zircon inclusions, even in valuable faceted stones, without damaging the host sapphire. The limiting conditions are the technical capabilities of the analytical devices on one hand and the characteristics of the zircon inclusions on the other (i.e. the sapphire must contain surface-reaching zircons, preferably on the girdle, that are large enough to analyse and lack fine-scale chemical zoning). The dating methods are applicable to any gemmological laboratory operating a LA-ICP-MS. Age data for zircon inclusions in sapphires provides useful information for origin determination, and can in some cases indicate the crystallization age of the host sapphire. Zircon ages that far exceed the inferred age of the surrounding sapphire can also provide valuable information. Depending on the error ranges, it may be more dependable to consider the data as minimum ages rather than the exact time of formation. This especially applies to those stones where heat treatment cannot be excluded. Although a discordant U-Pb age may be the consequence of a high-temperature (i.e. >1,200°C) heat treatment that was applied for a relatively long period, such discordance might also indicate that a high-grade metamorphic overprint caused loss of Pb and possibly U, or even point to a mixed age from sampling a complexly zoned zircon inclusion.

Although the routine age determination of zircon inclusions in sapphire is not yet frequently accomplished in gemmological laboratories, it is expected that this procedure will become more common in the future as LA-ICP-MS instrumentation becomes more available and better constraints are obtained on the ages of sapphires and their host rocks. It may even become an additional service requested by clients in addition to origin determination.

References

Abduriyim A. and Kitawaki H., 2006. Determination of the origin of blue sapphire using laser ablation inductively coupled plasma mass spectrometry (LA-ICP-MS). *Journal of Gemmology*, **30**(1–2), 23–36, http://dx.doi.org/10.15506/jog.2006.30.1.23.

Black R. and Liegeois J.-P., 1993. Cratons, mobile belts, alkaline rocks and continental lithospheric mantle: The Pan-African testimony. *Journal of the Geological Society*, **150**(1), 89–98, http://dx.doi.org/10.1144/gsjgs.150.1.0088.

Blackburn T., Bowring A., Schoene B., Mahan K. and Dundas F., 2011. U-Pb thermochronology: Creating a temporal record of lithospheric thermal evolution. *Contributions to Mineralogy and Petrology*, **162**(3), 479–500, http://dx.doi.org/10.1007/s00410-011-0607-6.

Breeding C.M., Shen A., Eaton-Magaña S., Rossman G.R., Shigley J.E. and Gilbertson A., 2010. Developments in gemstone analysis techniques and instrumentation during the 2000s. *Gems & Gemology* **46**(3), 241–257, http://dx.doi.org/10.5741/gems.46.3.241.

Cherniak D.J. and Watson B., 2003. Diffusion in zircon. In J.M. Hanchar and P.W.O. Hoskin, Eds., *Zircon*, Reviews in Mineralogy and Geochemistry, **53**, 113–143, http://dx.doi.org/10.2113/0530113.

Coenraads R.R., Sutherland F.L. and Kinny P.D., 1990. The origin of sapphires: U-Pb dating of

zircon inclusions sheds new light. *Mineralogical Magazine*, **54** (374), 113–122, http://dx.doi.org/10.1180/minmag.1990.054.374.13.

Corfu F., Hanchar J.M., Hoskin P.W.O. and Kinny P., 2003. Atlas of zircon textures. In J.M. Hanchar and P.W.O. Hoskin, Eds., *Zircon*, Reviews in Mineralogy and Geochemistry, **53**, 469–500, http://dx.doi.org/10.2113/0530469.

Dickin A.P., 2005. *Radiogenic Isotope Geology*. Cambridge University Press, Cambridge, 492 pp., http://dx.doi.org/10.1017/cbo9781139165150.

Elmaleh E., Karampelas S., Schmidt T. and Galster F., 2015. Zircon inclusions in blue sapphires. *34th International Gemmological Conference*, Vilnius, Lithuania, 26–30 August, 51–52.

Guillong M. and Günther D., 2001. Quasi 'non-destructive' laser ablation–inductively coupled plasma–mass spectrometry fingerprinting of sapphire. *Spectrochimica Acta B*, **56**(7), 1219–1231, http://dx.doi.org/10.1016/s0584-8547(01)00185-9.

Günther D. and Kane R.E., 1999. Laser ablation–inductively coupled plasma–mass spectrometry: A new way of analyzing gemstones. *Gems & Gemology*, **35**(3), 160–161.

Jackson S.E., Pearson N.J., Griffin W.L. and Belousova E.A., 2004. The application of laser ablation-inductively coupled plasma-mass spectrometry to in situ U–Pb zircon geochronology. *Chemical Geology*, **211**(1–2), 47–69, http://dx.doi.org/10.1016/j.chemgeo.2004.06.017.

Kröner A., Windley F.B., Jaeckelt P., Brewer S.T. and Razakamanana T., 1999. New zircon ages and regional significance for the evolution of the Pan-African orogen in Madagascar. *Journal of the Geological Society*, **156**(6), 1125–1135, http://dx.doi.org/10.1144/gsjgs.156.6.1125.

Ludwig K.R., 2003. Isoplot/Ex version 3.00: A geochronological toolkit for Microsoft Excel. Berkeley Geochronology Center, Berkeley, California, USA, www.bgc.org/isoplot_etc/isoplot.html.

Nasdala L., Wenzel M., Vavra G., Irmer G., Wenzel T. and Kober B., 2001. Metamictisation of natural zircon: Accumulation versus thermal annealing of radioactivity-induced damage. *Contributions to Mineralogy and Petrology*, **141**(2), 125–144, http://dx.doi.org/10.1007/s004100000235.

Rakotondrazafy A.F.M., Giuliani G., Ohnenstetter D., Fallick A.E., Rakotosamizanany S., Andriamamonjy A., Ralantoarison T., Razanatseheno M., Offant Y., Garnier V., Maluski H., Dunaigre C., Schwarz D. and Ratrimo V., 2008. Gem corundum deposits of Madagascar: A review. *Ore Geology Reviews*, **34**(1–2), 134–154, http://dx.doi.org/10.1016/j.oregeorev.2007.05.001.

Sláma J., Košler J., Condon D.J., Crowley J.L., Gerdes A., Hanchar J.M., Horstwood M.S.A., Morris G.A., Nasdala L., Norberg N., Schaltegger U., Schoene B., Tubrett M.N. and Whitehouse M.J., 2008. Plešovice zircon—A new natural reference material for U–Pb and Hf isotopic microanalysis. *Chemical Geology*, **249**(1–2), 1–35, http://dx.doi.org/10.1016/j.chemgeo.2007.11.005.

Sutherland F.L., Duroc-Danner J.M. and Meffre S., 2008. Age and origin of gem corundum and zircon megacrysts from the Mercaderes–Rio Mayo area, south-west Colombia, South America. *Ore Geology Reviews*, **34**(1–2), 155–168, http://dx.doi.org/10.1016/j.oregeorev.2008.01.004.

Sutherland F.L., Coenraads R.R., Abduriyim A., Meffre S., Hoskin P.W.O., Giuliani G., Beattie R., Wuhrer R. and Sutherland G.B., 2015. Corundum (sapphire) relationships, Lava Plains gem fields, NE Australia: Integrated mineralogy, geochemistry, genesis and geographical typing. *Mineralogical Magazine*, **79**, 545–581, http://dx.doi.org/10.1180/minmag.2015.079.3.04.

Váczi T., Nasdala L., Wirth R., Mehofer M., Libowitzky E. and Häger T., 2009. On the breakdown of zircon upon "dry" thermal annealing. *Mineralogy and Petrology*, **97**(1–2), 129–138, http://dx.doi.org/10.1007/s00710-009-0087-9.

Wang W., Scarratt K., Emmett J.L., Breeding C.M. and Douthit T.R., 2006. The effects of heat treatment on zircon inclusions in Madagascar sapphires. *Gems & Gemology*, **42**(2), 134–150, http://dx.doi.org/10.5741/gems.42.2.134.

Watson E.B., 1996. Dissolution, growth and survival of zircons during crustal fusion: Kinetic principles, geological models and implications for isotopic inheritance. *GSA Special Paper*, **315**, 43–56, http://dx.doi.org/10.1130/0-8137-2315-9.43.

Wetherill G.W., 1956. Discordant uranium-lead ages, I. *Eos—Transactions, American Geophysical Union*, **37**(3), 320–326, http://dx.doi.org/10.1029/tr037i003p00320.

The Author

Klemens Link is geochemical specialist at the Gübelin Gem Lab, Maihofstrasse 102, 6006 Lucerne, Switzerland.
Email: klemens.link@gubelingemlab.com

Acknowledgements

The author thanks the three anonymous reviewers for their helpful and constructive suggestions and the Gübelin Gem Lab team for its support whenever help was needed. Figure 3b was kindly supplied by Bulgari (Rome, Italy).

SSEF

SCHWEIZERISCHES GEMMOLOGISCHES INSTITUT
SWISS GEMMOLOGICAL INSTITUTE
INSTITUT SUISSE DE GEMMOLOGIE

ORIGIN DETERMINATION · TREATMENT DETECTION

DIAMOND GRADING · PEARL TESTING

EDUCATION · RESEARCH

THE SCIENCE OF GEMSTONE TESTING©

Aeschengraben 26, CH-4051 Basel, Switzerland Tel. +41 61 262 06 40 Fax + 41 61 262 06 41 admin@ssef.ch www.ssef.ch

Identification of a CVD Synthetic Diamond with a 'Tree Ring' Growth Pattern

Yan Lan, Rong Liang, Taijin Lu, Yong Zhu, Tianyang Zhang, Xuan Wang, Jian Zhang, Hong Ma and Zhonghua Song

The identification of CVD synthetic diamonds has become a challenge for the gem industry. Recently, a faceted 0.61 ct CVD synthetic diamond (VVS_2 clarity and L colour) was submitted to NGTC's Shenzhen Laboratory without disclosure. A bluish green fluorescence pattern similar to the 'tree ring' growth features seen in natural diamonds was observed in the table of the sample with the DiamondView. X-ray topography and Laue diffraction revealed that the crystallographic orientation of the table facet was inclined approximately 20° to the {111} octahedral plane, rather than being oriented in the typical {100} cubic direction. The appearance of this growth pattern could cause confusion, and vigilance is needed to assess the observed pattern in combination with the luminescence colour in differentiating between CVD synthetic and natural diamond. The X-ray topograph and Si-related photoluminescence (PL) doublet at 737.6/737.9 nm clearly indicate a CVD synthetic origin for this sample. The presence of PL peaks at 415 nm (N3) and 503.2 nm (H3), as well as mid-IR absorption at 3107 cm^{-1}, indicate that the sample underwent post-growth high-temperature, high-pressure (HPHT) treatment.

The Journal of Gemmology, 34(8), 2015, pp. 702–710, http://dx.doi.org/10.15506/JoG.2015.34.8.702

Introduction

During the last few decades, a considerable number of gem-quality synthetic diamonds produced by chemical vapour deposition (CVD) have entered the market. Most of them have reportedly come from Apollo Diamond Inc., Gemesis Corp. and others (Wang et al., 2003, 2007b, 2012; Martineau et al., 2004; Wang and Moses, 2011). In 2003, the Gemological Institute of America (GIA) laboratory described a near-colourless gem-quality CVD synthetic diamond grown by Apollo Diamond (Wang et al., 2003). Subsequently, Wang et al. (2007b, 2010) reported on colourless, brown and orange-pink gem-quality CVD-grown synthetics from Apollo Diamond. Martineau et al. (2004) presented analytical results from the Diamond Trading Co. (DTC) Research Centre on CVD synthetic

diamond samples grown for research purposes by Element Six; these included as-grown and HPHT-treated nitrogen-doped samples, as well as boron-doped and high-purity CVD synthetic diamonds. Gemesis Corp. announced plans to market CVD-grown synthetics in November 2010, and these were described by GIA in 2011 (Wang and Moses, 2011). Subsequently, Wang et al. (2012) reported additional gemmological and spectroscopic properties of Gemesis CVD synthetic diamonds.

In recent years, greater identification challenges for CVD synthetic diamonds have resulted from refinements in their growth and processing, which have yielded products that are very similar to natural diamond in appearance, with variable properties according to the added impurities or post-growth treatment. In the past few years, undisclosed CVD synthetic diamonds have been submitted to the International Gemological Institute, National Gemstone Testing Centre (NGTC), Tokyo Central Gem Laboratory and others (e.g. Song et al., 2012; Kitawaki et al., 2013, 2015).

NGTC has carried out significant research on CVD synthetic diamonds, and has developed effective identification protocols using ultraviolet-visible–near infrared (UV-Vis-NIR) and infrared absorption spectroscopy, the DiamondView instrument, PL spectroscopy, etc. Of these, DiamondView fluorescence imaging is one of the most useful identification methods, since it reveals the striations associated with the layered growth of CVD synthetics (Martineau et al., 2004; Wang et al., 2010). However, this article documents a 'tree ring' growth pattern seen with the DiamondView in the table of a faceted CVD synthetic diamond that is similar to patterns seen in some natural diamonds. The gemmological characteristics of this sample are presented, and the reason for the unusual appearance of its growth pattern is analysed using X-ray topography and Laue diffraction to determine the crystallographic orientation of the synthetic diamond relative to the table facet.

Materials and Methods

A 0.61 ct round brilliant (Figure 1) was submitted to NGTC's Shenzhen Laboratory for a grading report in February 2015. It was identified as a CVD synthetic diamond, and received a low colour grade (L) but showed good clarity (VVS_2). The following investigations were carried out at NGTC, except for X-ray topography and Laue diffraction, which were carried out at De Beers Technologies in Maidenhead.

Figure 1: This 0.61 ct CVD synthetic diamond was submitted to NGTC without disclosure. Photo by Y. Lan.

The sample's fluorescence and phosphorescence to UV radiation were observed using 254 nm (short-wave) and 365 nm (long-wave) 4-watt UV lamps, and also with the DiamondView deep-UV (<230 nm) imaging system.

Infrared absorption spectra were recorded in the mid-infrared range (6000–400 cm^{-1} and 2 cm^{-1} resolution) at room temperature, with a Nicolet 6700 Fourier-transform infrared (FTIR) spectrometer equipped with a KBr beam splitter. UV-Vis-NIR absorption spectra in the range of 230–1000 nm were collected with an Ocean Optics GEM-3000 Jewel Identifying Instrument at liquid-nitrogen temperature. The sample was also tested using the DTC DiamondSure and DiamondPLus instruments.

Photoluminescence spectra were acquired with four different laser excitations (325, 473, 532 and 785 nm) using a Renishaw InVia Raman confocal micro-spectrometer with the sample cooled to liquid-nitrogen temperature.

X-ray topography (Mo $K\alpha$ radiation, {533} reflection) using a Marconi GX20 rotating anode X-ray generator was done to visualize strain associated with dislocations that formed during the sample's growth. The crystallographic orientation of the

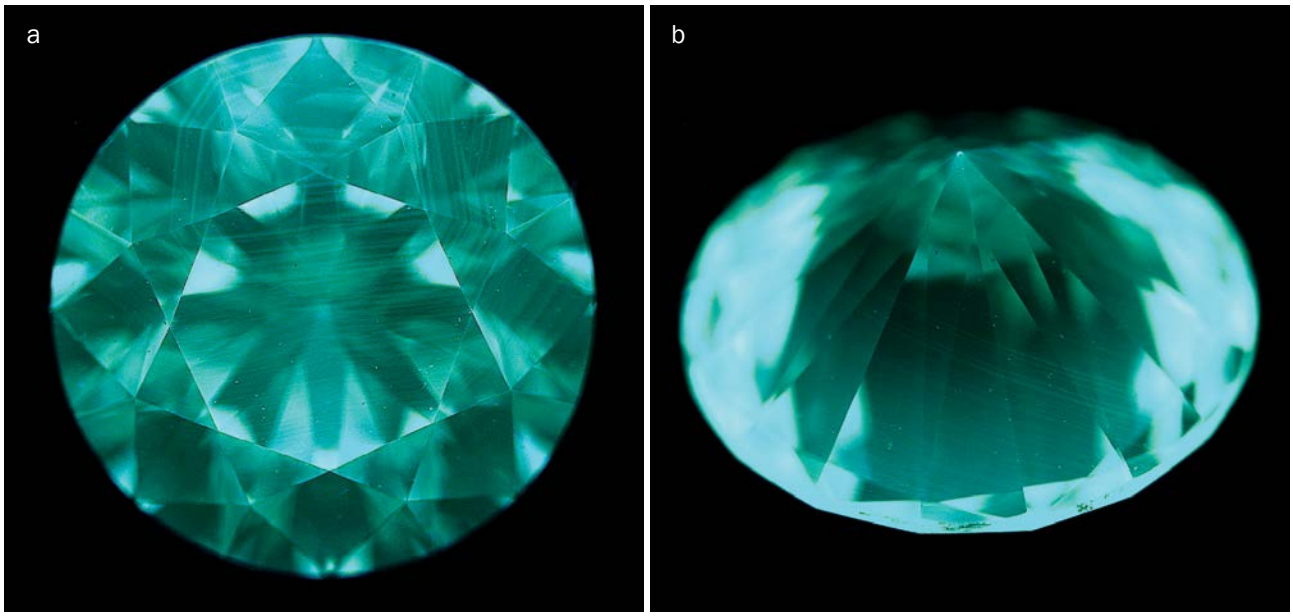

Figure 2: DiamondView images of the 0.61 ct CVD sample show bluish green UV fluorescence patterns with a 'tree ring' growth pattern seen in the table-up orientation (a) and a layered growth pattern viewed through the pavilion (b). Photos by Y. Lan.

table facet was determined by Laue diffraction, using a Bruker SMART 1000 CCD single-crystal diffractometer. Laue diffraction patterns are useful for revealing the crystallographic orientation of a faceted sample. Named after Max von Laue, such images provide a photographic record of the diffraction pattern that is produced when an X-ray beam passes through a crystal (Warren, 1969). The patterns show a regular array of spots on a photographic emulsion resulting from X-rays scattered by certain groups of parallel atomic planes within the crystal. Those X-rays oriented at just the proper angle to a group of atomic planes will combine in-phase to produce intense, regularly spaced spots on the film or plate that indicate the sample's crystallographic orientation relative to the X-ray beam.

Results

Luminescence

The sample was inert to long-wave UV radiation and showed moderate-to-strong green fluorescence to the short-wave UV lamp. No obvious phosphorescence was seen.

In the DiamondView, the sample displayed bluish green fluorescence with layered growth striations (Figure 2). Unlike previously reported CVD synthetic diamonds, when observed table-up the sample showed a 'tree ring' growth pattern, similar to that seen in some type I natural diamonds (Wang et al., 2007a; Sun et al., 2012; see Figure 2a). By contrast, when viewed from the pavilion the sample showed the characteristic parallel layers associated with the growth of CVD synthetic diamond (Figure 2b). As far as we are aware, the 'tree ring' pattern has not been previously reported in CVD synthetic diamond (cf. Martineau et al., 2004; Wang et al., 2007b).

Infrared and UV-Vis-NIR Absorption Spectroscopy

The absorption spectrum in the mid-infrared region (Figure 3) showed that the sample was type IIa, with very weak N-related absorption at 1344 cm^{-1}. Other features included H-related lines at 3107, 3029, 2919, 2880 and 2831 cm^{-1}, and weak bands at 1340, 1332, 1296 and 1128 cm^{-1}. Note that the weak line at 3107 cm^{-1} and the missing 3123 cm^{-1} line (a characteristic H-related feature in CVD synthetic diamond) provide strong evidence that the sample had been HPHT treated (Martineau et al., 2004).

The UV-Vis-NIR absorption spectrum revealed an N-related peak at 270 nm and decreasing absorbance from 300 to 700 nm (Figure 4). Neither the Si-V^{-}-related peak at 737 nm (typical of some CVD synthetic diamonds: Martineau et al., 2004; Wang et al., 2012) nor the N3 absorption at 415 nm (common in natural diamond) were detected.

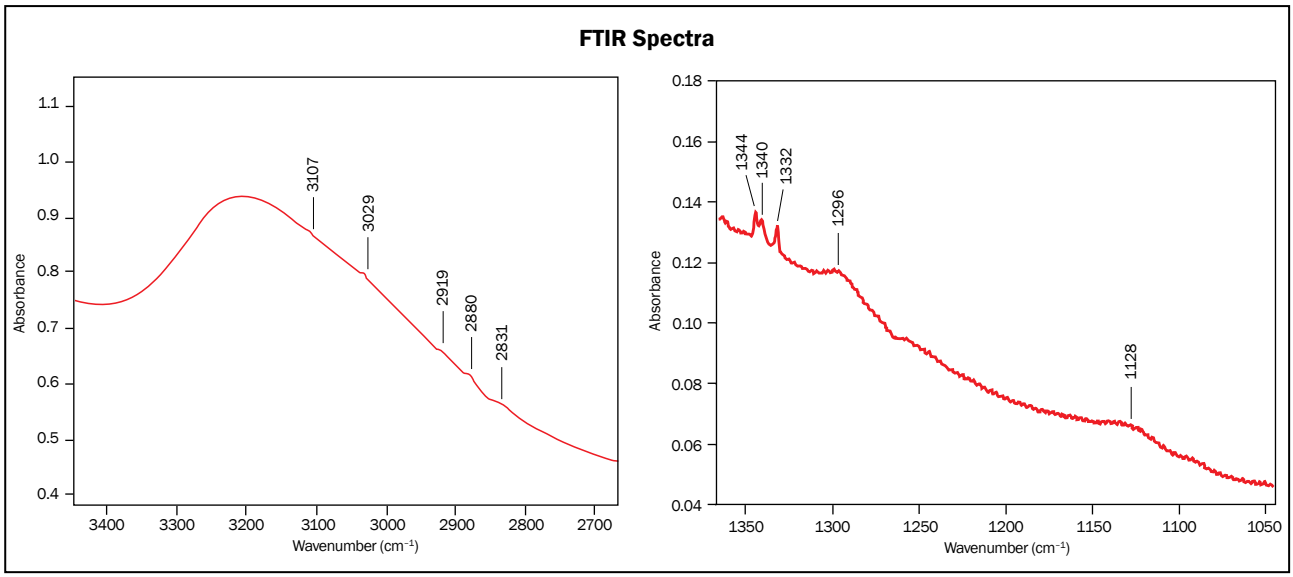

Figure 3: Infrared spectroscopy of the CVD synthetic diamond shows H-related lines at 3107 cm^{-1} etc. (left) and very weak N-related 1344 cm^{-1} absorption (right). The missing CVD-characteristic H-related absorption band at 3123 cm^{-1} reveals that the sample has been HPHT treated.

Verification Instruments

Testing with the DiamondSure resulted in 'refer for further test: type II', and the DiamondPLus indicated 'Refer CVD' from the PL measurement of the 737 nm Si-V^- centre.

Photoluminescence Spectroscopy

325 nm Excitation: A weak PL peak at 415.1 nm was excited by the 325 nm laser (Figure 5). This peak is attributed to the N3 defect (three nitrogen atoms in a {111} plane associated with a vacancy: Davies, 1974; Davies et al., 1978), which usually occurs in cape diamonds. Nitrogen in CVD synthetic diamond is commonly present in the form of single nitrogen, but may be aggregated during HPHT treatment to produce the N3 defect, particularly after prolonged annealing at 2,200°C (Martineau et al., 2004). In addition, a series of weak PL peaks in the 388–503 nm range were detected.

Figure 4: The UV-Vis-NIR absorption spectrum of the CVD synthetic diamond shows a broad absorption band centred at ~270 nm attributed to isolated nitrogen.

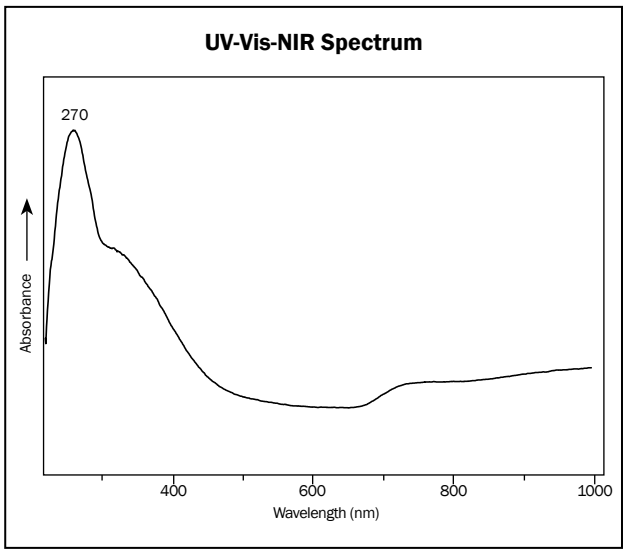

Figure 5: The PL spectrum of the CVD synthetic diamond sample excited by the 325 nm laser at liquid-nitrogen temperature shows a weak emission at 415.1 nm from the N3 optical centre.

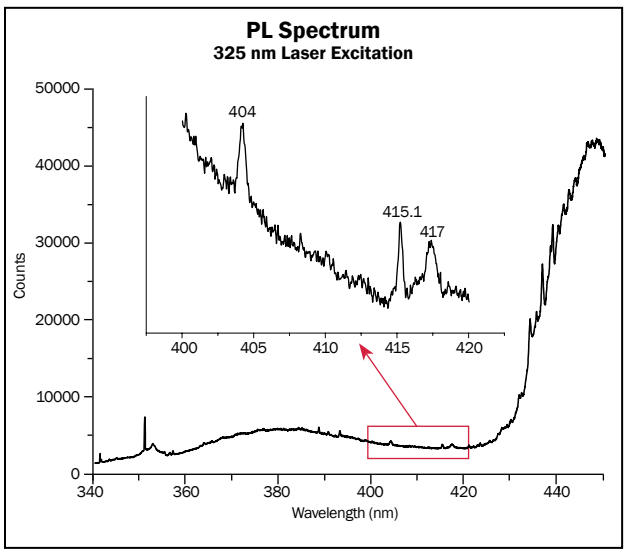

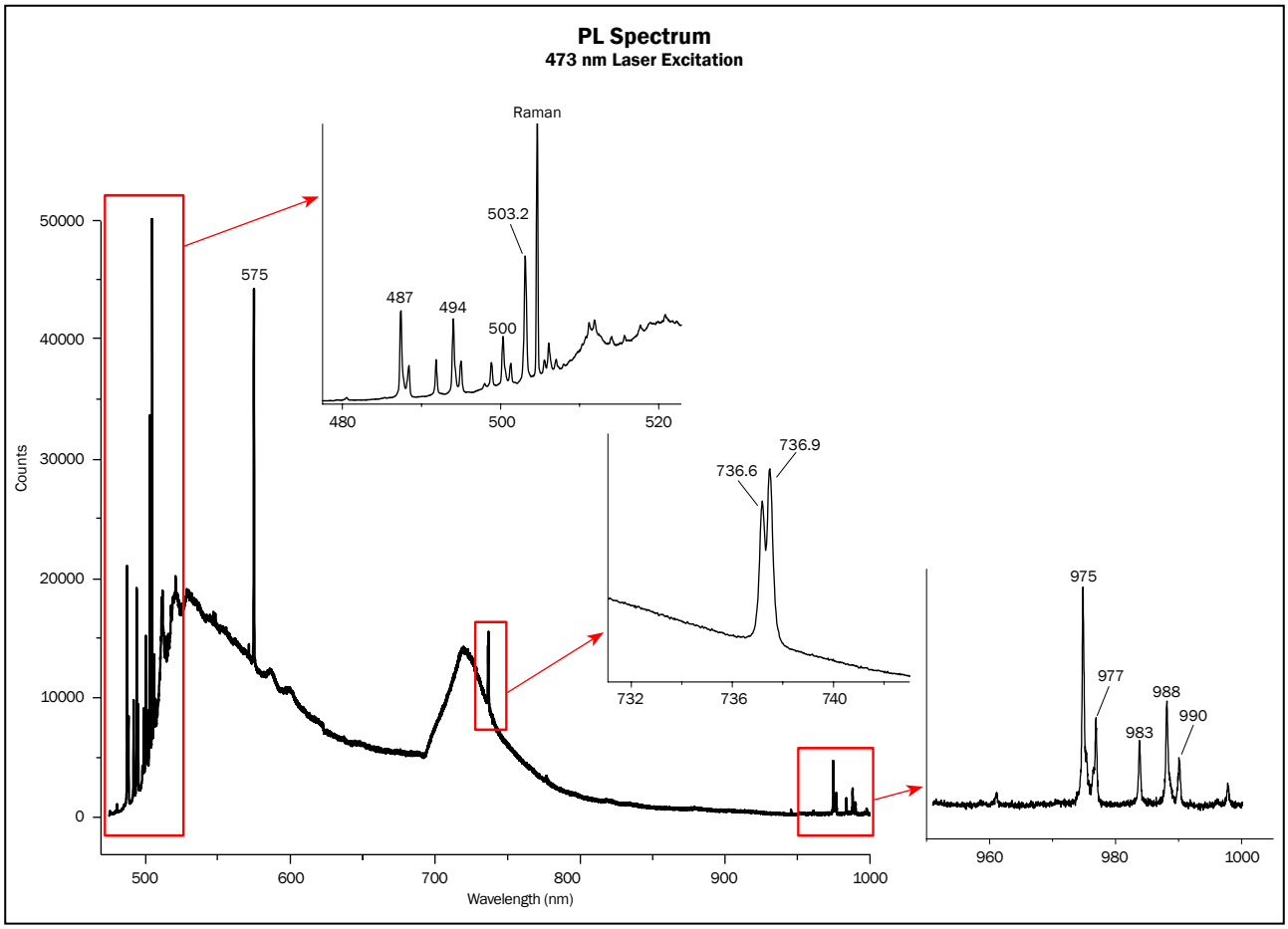

Figure 6: The PL spectrum of the CVD synthetic diamond sample collected with 473 nm laser excitation at liquid-nitrogen temperature shows emissions of H3 (503.2 nm), NV^0 (575 nm) and $Si\text{-}V^-$ (736.6/736.9 nm) centres. Also, numerous sharp peaks were recorded in the 480–520 nm and 960–1000 nm regions.

473 nm Excitation: The PL spectrum excited by the 473 nm (blue-green) laser is shown in Figure 6. The strongest zero-phonon-line (ZPL) emissions were at 575, 503.2 and 736.6/736.9 nm.

The 575 nm emission is from the NV^0 centre, which is commonly detected in CVD synthetic diamond due to the presence of single nitrogen and vacancies that are inevitably introduced during the growth process (Martineau et al., 2004).

The 503.2 nm ZPL is attributed to the H3 defect ($[N\text{-}V\text{-}N]^0$), which can be produced by irradiation in diamond containing aggregated nitrogen, followed by annealing at approximately 800°C. Vacancies are generated during the irradiation and annealing, and are trapped at nitrogen A-aggregates (a nearest-neighbour pair of nitrogen atoms) to form H3 centres. In CVD synthetic diamond, this defect is produced when there is nitrogen and a source of vacancies in the pre-treated material. H3 defects also can be formed by high-temperature annealing without irradiation (Charles et al., 2004; Martineau et al., 2004; Meng et al., 2008). According to Meng et al. (2008), when the annealing temperature exceeds 1,700°C, H3 defects may be observed in CVD synthetic diamond. This defect is responsible for the green fluorescence excited by the short-wave UV lamp and the DiamondView (Wang et al., 2012).

The 736.6/736.9 nm doublet and its corresponding vibronic structure are attributed to the $Si\text{-}V^-$ centre. Silicon is often introduced into CVD synthetic diamond by the etching of Si-containing components forming the reactor (Robins et al., 1989; Barjon et al., 2005; Wang et al., 2012). The defect can exist stably after HPHT treatment (Martineau et al., 2004), and is usually regarded as one of the identification characteristics of CVD synthetic diamond (although not definitive, as a small number of natural diamonds also have this defect: Breeding and Wang, 2008).

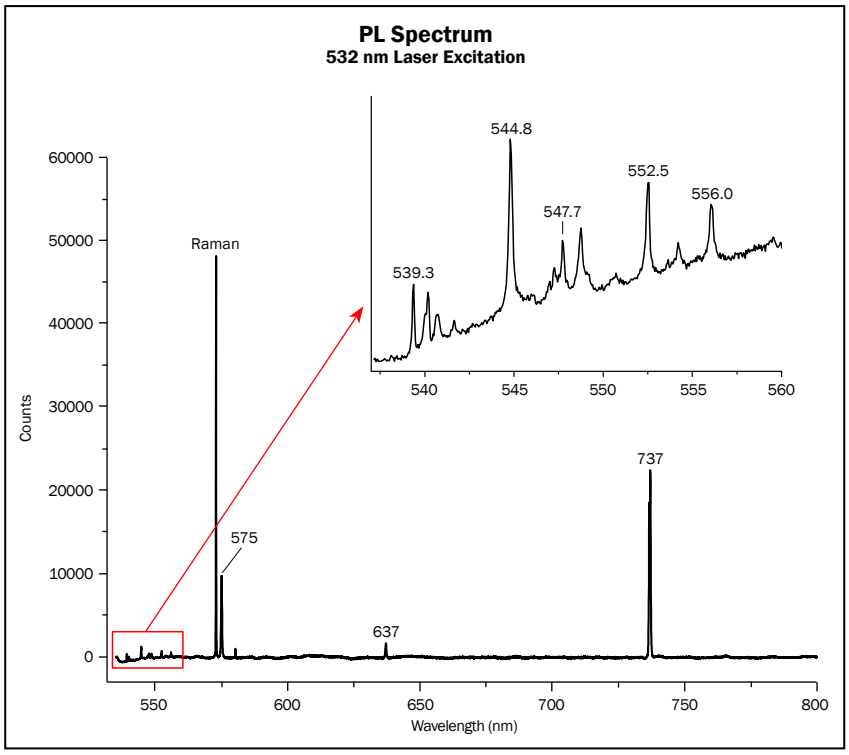

Figure 7: Green laser (532 nm) excitation of the CVD sample produced strong PL emissions at 575 nm (NV^0) and 737 nm ($Si\text{-}V^-$). In addition, numerous weak peaks were recorded in the 535–560 nm region.

The 473 nm laser also excited many unidentified sharp peaks, including those at 487, 488, 494, 495, 500, 501, 506 and 507 nm, as well as those at 975, 977, 983, 988 and 990 nm in the infrared region (not all peaks are shown in Figure 6).

532 nm Excitation: Photoluminescence peaks at 575 nm (NV^0) and 736.6/736.9 nm ($Si\text{-}V^-$) were detected in the sample when excited by the 532 nm laser (Figure 7). In addition, 637 nm emission attributed to the NV^- centre was recorded. Several unattributed emission peaks were detected in the 539–556 nm region, including those at 539.3, 540.1, 540.6, 541.6, 544.8, 547.7, 548.7, 552.5, 554.2 and 556.0 nm (not all peaks are shown in Figure 7).

Figure 8: The PL spectrum of the CVD synthetic diamond excited by the 785 nm laser revealed unidentified weak peaks at 819.3, 824.5, 850.1 and 853.3 nm.

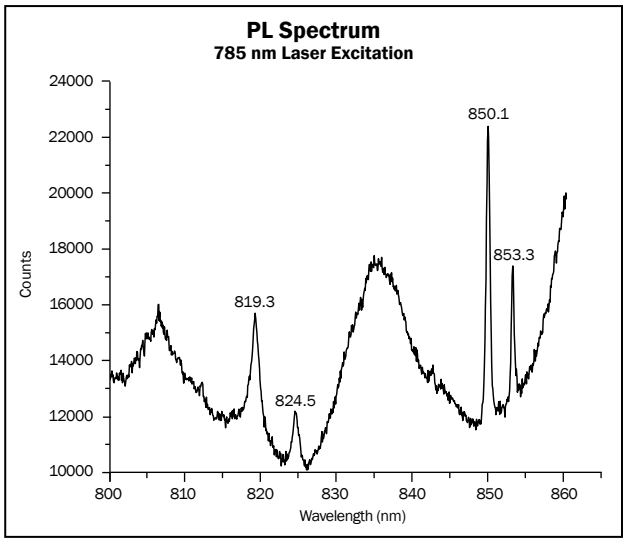

785 nm Excitation: Weak PL peaks at 819.3, 824.5, 850.1 and 853.3 nm were detected in the sample when excited with the 785 nm laser (Figure 8). The defects responsible for these PL peaks have not been identified.

X-ray Topography

The X-ray section topograph of the sample is similar to those previously reported in CVD synthetic diamond (Martineau et al., 2004), showing a columnar texture with linear contrast streaks parallel to the growth direction (Figure 9). This appearance is quite different from that seen in topographs of natural diamonds (cf. Diehl and Herres, 2004). The contrast streaks are believed to be caused by the dislocations produced during the growth process. If the X-ray beam sampled a direction perpendicular to the growth direction, these dislocation bundles would appear as dark spots in the resultant topograph (Martineau et al., 2004). The X-ray topograph shows that the table of the faceted CVD synthetic diamond is oriented at a significant oblique angle to the crystal's growth

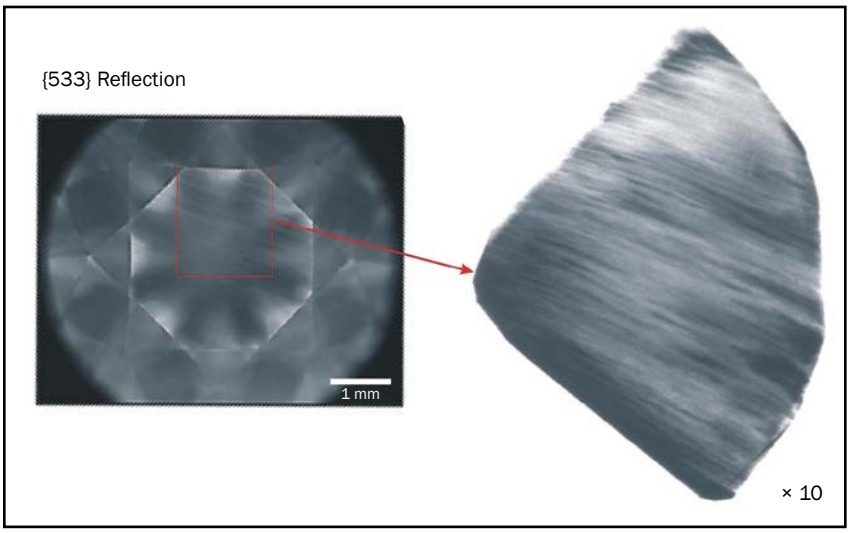

Figure 9: A columnar texture is evident in this X-ray topograph taken through the table facet of the CVD sample, in which a cross-sectional slice parallel to the growth direction was sampled by the X-ray beam. Courtesy of De Beers Technologies.

direction, in contrast to that reported by Martineau et al. (2004) where the table was approximately perpendicular to the growth direction.

Laue Diffraction

A Laue diffraction image taken with the table parallel to the plane of the image (Figure 10) showed that the table facet of the CVD synthetic diamond was oriented approximately 20° to the {111} octahedral plane, in the {100} cubic direction.

Discussion

The angle between the octahedral and cubic planes in diamond is 54.7°. Laue diffraction allows the orientation of the CVD synthetic diamond's table facet to be calculated (Figure 11), showing a deviation from the {100} cubic plane toward the {111} octahedral plane. In general, CVD synthetic diamonds are grown on plates oriented parallel to the {001} plane, producing growth in the <001> direction. The table facet is typically oriented approximately parallel to the seed plate plane (i.e. perpendicular to the growth direction of CVD synthetic diamond) to improve the cutting yield. The Laue diffraction pattern indicates that the 'tree ring' growth pattern observed on the table of the CVD synthetic diamond sample with the DiamondView is due to the orientation of the

Figure 10: Indexing of this X-ray Laue diffraction pattern of the CVD sample revealed that the table facet has an orientation that is inclined approximately 20° to the {111} octahedral plane toward the {100} cubic direction.

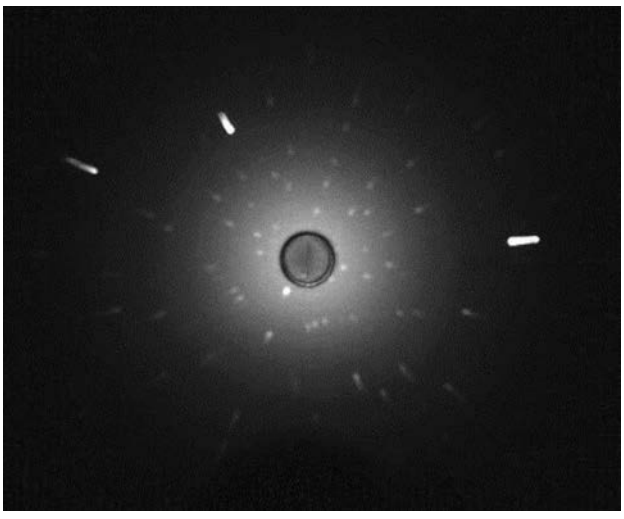

Figure 11: This schematic diagram of the cutting direction of the CVD sample shows that the crystallographic orientation of the table facet deviates from the {100} cubic plane and approaches the {111} octahedral plane. This differs from typical faceted CVD synthetic diamond, in which the table is oriented approximately parallel to the {001} plane.

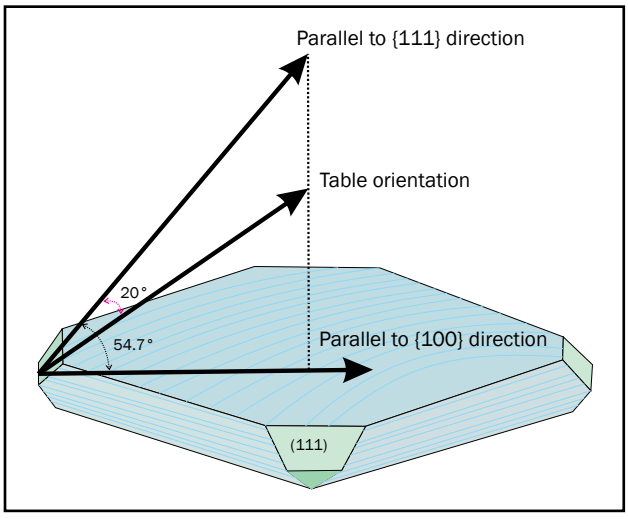

table at just the right angle to the growth direction to produce very shallow angles between the growth planes and the table and crown facets at one position at the edge of the table. This results in the concentric ring-like appearance where the striations intersect the facets.

Conclusion

Refinements in CVD synthetic diamond growth technology, and the resulting increase in crystal size, have resulted in more flexibility regarding the cutting orientation used to facet such products. The 'tree ring' growth structure observed with the DiamondView in the table of a 0.61 ct CVD synthetic diamond is due to the crystallographic orientation of the table facet deviating from the {100} cubic direction toward the {111} octahedral plane to produce very shallow angles between the growth planes and the table and crown facets. This concentric pattern is different from the dislocation and 'mosaic' structures seen in DiamondView images of natural type IIa diamond (Martineau et al., 2004), but may resemble those patterns observed in natural type Ia stones; however, the luminescence of the latter gems shows a blue colour that is very different from that seen in CVD synthetics (Wang et al., 2007a; Sun et al., 2012). Also, compared to the regular striations in CVD synthetics, the growth patterns in natural diamond are more complicated and less orderly because of the complex geological environment of their formation. In addition, the CVD sample showed the Si-V^--related doublet at 737.6/737.9 nm in PL spectra. This defect can be used to identify CVD synthetic diamond but is also seen very occasionally in natural diamond. The columnar texture of the X-ray topograph may be useful as an indicator of CVD synthesis (cf. Diehl and Herres, 2004; Martineau et al., 2004). The presence of the N3 (415 nm) and H3 (503.2 nm) defects, and also the 3107 cm^{-1} absorption seen in the mid-IR spectrum, indicate that the CVD synthetic diamond has been HPHT treated. The 480–524 nm PL peaks excited by the 473 nm laser and the 535–560 nm PL peaks excited by the 532 nm laser have also been detected in other CVD synthetic diamonds that show green fluorescence and characteristics of HPHT treatment, and may be used as further indicators of CVD synthetic diamond.

References

Barjon J., Rzepka E., Jomard F., Laroche J.M., Ballutaud D., Kociniewski T. and Chevallier J., 2005. Silicon incorporation in CVD diamond layers. *Physica Status Solidi (a)*, **202**(11), 2177–2181, http://dx.doi.org/10.1002/pssa.200561920.

Breeding C.M. and Wang W., 2008. Occurrence of the Si-V defect in natural colourless gem diamonds. *Diamond and Related Materials*, **17**(7–10), 1335–1344, http://dx.doi.org/10.1016/j.diamond.2008.01.075.

Charles S.J., Butler J.E., Feigelson B.N., Newton M.E., Carroll D.L., Steeds J.W., Darwish H., Yan C.S., Mao H.K. and Hemley R.J., 2004. Characterization of nitrogen doped chemical vapor deposited single crystal diamond before and after high pressure, high temperature annealing. *Physica Status Solidi (a)*, **201**(11), 2473–2485, http://dx.doi.org/10.1002/pssa.200405175.

Davies G., 1974. Vibronic spectra in diamond. *Journal of Physics C: Solid State Physics*, **7**(20), 3797–3809, http://dx.doi.org/10.1088/0022-3719/7/20/019.

Davies G., Welbourn C.M. and Loubser J.H.N., 1978. Optical and electron paramagnetic effects in yellow type Ia diamonds. *Diamond Research 1978*, De Beers Industrial Diamond Division, Ascot, 23–30.

Diehl R. and Herres N., 2004. X-ray fingerprinting routine for cut diamonds. *Gems & Gemology*, **40**(1), 40–57, http://dx.doi.org/10.5741/gems.40.1.40.

Kitawaki H., Yamamoto M., Hisanaga M., Okano M. and Emori K., 2013. Gem News International: Undisclosed samples of large CVD synthetic diamond. *Gems & Gemology*, **49**(1), 60–61.

Kitawaki H., Hisanaga M., Yamamoto M. and Emori K., 2015. Type Ib yellow to brownish yellow CVD synthetic diamonds seen at CGL. *Journal of Gemmology*, **34**(7), 594–604, http://dx.doi.org/10.15506/JoG.2015.34.7.594.

Martineau P.M., Lawson S.C., Taylor A.J., Quinn S.J., Evans D.J.F. and Crowder M.J., 2004. Identification of synthetic diamond grown using chemical vapor deposition (CVD). *Gems & Gemology*, **40**(1), 2–25, http://dx.doi.org/10.5741/gems.40.1.2.

Meng Y.-F., Yan C.-S., Lai J., Krasnicki S., Shu H., Yu T., Ling Q., Mao H.-K. and Hemley R.J., 2008. Enhanced optical properties of chemical vapor deposited single crystal diamond by low-pressure/high-temperature annealing. *Proceedings of the National Academy of Sciences*, **105**(46), 17620–17625, http://dx.doi.org/10.1073/pnas.0808230105.

Robins L.H., Cook L.P., Farabaugh E.N. and Feldman A., 1989. Cathodoluminescence of defects in

diamond films and particles grown by hot-filament chemical-vapor deposition. *Physical Review B*, **39**(18), 13367–13377, http://dx.doi.org//10.1103/PhysRevB.39.13367.

Song Z., Lu T., Lan Y., Shen M., Ke J., Liu J. and Zhang Y., 2012. The identification features of undisclosed loose and mounted CVD synthetic diamonds which have appeared recently in the NGTC laboratory. *Journal of Gemmology*, **33**(1–4), 45–48, http://dx.doi.org/10.15506/jog.2012.33.1.45.

Sun Y., Chen H., Qiu Z., Lu T., Liang W., Zhang J., Li L., Wang Q. and Mo M., 2012. The DiamondView images of natural diamonds from three commercial diamond localities in China and their significance. *Acta Petrologica et Mineralogica*, **31**(2), 261–270 (in Chinese with English abstract).

Wang W. and Moses T.M., 2011. Lab Notes: Gem-quality CVD synthetic diamonds from Gemesis. *Gems & Gemology*, **47**(3), 227–228.

Wang W., Moses T., Linares R.C., Shigley J.E., Hall M. and Butler J.E., 2003. Gem-quality synthetic diamonds grown by the chemical vapor deposition method. *Gems & Gemology*, **39**(4), 268–283, http://dx.doi.org/10.5741/gems.39.4.268.

Wang W., Hall M. and Breeding C.M., 2007a. Natural type Ia diamond with green-yellow color due to Ni-related defects. *Gems & Gemology*, **43**(3), 240–243, http://dx.doi.org/10.5741/gems.43.3.240.

Wang W., Hall M.S., Moe K.S., Tower J. and Moses T.M., 2007b. Latest-generation CVD-grown synthetic diamonds from Apollo Diamond Inc. *Gems & Gemology*, **43**(4), 294–312, http://dx.doi.org/10.5741/gems.43.4.294.

Wang W., Doering P., Tower J., Lu R., Eaton-Magaña S., Johnson P., Emerson E. and Moses T.M., 2010. Strongly colored pink CVD lab-grown diamonds. *Gems & Gemology*, **46**(1), 4–17, http://dx.doi.org/10.5741/gems.46.1.4.

Wang W., D'Haenens-Johansson U.F.S., Johnson P., Moe K.S., Emerson E., Newton M.E. and Moses T.M., 2012. CVD synthetic diamonds from Gemesis Corp. *Gems & Gemology*, **48**(2), 80–97, http://dx.doi.org/10.5741/gems.48.2.80.

Warren B.E., 1969. *X-ray Diffraction*. Dover Publications Inc., New York, New York, USA.

The Authors

Yan Lan, Rong Liang, Tianyang Zhang and Hong Ma
National Gemstone Testing Center (NGTC)
Gems & Jewelry Institute of Shenzhen
13F NGTC Building, 4 # Beili South Road
Luohu District, Shenzhen 518020, China
Email: 858lan@163.com

Yong Zhu and Xuan Wang
Chongqing Academy of Metrology and Quality Inspection, 1 # Yangliu North Road
Yubei District, Chongqing 401123, China

Dr Taijin Lu, Jian Zhang and Zhonghua Song
NGTC, Gems & Jewelry Institute of Beijing
22F Tower C, Global Trade Center
36 # North Third Ring East Road
Dongcheng District, Beijing 100013, China

Acknowledgements

Special thanks to John Freeth and David Fisher of De Beers Technologies, Maidenhead, who provided assistance with the X-ray diffraction and topographic analysis of the sample.

Thank You, Guest Reviewers

The following individuals served as guest reviewers during the past publication year. The editors extend their special thanks to all of them for lending their expertise to reviewing manuscripts submitted to *The Journal*. Together with the Associate Editors, these individuals have enhanced the quality of *The Journal* through their knowledge and professionalism.

Dr Ahmadjan Abduriyim
Gemological Institute of America, Tokyo, Japan
Dr James Butler
Huntingtown, Maryland, USA
Maggie Campbell Pedersen
Organic Gems, London
Dr Laurent Cartier
Swiss Gemmological Institute SSEF, Basel, Switzerland
Gagan Choudhary
Gem Testing Laboratory, Jaipur, India
Dr Eloïse Gaillou
Musée de Minéralogie, Mines ParisTech, Paris, France
Al Gilbertson
Gemological Institute of America, Carlsbad, California, USA
Alan Hodgkinson
Ayrshire, Scotland
Dr Mary Johnson
Mary Johnson Consulting, San Diego, California, USA
Dr Taijin Lu
National Gemstone Testing Center Laboratory, Beijing, China
Dr Alexander Makhrov
Russian Academy of Sciences, Moscow
Dr Andy H. Shen
China University of Geosciences, Wuhan, China
Jeremy Shepherd
Pearl Paradise, Los Angeles, California, USA
Dr Frederick L. Sutherland
Port Macquarie, Australia
Dr Richard P. Taylor
The University of St Andrews, Fife, Scotland

Conferences

CGA Conference

The annual conference of the Canadian Gemmological Association took place 17–18 October 2015 in Vancouver, British Columbia, Canada. The 118 people in attendance represented approximately 11 countries.

CGA president **Donna Hawrelko** introduced the conference, which was kicked off with a presentation by **Gary Roskin** (International Colored Gemstone Association, New York, New York, USA) on communicating colour. He asked the audience whether gem laboratory reports should be using scientific colour descriptions (i.e. hue, tone and saturation) or popular colour designations (e.g. 'Pigeon's Blood' red or 'Royal' blue) that gem traders can use as marketing tools. For the latter case, he recommended that labs should be consistent and have well-defined and published ranges for such colour terminology. Next, **Dr Cigdem Lule** (Gemworld International Inc., Glenview, Illinois, USA) warned against the abuse of commercial colour terms for marketing purposes when dealers "sell the report, not the stone". She gave an example of the term 'Pigeon's Blood' appearing on an overly high percentage of ruby reports (90% of some 500+ surveyed), for stones that ranged from $450/ct to $50,000/ct. She, too, emphasized the need to establish clear gemmological nomenclature and be consistent in the way it is applied.

Dr James Shigley (Gemological Institute of America [GIA], Carlsbad, California, USA) provided an update on the identification of synthetic diamonds. He emphasized that only a small number are submitted to the GIA Laboratory (perhaps 10–15/month), and they continue to be readily distinguishable by well-equipped labs. **Richard Drucker** (Gemworld International Inc., Glenview) reviewed the pricing of synthetic and treated diamonds. Synthetic colourless diamonds are generally priced at 50% (up to 65% for larger sizes) of natural stones, except for melee which is ~US$100/ct less than natural diamonds. High-pressure, high-temperature (HPHT)-treated D–G colour diamonds typically are discounted by 40%–55% compared to equivalent untreated natural stones. Drucker also gave pricing data for fancy-colour synthetic and treated-colour natural diamonds in an informative handout. **Alex Grizenko** (Lucent Diamonds Inc., Los Angeles, California, USA) reviewed diamond colour enhancement, with an emphasis on multi-treatments involving HPHT annealing, irradiation, and further heat treatment at lower temperatures. Interestingly, he is asking the same price for both natural and synthetic Imperial Red diamonds (multi-treated type Ia). **Art Samuels** (Vivid Diamonds & Jewelry and EstateBuyers.com, Florida, USA) passed along many diamond-buying tips gleaned throughout his career. For example, he explained how strongly blue-fluorescent stones (which are unnecessarily punished by the trade) and fancy shapes can be great bargains. He also recommended examining a gemstone closely both before and after obtaining a laboratory report to calibrate one's observational skills, and to learn pricing by attending shows and asking questions.

Dr Lee Groat (University of British Columbia, Vancouver, Canada) surveyed Canadian gem localities. Diamond production is planned to begin during the second half of 2016 from the Gahcho Kué deposit in Northwest Territories and the Renard project in Québec, both of which are currently under construction. Canada also hosts significant deposits of nephrite and the world's only commercial occurrence of Ammolite (iridescent fossilized ammonite). Other gems include amethyst from Thunder Bay, Ontario; tourmaline from O'Grady, Northwest Territories; sodalite from Bancroft, Ontario; opal from British Columbia; sapphire from Baffin Island and Revelstoke, British Columbia; emerald from Taylor 2 (Ontario), Anuri (Nunavut) and three additional localities in north-western Canada; aquamarine from the True Blue occurrence in Yukon Territory; green beryl from Mountain River, Northwest Territories; and spinel from Baffin Island. **Simon O'Brien** (De Beers Group of Companies, Toronto, Ontario, Canada) gave an update on De Beers' diamond mining activities in Canada (i.e. Snap Lake, Gahcho Kué and Victor), and then described the evaluation of rough diamonds (e.g. Figure 1). The diamonds are (1) sieved into various

Figure 1: Rough diamonds such as these are evaluated according to numerous criteria including size, shape, clarity and colour. The largest diamond crystal shown here weighs 174.25 ct. Courtesy of De Beers Group of Companies.

sizes; (2) evaluated into sawable and makeable groups followed by sorting according to their shape; (3) separated according to their clarity into gem, near-gem and industrial categories; and (4) assessed for their colour. Further sorting within the various categories leads to a total of 12,000 price points.

Andrew Fagan (True North Gems, Vancouver, Canada) described the geology and gemmology of the Fiskenaesset gem district in Greenland, where his company is preparing to open a ruby and pink sapphire mine at Aappaluttoq. Core drilling (to 220 m depth) and bulk sampling have been used to define the ore zone, and plans call for constructing two open pits up to 65 m deep with a predicted nine-year mine life. The mine economics are modelled on melee-sized material, although some larger stones will be produced. True North will sell the rough to suppliers (initially in 2016), and by 2017 they will be in full production with 20,000–30,000 tonnes/year of ore mined.

Robert Weldon (GIA, Carlsbad) recounted the history of the Chivor emerald mine in Colombia. Many famous emeralds have come from Chivor, and the height of commercial production occurred in the 1930s, when the mine was operated by Peter Rainier.

Dr Edward (Shang-i) Liu (The Hong Kong Institute of Gemmology) described several types of *fei cui* jade, consisting of various amounts of jadeite ± omphacite and kosmochlor. He demonstrated how different minerals can be present in various parts of the same cabochon, leading to challenges in proper identification and nomenclature. For the purposes of the gem trade, he advocated simplifying the terminology to indicate 'natural *fei cui*' on lab reports, with major mineral constituents specified upon the client's request.

Shawn O'Sullivan (Eternity Natural Emeralds, Ridgewood, New Jersey, USA) described the impact of clarity treatment on emerald and tourmaline. He stated that there is generally a 5–10% improvement in appearance after treatment, and that it is difficult for gem laboratories to tell the amount of clarity enhancement because they do not see the stone's appearance after it is cleaned and before its fractures/cavities are filled.

Alan Hodgkinson (Ayrshire, Scotland) highlighted various stones that he encountered at last year's Tucson gem shows, and illustrated how they could be separated or identified using his techniques of 'visual optics'. Ruby and diamond are the only gems that can be specifically identified using visual optics, and otherwise these techniques are good for eliminating possibilities, thus narrowing potential candidates.

Kelly Ross (owner of Ross Inc., Edmonton, Alberta, Canada, and formerly diamond program coordinator for the Royal Canadian Mounted Police) explained why jewellery is so common in 'money laundering', which he defined as the proceeds of a crime that must be sold to obtain cash and real property (i.e. fixed property such as land and buildings). Along with electronics and power tools, jewellery is commonly desired by burglars because (according to the acronym CRAVED) it is concealable, removable, available, valuable, enjoyable and disposable. Jewellers who are approached to buy possible stolen goods can help by reporting suspicious transactions, by keeping good records (of lab reports, etc.), and by getting the seller's identification information.

The conference was preceded by a short-course on the geology of gem deposits and was followed by a jadeite identification and valuation workshop, both of which were filled to capacity.

Brendan M. Laurs

First World Emerald Symposium

'Be Part of the Change' was the theme of the First World Emerald Symposium (WES), held at the Sheraton Convention Center in Bogotá, Colombia, 13–15 October 2015 (Figure 2). The advance registration was capped at 350 participants, and many more tickets were sold at the door (mostly to local Colombians), for a total attendance of 471. The WES was organized by the Colombian government and the Colombian emerald industry umbrella association Fedesmeraldas, an alliance of miners, manufacturers and wholesalers. The two most prominent corporate sponsors were Muzo International (Geneva, Switzerland) and Gemfields (London). Muzo International is the owner of the world-famous Muzo emerald mine, where they first began operations in 2009. Gemfields announced in September 2015 their acquisition of the historic Coscuez mine, some 10 km north of Muzo.

An important message from the WES is that, for the first time in history, Colombia is no longer the number-one producer of emerald in the world. Zambia now leads in annual emerald production by volume and by value. The precipitous drop in Colombia's emerald production is due to the lack of investment by Colombians in their mines.

Zambia's Minister of Mines, **Dr Christopher B. Yaluma**, spoke eloquently on his country's success in the emerald market. Unlike Colombia, where emeralds have been mined continuously for 1,500 years, emeralds were discovered relatively recently (1929) in Zambia. Next, the Vice-Minister of Mines for Colombia, **Dr Maria Isabel Ulloa**, focused on the scourge of 'illegal' emerald mining. By her estimate, half of the small-scale emerald miners in Colombia lack proper title to the land. In the miners' defence, government delays in issuing proper title under the updated mining law of 2012 have led to a three-year backlog in pending reviews and approvals. Minister Ulloa also stated that over 90% of the emerald licences are idle. **Dr Carolina Rojas Hayes** of the Colombian National Mining Agency reported that there were 1,496 exploration permits for some 7,500 prospectors, and another 359 licences for land parcels, with 178 parcels partially certified and another 49 under review. By her count, only two licences have been fully vetted, those of Gemfields and Muzo International.

Principals of coloured gemstone industry organizations discussed and then debated how guild organizations can promote business in a dynamic global market. ICA president **Benjamin Hackman** emphasized the need for full disclosure of treatments, saying: "Synthetic emeralds are better documented than natural emeralds that have been treated and enhanced." **Roland Naftule** with CIBJO highlighted the economic power of the emerging generation of millennials, and contrasted their motivations for buying gemstones and jewellery with those of the 'baby boomer' generation, leading to the creation of new market channels rewarding ample information and social consciousness. **Gerry Manning** with AGTA stressed the importance for national organizations to represent collective interests to both recalcitrant government regulators and hostile media. He said, "Misinformation is pandemic, and clarity is critical to value." Fedesmeraldas president **Oscar Baquero** hoped that the lasting impact of the WES would be closer coordination between Colombians and their international colleagues. Baquero reported officially that the 2014 emerald export for Colombia totalled US$145 million, derived from some 347 licences of which only 10% were active.

Figure 2: The theme of the First World Emerald Symposium was 'Be Part of the Change'. Here, Philippe Scordia discusses emerald selection criteria used by luxury jewellery brands. Photo by W. Rohtert.

International gemstone laboratories were well represented during an afternoon session. In summary, the labs are confident they can distinguish Colombian emeralds from those of other sources, and can differentiate synthetics as well. Admittedly, the cost of testing melee parcels is prohibitive, rendering a risk of blended stock escaping detection. Although technology permits the identification of specific emerald fillers, there is presently no systematic reportage for treatments, nor any plans for such structure. **Dr Thomas Hainschwang** (GGTL Laboratories, Balzers, Liechtenstein) reviewed the standards and protocols for verifying emeralds in gem labs, especially infrared spectroscopy to differentiate fillers and fluorescence

microscopy to map their distribution in a stone. **Kenneth Scarratt** (formerly of the GIA Laboratory in Bangkok, Thailand) spoke on the history of emerald enhancement, elucidating the multiple cycles of cleaning, treating and filling that any emerald might experience, as well as the breakdown over time of some fillers. **Shane McClure** (GIA Laboratory, Carlsbad) addressed the harmonization of reports, protocols and specific wording for emerald documentation. **Ronald Ringsrud**, speaking for Muzo International, focused on residues and other substances mistakenly classified as enhancements in emeralds—especially simple manufacturing residues. Ringsrud also delivered a passionate sermon on the importance of 'romance and glamour' as the driving factors in emerald sales, not scientific certificates. **Dr Dietmar Schwarz** (AIGS Lab, Bangkok) illustrated the many physical and chemical distinctions of Colombian emeralds as compared to those from other sources, notably their high Cr+V content and diagnostic three-phase inclusions, as well as characteristic growth features such as first-order prisms and pinacoids. **Carlos Julio Cedeño** (CDTEC Gemlab, Bogotá) provided insight into some of the unique crystallographic features of Colombian emeralds derived from their growth within open spaces in a hydrothermal environment.

Muzo International president **Charles Burgess** delivered a keynote address focusing on the social responsibility of a modern gem mining company. Burgess said that "six years of positive social transformation has been key to Muzo's commercial success" in Colombia. Corporate social responsibility is a foundation commitment, not an optional extravagance, he claimed. When they arrived at Muzo, they confronted a health-social-cultural crisis that was exacerbated by the modernization and mechanization of an historic mine site. There was a general lack of law and order, a legacy of rampant environmental damage, the constant risk of invasion by squatters and an absence of social services. To succeed, Muzo International assumed a proactive role normally assigned to government in addressing the challenges of unemployment, the need for schools and clinics, and support for the disabled and elderly. Muzo International financed outreach to the community and empowered women by financing local tailors to deliver clothing for miners, and by hiring women to engage in environmental restoration of the riparian environment along the Río Minero. Today, the mine employs over 600 workers and sustains a surrounding community of more than 2,500 people.

ICA director of communications **Jean Claude Michelou** spoke next on the traceability of coloured stones, with an update on ongoing initiatives and a way forward. He emphasized that documentation of provenance was critical to product branding and to building confidence with consumers. **Captain Torres** with the Colombian National Police then spoke on corporate and social traceability, and detailed the considerable capacity of the Colombian police and security forces in Boyacá, the state where the major emerald mines are located. **Jaime Loder** (Aegis Defense Services, London) and **Adam Brown** (Anuera Security, London) addressed private protection forces for the emerald industry in a high-risk environment, where safety originates in the village, and defence ultimately extends internationally to family, friends and business colleagues.

Another block of presentations concentrated mostly on the technical aspects of emeralds. **Dr Gaston Giuliani** (Centre de Recherches Pétrographiques et Géochimiques, Nancy, France) started the session with a review of the geology and gemmology of emerald deposits worldwide, highlighting laboratory determinative techniques for the differentiation of emeralds that are derived, ultimately, from differences in the style of mineralization. **Marcelo Ribeiro**, owner of the Belmont emerald mine in Minas Gerais, Brazil, gave a stunning presentation on their modern, mechanized, surface and underground, emerald mining operations. Belmont is a type example of how to correctly mine emerald deposits in South America, from the use of optic sorters to integration with a national marketing campaign. **Clarissa Maciel** (Brazilian Institute of Gems and Precious Metals, Brazilia) expounded on how her organization—a partnership between the government and private sector—promotes the gem business (including Belmont), nationally and internationally. **Warren Boyd** (R.T. Boyd Ltd., Oakville, Ontario, Canada) provided an interesting review and update on the geology and gemmology of the Malysheva emerald mine in the Ural Mountains of Russia. He noted that the 'seizure' of Malysheva from Canadian-owned Tsar Emerald Corp. coincided with Vladimir Putin's shell companies consolidating control over the remnants of the beryllium industry of the former Soviet Union. Malysheva is Russia's primary source of beryllium for their nuclear industry. Next, **Gary Bowersox** (GeoVision Inc., Honolulu, Hawaii, USA) covered the extensive history of emerald mining in Afghanistan, providing, as always, his own considerable personal experience in south-central Asia. He painted a hopeful picture of the Afghan emerald miners, emerging from decades of war, improving their lives and circumstances, despite difficulties that continue to this day. **This author** spoke next for SRK Consulting (a global mining engineering firm working with diamond, emerald, ruby and sapphire), describing

new mining and recovery tools and technologies useful in the Colombian emerald industry.

Vijay Kedia (Jewelers Association of Jaipur, India) recounted the Indian tradition with emerald of all origins and the market perception of Jaipur as one of the largest buyers and cutters. Left unresolved was the issue of blended melee parcels combined from multiple sources of supply. **Philippe Scordia** (Christian Dior Joaillerie, Paris, France) described the purchasing criteria, selection and certification of suppliers for luxury jewellery brands, and the increasing importance of provenance and social responsibility. Luxury designer **Erica Courtney** (Los Angeles, California, USA) illustrated how social media can be used to promote gems and jewellery, including emerald, to a new generation of media-saturated and techno-savvy buyers.

On the third and final day, **Jaime Rotlewicz** (C.I. Gemtec, Bogotá) began with a demonstration of acoustics and geo-gemmology, using various devices to amplify and record sonic signals, music and noise, from gemstone samples in his lab. **David Lihgtle** (The Wright Brothers, Dayton, Ohio, USA) re-emphasized the importance of global branding for service as well as product. **Gabriel Angarita**, a member of the WES organizing committee and president of the Colombian Association of Emerald Exporters, delivered a resounding review of Colombian emerald branding and lack of branding, ending with a plea for increased cooperation from all elements of the national industry. **Andy Lucas** (GIA, Carlsbad) gave a broadcast-quality still-and-video presentation on educating retailers and the global supply chain from mine to market, using specific examples from Asia and Africa.

Executive director of Gemfields **Sean Gilbertson** recounted the history of his company's activities in the coloured gemstone sector, focusing mainly on exploring and developing the Coscuez emerald district. **Dr Sixtus C. Mulenga** with Zambia's Extractive Industry Transparency Initiative considered the foundations for global gemstone growth to be honest and responsible practices.

Darwin Fortaleche, CDTEC Gemlab's chief gemmologist, presented research into a new emerald enhancement developed in Colombia, where the treatment of emeralds is routine and ever-evolving. **Oded Ben Shmuel** (Sarine Technologies Ltd., Kfar Saba, Israel) gave an update on his company's tools applicable to the emerald trade, borrowing new technology from the electronics and aerospace industries. **Dr Adolf Peretti** (GRS Gemlab, Lucerne, Switzerland) discussed his colour terminology for gem reports, and emphasized its use as a marketing and communication tool. **Hypone-Phyo Kan-Nyunt** (Gübelin Gem Lab Ltd., Hong Kong) detailed the ultra-trace-element analysis of emeralds through a combination of techniques. **Wei Ran** (National Gemstone Testing Center [NGTC], Beijing, China) concluded the WES with a description of emerald investigations underway in the Research Department at NGTC.

A post-conference field trip brought participants to various emerald mines in Colombia. Although the symposium was organized rather quickly, it came together with resounding success.

William Rohtert (william.rohtert@cox.net)
William Rohtert Consulting LLC
Phoenix, Arizona, USA

and FEEG Symposium

Gem-A Conference

incorporating the 18th Federation for European Education Symposium

The annual Gem-A Conference took place in London on 21–22 November 2015, and was attended by 190 people from 20 countries.

The event was introduced by Gem-A's interim CEO **Nick Jones**. Then, **Jörg Gellner** (Gellner, Bochum, Germany) provided a detailed description of pearl quality factors, which he referred to as the '5 S's': size, shape, shade, surface and shine. He gave the typical size ranges of various types of cultured pearls, and for each millimetre above the benchmark size he said the value should be adjusted by +35%. For shape, round is ideal and all other shapes correspond to reductions in value except for matched pairs of drop shapes, which are adjusted by +150%–200%. For shade (colour), different value factors are applied for white or black cultured pearl varieties (e.g. South Sea or Tahitian). Surface is evaluated according to 'spot level', with five categories differing in their value factors by 1.5× (e.g. 100% for no spots and 67% for the next category of lightly spotted). Shine (lustre) is also adjusted by 1.5× between categories, of which there are four (AAA, AA, A and B).

Jean Pierre Chalain (Swiss Gemmological Institute SSEF, Basel, Switzerland) recounted the history of developments surrounding the identification of HPHT-

treated diamonds. After the 1999 announcement by General Electric (GE) and Lazare Kaplan International about their 'undetectable' and 'permanent' diamond decolorization process, a close collaboration between SSEF and researchers from various centres including the University of Nantes and CIBJO laboratories helped develop, one year later, final identification criteria. Additional collaborations with De Beers and the Natural Historic Museum of Vienna later helped in consolidating the identification criteria of HPHT-treated type Ia diamonds.

Adolf Peretti (GRS GemResearch Swisslab Ltd., Lucerne, Switzerland) surveyed some commercially important ruby and sapphire sources, including Myanmar (Mogok and Mong Hsu), Madagascar (Didy and Ilakaka), Sri Lanka (Kataragama), Cameroon, Kashmir, Tanzania (Winza), Vietnam (Luc Yen), Tajikistan and Mozambique. The availability of abundant rough material from Mozambique has allowed the cutting of large ruby suites that were previously very difficult and time consuming to put together. Peretti showed video clips from his visits to some of the mines, and also screened a film that documented the cutting of a notable Mozambique ruby.

Dr Ilaria Adamo (Italian Gemmological Institute, Milan) reviewed the geology and gemmology—including origin determination—of demantoid sources. Serpentine-associated deposits are found in Russia (central Ural Mountains), Italy (Val Malenco), Pakistan (Kaghan Valley and Baluchistan) and Iran (Kerman Province), while skarn-hosted occurrences are in Namibia (Erongo) and Madagascar (Antetezambato). Adamo noted several differences according to the two source types, including their inclusions, reaction to heat treatment and chemical composition.

Dr Paul Rustemeyer (Gundelfingen, Germany) documented colour zoning and growth phenomena in tourmaline crystals. Colourful photographs of slices oriented both perpendicular and parallel to the c-axis showed a wide variety of features, including sequential and face-selective incorporation of chromophore ions, parallel crystal aggregates, re-growth or 'healing', corrosion intervals and delta structures corresponding to the appearance of a second colour phase crystallizing on the same face.

Dr Raquel Alonso-Perez (Harvard Mineralogical & Geological Museum, Cambridge, Massachusetts, USA) examined the historic Hamlin Collection of tourmalines from Mount Mica, Maine, USA. Raman spectra showed four peaks in the 3650–3450 cm^{-1} region (corresponding to OH-stretching vibrations) that could be correlated to the colour of the tourmalines.

Figure 3: Australia's Lightning Ridge mining area is the source of these black opals (~2–70 ct). Courtesy of Cody Opal Australia Pty. Ltd.; photo by Damien Cody.

Andrew Cody (Cody Opal Australia Pty. Ltd., Melbourne, Victoria, Australia) reviewed the global sources of opal, including Australia (e.g. Figure 3), Brazil, Ethiopia, Honduras, Mexico, Indonesia, Slovakia and USA. He indicated that Australia's opal production was formerly worth US$500 million/year, and although many deposits have played out, Australia still supplies 90% of the world's opal by value.

Grant Hamid (Hamid Bros. Gem Merchants, Melbourne) reviewed important historical developments in the sources, supply, treatment and synthesis of gem corundum. He also showed how possessing good gemmological knowledge can be helpful for one's business: he bought a 7.44 ct 'synthetic sapphire' cabochon for $300, and upon examining its inclusions he discovered it was actually a natural Kashmir sapphire.

Richard Drucker (Gemworld International Inc., Glenview) discussed various issues of current interest in the gem trade: coloured stone treatments; nomenclature issues surrounding colour terminology (on lab reports), geographical origin and trade names for gem varieties; and recent developments in synthetic diamond growth and production.

Martin Steinbach (Steinbach – Gems with a Star, Idar-Oberstein, Germany) covered asterism in gems, noting that 50 gem varieties are known to display asterism when cut as cabochons or spheres, and in 90% of the cases the star is due to rutile 'silk'. He described several famous star rubies and sapphires, and also showed examples of rarities as well as asterism resulting from treatments.

Fabian Schmitz (German Gemmological Association, Idar-Oberstein) provided an overview of the coloration and identification of natural and synthetic quartz. The various colours shown by quartz are due to colour centres (natural as well as laboratory-induced) and inclusions. In general, synthetic quartz may show swirl-like colour zoning, 'breadcrumb' inclusions or a seed plate, while natural quartz can display twin structures. Infrared spectroscopy is useful for separating them, but it is important to look at the entire spectrum rather than just one portion of it.

Shane McClure (GIA Laboratory, Carlsbad) described various oddities and scams that he has encountered in the GIA Laboratory over the years. Some standouts include 'rainbow calsilica' from Mexico consisting of dyed colour-banded calcite of an unknown (but clearly manufactured) origin; 'night-glowing pearls' that display strong green fluorescence and phosphorescence due to a coating containing rare-earth elements; various fake mineral specimens and gem crystals; and 'Arabian sand diamonds' consisting of quartz pebbles that were collected in Saudi Arabia by unsuspecting clients and then supplied to a gem cutter, with the resulting 'gems' actually being faceted cubic zirconia.

After the conference, three workshops covered coloured stone grading and pricing, visual optics and pearls, and private museum tours brought participants to the Natural History Museum (gem and mineral collection), the Tower of London (British Crown Jewels) and the Victoria and Albert Museum (Bejewelled Treasures: The Al Thani Collection).

Brendan M. Laurs

GSA 2015

A session on various aspects of research on gem materials was organized by GIA at the 2015 annual meeting of the Geological Society of America (GSA) in Baltimore, Maryland, on 1–4 November 2015. Abstracts of the oral presentations can be viewed at https://gsa.confex.com/gsa/2015AM/webprogram/Session37638.html, and poster session abstracts are available at https://gsa.confex.com/gsa/2015AM/webprogram/Session38771.html.

The talks were led off by **Dr George Harlow** (American Museum of Natural History, New York, New York), who cited three examples where the study of gem minerals has benefited from recent advances in the geological sciences. Occurrences of jadeite jade are related to particular formation conditions that are created by continental subduction. The trace-element study of ruby and sapphire using laser ablation–inductively coupled plasma–mass spectrometry has provided a new approach to understanding the geological environments (igneous and metamorphic) of gem corundum. Large gem-quality forsterite (peridot) crystals appear to grow from hydrous fluids along tension gashes in igneous dunite bodies.

In a presentation made in the absence of a speaker who could not attend the conference, **Dr Wuyi Wang** (GIA Laboratory, New York) described the occurrence of the silicon-vacancy defect in synthetic diamonds, which can be detected by photoluminescence spectroscopy, and which represents one of the most diagnostic features of synthetic diamonds grown by the chemical vapour deposition method.

Dr Karen Smit (GIA Laboratory, New York) and co-authors investigated sulphide inclusions in rare, bright-yellow type Ib diamonds from the Zimmi region of Sierra Leone. Re-Os isotopic compositions of the inclusions give a Pan-African diamond-growth age (~650 million years ago) that correlates with the assembly of the Gondwana supercontinent.

Dr Steven Shirey (Carnegie Institution of Washington, Washington DC, USA) and co-authors described the study of mineral inclusions in diamonds from the Juina area of Brazil, which are rather unique geologically because of their 'superdeep' origin (below the lithosphere from depths of 300–800 km). Such diamonds from the Collier 4 kimberlite are believed to have crystallized from carbonatitic melts derived from the recycling of oceanic lithosphere.

Using an 1851 plaster cast and a modern cubic zirconia replica of the original facet shape of the famous Koh-i-Noor diamond (now a 105.6 ct oval-cut stone in the Coronation Crown of the British Crown Jewels), **Alan Hart** of The Natural History Museum in London described how directional hardness anisotropy was a major constraint to the ancient polishing of the so-called Mogul-cut form of this diamond. Although a centrepiece display of the 1851 Great Exhibition in London, this diamond proved a visual disappointment to many exhibit visitors due to its lack of fire and brilliance, and it was subsequently recut to its present form.

Dr Keal Bryne (Smithsonian Institution, Washington DC) and co-authors investigated the luminescence behaviour of two classes of diamonds that exhibit a colour change when exposed to different

temperatures or light sources. Pink/brown diamonds display luminescence reactions that appear related to optical defects associated with their coloration. So-called chameleon diamonds display a characteristic luminescence peak centred near 560 nm with an intensity that is strongly temperature-sensitive.

The Hamlin Necklace, a unique 19th century jewellery piece containing tourmaline and beryl from Mount Mica in Maine, USA, was investigated by **Dr Raquel Alonso-Perez** (Harvard University, Cambridge, Massachusetts, USA). She used Raman spectroscopy and non-destructive chemical analytical methods to prove that the tourmalines in the necklace are elbaite.

Dr Aaron Palke (GIA Laboratory, Carlsbad) and co-authors documented glassy melt inclusions in alluvial sapphires from Montana. These sapphires are believed to have a metamorphic origin followed by transport to the surface in rhyolitic to dacitic volcanic eruptions. The melt inclusions are hypothesized to be the product of partial melting during high-grade metamorphism of the parent rock, which produced a silica-rich melt and an alumina-rich residue from which the sapphires crystallized.

John Koivula (GIA Laboratory, Carlsbad) and co-authors heated two kinds of synthetic rubies and sapphires in air at temperatures above 1,800°C, and were able to produce partially healed fractures (e.g. Figure 4) and web-like parting planes. These features display a similar appearance to those seen in heat-treated gem corundum that has been interpreted by gemmologists as having been formed during a flux-healing process. The authors conclude that if no contradictory visual evidence exists, synthetic gem corundum containing these visual features could erroneously be mistaken for heat-treated natural gems.

Dr Laurent Cartier (Swiss Gemmological Institute SSEF, Basel) and co-authors discussed the potentially valuable information that DNA testing can reveal about the formation conditions of organic gems such as pearl, coral and ivory that are the result of biomineralization processes. In the case of pearls (cultured or natural), the analytical method has been improved so that it is quasi-non-destructive. This method can provide information on the oyster species, and also geographic origin.

Xiayang Lin and **Dr Peter Heaney** (Pennsylvania State University, University Park, USA) reported on quartz crystals that display natural iridescence from cavities in the Deccan Trap basalts of India. The small iridescent *z* faces exhibit tiny periodic ridges visible with the atomic force microscope, and these ridges act as a diffraction grating for visible light. Non-iridescent *r* faces lack these periodic ridges. The authors interpret the formation of the surface topography of the *z* faces as the result of preferential dissolution.

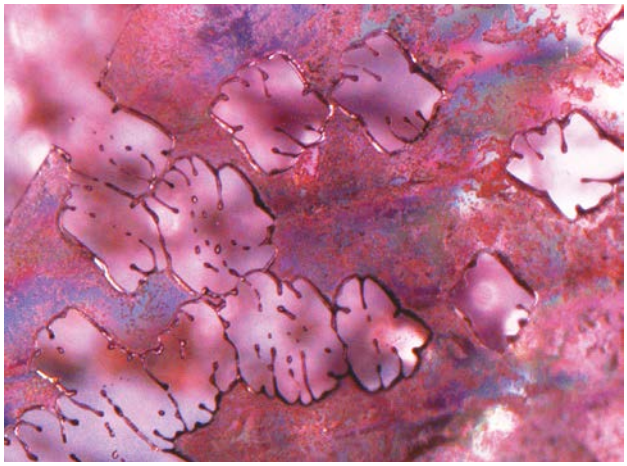

Figure 4: This crack in a Czochralski-pulled pink synthetic sapphire was partially healed by heating the gemstone in air at temperatures exceeding 1,800 °C. Photomicrograph by John I. Koivula/GIA; image width ~0.30 mm.

Yury Klyukin (Virginia Institute of Technology, Blacksburg, USA) and co-authors investigated emeralds from the North American Emerald mine (at the former Rist mine site) near Hiddenite, North Carolina, USA. The gems occur in cavities associated with quartz, muscovite and carbonate minerals. The emeralds have fluid inclusions that contain two fluid phases (CO_2-rich and H_2O-rich). The presence of a CO_2-rich fluid suggests that the emeralds formed in a medium-grade metamorphic environment.

Dr William Simmons (Maine Mineral and Gem Museum, Bethel, USA) and co-authors described gem pollucite from the Mount Mica pegmatite near Oxford, Maine. The dyke is cavity-rich, averaging one pocket about every three metres. Gem-quality pollucite is rare in pegmatites, but one pocket found in 2014 contained a number of strongly-etched crystals measuring 2–3 cm in diameter.

The final oral presentation was made by **Dr Michael Wise** (Smithsonian Institution, Washington DC), who reported on emerald and hiddenite (Cr-bearing spodumene) deposits near Hiddenite, North Carolina. Both minerals occur in quartz-carbonate Alpine-type veins within Precambrian migmatitic schists and gneisses. The gems appear to have been formed from hydrothermal fluids under low-temperature (<250°C) and low-pressure (~1 kbar) conditions. The host rocks are the most likely source of Cr, and local outcrops of granitic rocks provide evidence for the Be needed for emerald mineralization. However, recent discoveries of aquamarine in leucosomes within the migmatite indicate that the latter rocks may provide an alternative source of Be.

James E. Shigley (jshigley@gia.edu)
GIA, Carlsbad, California, USA

An innovator in gemstone reporting

• Identification of colored gemstones • Country of origin determination • Full quality and color grading analysis

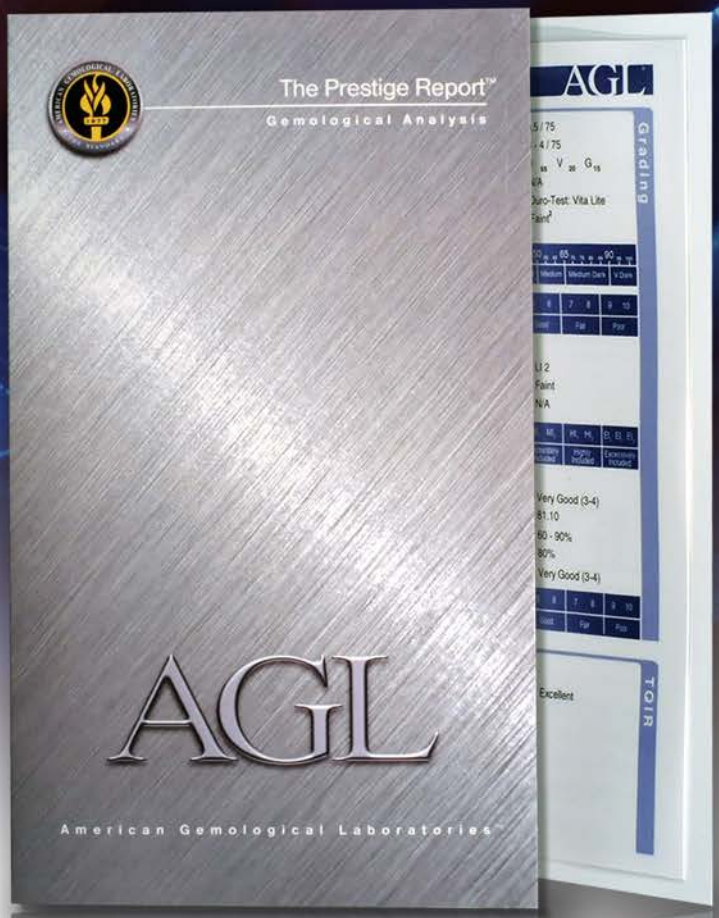

AMERICAN GEMOLOGICAL LABORATORIES AGL

580 5th Ave • Suite 706 • New York, NY 10036, USA
www.aglgemlab.com • +1 (212) 704 - 0727

Gem-A Notices

GEM-A CONFERENCE AND 18th INTERNATIONAL FEEG SYMPOSIUM

The 2015 Gem-A Conference and 18th International Federation for European Education in Gemmology (FEEG) Symposium was held at Royal Institute of British Architects in Portland Place, London, on 21 and 22 November. A full report of the Conference and events was published in the January/February 2016 issue of *Gems&Jewellery*. Highlights of the presentations are given in the Conferences section, pages 716–718.

Seminars and workshops were presented on 23 November at the Gem-A headquarters. Visits were arranged on 24 November to the Victoria and Albert Museum to see 'Bejewelled Treasures: The Al Thani Collection', to the Natural History Museum for a guided tour of the Mineral Gallery, and to the Tower of London for a private viewing of the Crown Jewels.

Conference Sponsors and Supporters

The Association is most grateful to the following for their support:

Platinum Sponsor

Jewelry Television (JTV)
www.jtv.com

Silver Sponsors

American Gemological Laboratories (AGL)
www.aglgemlab.com

AnchorCert Gem Lab
www.anchorcert.co.uk

Canadian Gemmological Association
www.canadiangemmological.com

Gemworld
www.gemguide.com

Marcus McCallum FGA
www.marcusmccallum.com

Bronze Sponsors

Fellows Auctioneers & Valuers
www.fellows.co.uk

T.H. March, Insurance Brokers
www.thmarch.co.uk

We would also like to thank **DG3 Diversified Global Graphics Group** for sponsoring conference materials.
www.dg3.com

GRADUATION CEREMONY

The Graduation Ceremony and Presentation of Awards for both Gem-A and FEEG was held at the Mermaid Conference and Events Centre, Puddle Dock, Blackfriars, London, on 23 November.

Nick Jones, Interim Chief Executive Officer of Gem-A, opened the ceremony by welcoming those present. **Kathryn Bonanno** (pictured right), a newly-elected Gem-A Trustee, addressed the graduates before presenting the Gem-A diplomas and awards.

Dr Loredana Prosperi, president of FEEG, introduced the FEEG delegates and presented the diplomas to the FEEG graduates.

Gem-A president **Harry Levy** gave the closing remarks before graduates and guests enjoyed a reception in a room overlooking the River Thames.

GIFTS TO THE ASSOCIATION

The Association is most grateful to the following for their gifts for research and teaching purposes:

John Bradshaw, Coast-to-Coast Rare Stones International, Nashua, New Hampshire, USA, for 21 bags containing part-cut crystals of: apatite (Canada and Mexico), cassiterite (Namibia), celestine (Kansas, USA), cerrusite (Namibia), crocoite (Tasmania, Australia), diaspore (Turkey), oligoclase (Kenya), pollucite (Conneticut, USA), scheelite (Pakistan and Arizona, USA), smithsonite (Namibia), sphalerite (Spain), tourmaline (Maine, USA, and Afghanistan), tugtupite (Greenland), willemite/leucophoenicite (New Jersey, USA) and zincite on calcite (New Jersey); and also for 95 faceted mixed-shape tourmalines, mostly pink, green and blue.

From the estate of **Ingeborg Bratman**, a large collection of rough and fashioned gem materials.

Boris Brianceau, Nantes, France, for large faceted samples of fluorite and amethyst.

Andrew Cody, Cody Opal, Melbourne, Australia, for copies of the book *The Opal Story: A Guidebook* (with DVD) by Andrew and Damien Cody, to sell at the Gem-A Conference, which raised a total of £630.

Roy Duran, Finer Jewelry Inc., Chicago, Illinois, USA, for assorted orange and colour-change sapphires; small Colombian emerald crystals; a carved amethyst; a jadeite bead; cabochons of synthetic ruby, tourmaline and 'white garnet'; and faceted aquamarine, garnet, peridot and sapphire.

Kwong Pui Ho (John Ho), Yangon, Myanmar, for assorted Ammolite, chrome tourmaline, hackmanite, thorite and ruby-in-quartz; rough amber, apatite, corundum, gypsum, jadeite, mica, moonstone, pollucite and tourmaline; crystals of spinel and zircon; cabochons of hematite, kyanite, opal and pargasite; and faceted quartz, spinel and tanzanite.

Alistair Laidlaw and **Christine Marsden**, Fort Augustus, Scotland, for a copy of *Dreams of Diamonds* authored by them.

Bill Larson, Palagems.com, Fallbrook, California, USA, for rough pieces of iridescent andradite from Mexico and a slab of jadeite from Russia.

Claire Mitchell FGA DGA, London, for a reconstituted malachite/azurite, two reconstituted turquoises, two sugilite simulants, and rough and cabochon-cut samples of omphacite jade from Val Pellice-Alpi Cozie, Piemonte-Nord, Italy.

Dominic Mok FGA DGA, AGIL, Hong Kong, for a jadeite colour master set guide.

Saeko Nasao, Fukushima, Japan, for rough opal.

Adolf Peretti FGA, GemResearch Swisslab Ltd., Lucerne, Switzerland, for four issues of his book *Contributions to Gemology* (Nos. 4, 5, 7 and 11) to sell at the Gem-A Conference, which raised a total of £290.

Prof. Chiu Mei Ou Yang FGA, Hong Kong Institute of Gemmology, for a selection of jadeites of various colours and trade names.

Michiko Shimomura FGA, Tokyo, Japan, for a copy of *The Book of the Pearl: The History, Art, Science and Industry of the Queen of Gems* by George Frederick Kunz and Charles Hugh Stevenson.

Tay Thye Sun FGA, Far East Gemological Laboratory, Singapore, for several pieces of tumbled amber.

MEMBERSHIP

At a meeting of the Council held on 9 October 2015, Diploma graduates of the examinations held in June 2015 (included in lists on pages 723–733) were elected or transferred to Fellowship or Diamond Membership as appropriate.

At a meeting of the Council held on 4 November 2015 the following were elected to membership:

Fellowship and Diamond Membership (FGA DGA)

Feng Wei, *Guangzhou, Guangdong, P.R. China*
Pei Yu, *Beijing, P.R. China*

Fellowship (FGA)

Hsu Yen Hsin, *Taipei City, Taiwan, R.O. China*
Reuser, Laetitia, *Amsterdam, The Netherlands*

Diamond Membership (DGA)

Wong Ching Man, *Discovery Bay, Hong Kong*

Associate Membership

Brown, Victoria, *Edinburgh*
Fiebig, Jim, *West Des Moines, Iowa, USA*
Quigg, Gloria, *Tucson, Arizona, USA*

At a meeting of the Council held on 23 November 2015 the following was elected to membership:

Corporate Membership

Fabula, *Thornhaugh, Cambridgeshire*

GEM-A AWARDS

In the Gem-A examinations held in January, February and June 2015, 413 students qualified in the Gemmology Diploma examination, including 36 with Distinction and 51 with Merit, and in the Foundation Certificate in Gemmology examination 606 qualified. In the Gem Diamond examination 135 qualified, including 19 with Distinction and 22 with Merit.

In the **Gemmology Diploma** examinations the **Christie's Prize for Gemmology** for the best candidate of the year was awarded to **Mei Mei Sit** of Central, Hong Kong. The **Anderson Bank Prize** for the best set of theory papers was awarded to **Emilie Disner** of Geneva, Switzerland. The **Read Practical Prize** for excellence in the practical examination was awarded to **Ka Yi Man** of Hong Kong.

In the **Foundation Certificate in Gemmology** examination, the **Anderson Medal** for the candidate who submitted the best set of answers which, in the opinion of the examiners, were of sufficiently high standard, was awarded to **Christina Khoudian** of Colchester, Essex.

In the **Diamond Diploma** examination, the **Bruton Medal** for the best set of theory answer papers of the year was awarded to **Valentina Molon** of Varese, Italy.

The **Deeks Diamond Prize** for the best candidate of the year was awarded to **Kathryn Williams** of Dover, Kent.

The **Diamond Practical Prize** for excellence in the Diamond Practical examination, sponsored by Dominic Mok from AGIL, Hong Kong, was awarded to **Louise Van Colen** of Montreal, Quebec, Canada.

The **Tully Medal** was not awarded.

The names of the successful candidates are listed below.

Examinations in Gemmology

Gemmology Diploma

Qualified with Distinction

Aron-Brunetiere, Patricia, *Raray, France*
Arrive, Elodie Jacquinot, *Annecy, France*
Bai Qing, *Beijing, P.R. China*
Beaumont, Elizabeth, *Montreal, Quebec, Canada*
Chow Hiu Yan Bona, *Central, Hong Kong*
Griziot, David, *Marseille, France*
Guay, Richard, *Saint-Justin, Quebec, Canada*
Herbin, Thomas, *Lésigny, France*
Ito, Claire, *Carlsbad, California, USA*
Jacmain, Irina, *Noisy-le-Sec, France*
Jin Xinyu, *Beijing, P.R. China*
Jonas, Helen C., *Shellingford, Oxfordshire*
Lai Hsin Han, *Kaohsiung City, Taiwan, R.O. China*
Lam Wai Chun, *Tuen Mun, Hong Kong*
Li Huan, *Beijing, P.R. China*
Liu, Dan, *Yongxiu, Jiangxi, P.R. China*
Nian Bofeng, *Shanghai, P.R. China*
Qi Zhaohui, *Beijing, P.R. China*
Qiao Lei, *Beijing, P.R. China*
Quan Xiaoyun, *Beijing, P.R. China*
Reich, Mary, *Albuquerque, New Mexico, USA*
Ren Weina, *Beijing, P.R. China*
Shen Jingyao, *Beijing, P.R. China*
Sit Mei Mei, *Central, Hong Kong*
Smith, Fiona, *Hoddesdon, Hertfordshire*
Soonthorntantikul, Wasura, *Bangkok, Thailand*
Tian Xiufang, *Beijing, P.R. China*
Wang Tian Xin, *Tiu Keng Leng, Hong Kong*
Williamson, Anna Frances, *Hamilton, New Zealand*
Wu Oi Lam, *Kwai Chung, Hong Kong*
Ying Zongqi, *Le Pontet, Vaucluse, France*
Yong Chenying, *Beijing, P.R. China*
Zhang Chen, *Shanghai, P.R. China*
Zhang Hongqing, *Beijing, P.R. China*
Zhang Yiwen, *Beijing, P.R. China*
Zhao Tian, *Beijing, P.R. China*

Qualified with Merit

Au Cheuk Yin, *Yuen Long, Hong Kong*
Bailey, Rachel, *Edinburgh*
Barrett, Andrew, *Sliema, Malta*
Bernard, Edmund, *Clanfield, Oxfordshire*
Burton, Amy Louise, *London*
Caplan, Candice, *Monnetier, France*
Chang Xing, *Shanghai, P.R. China*
Chen Naixi, *Huangshi, Hubei, P.R. China*
Deng Yihong, *Beijing, P.R. China*
Disner, Emilie, *Geneva, Switzerland*
Dong Yiyuan, *Beijing, P.R. China*
Dufour, Jean Yves, *Velaux, France*
Guo Rui, *Beijing, P.R. China*
Guo Yilin, *Beijing, P.R. China*
Huang Chanyuan, *Beijing, P.R. China*
Huang I-Ping, *New Taipei City, Taiwan, R.O. China*
Huang Shu, *Beijing, P.R. China*
Huang Yi, *Beijing, P.R. China*
Izzard, Georgina Sara, *Stansted, Essex*
Ji Bin, *Rizhao, Shandong, P.R. China*
Lam Lai Yuen, *Tseung Kwan O, Hong Kong*
Lei Kaixi, *Wuhan, Hubei, P.R. China*
Lei Yunqing, *Heyuan, Guangdong, P.R. China*
Lemoine, Mathilde, *Vouziers, France*
Levenez, Orianne, *La Forêt-Fouesnant, France*
Li Yanbin, *Beijing, P.R. China*

Li Zhechen, *Beijing, P.R. China*
Lin Moqing, *Tseung Kwan O, Hong Kong*
Li Yu-Chun, *Taipei City, Taiwan, R.O. China*
Ma Sin Yue, *Kowloon, Hong Kong*
Pan Yanmei, *Beijing, P.R. China*
Renfro, Nathan, *Carlsbad, California, USA*
Shi Jiaqing, *Beijing, P.R. China*
Shi Shuang, *Beijing, P.R. China*
Simard, Camille, *Voinsles, France*
Song Qingzhuo, *Shanghai, P.R. China*
Suzuki, Mari, *Ginowan City, Okinawa, Japan*
Tan Yongting, *Beijing, P.R. China*
Tang Kit Yui Jo Jo, *Shatin, Hong Kong*
Wang Juan, *Shanghai, P.R. China*
Wang Sisi, *Beijing, P.R. China*
Wen Xinyu, *Beijing, P.R. China*
Wu Xuxu, *Beijing, P.R. China*
Xu Huanling, *Wuhan, Hubei, P.R. China*
Yang Yanfei, *Beijing, P.R. China*
Zhang Linqi, *Beijing, P.R. China*
Zhang Peng, *Shanghai, P.R. China*
Zhang Yu, *Beijing, P.R. China*
Zhao Zhiyang, *Shanghai, P.R. China*
Zheng Tianyu, *Beijing, P.R. China*
Zhu Qianwen, *Shanghai, P.R. China*

Qualified

Aubert, Lea, *Caen, France*
Azad, Ahmed Anfas, *Colombo, Sri Lanka*
Badjan De Junnemann, Johanna, *Doussard, France*
Bai Qiuwen, *Wuhan, Hubei, P.R. China*
Bassil, Sophie-Marie, *Malakoff, France*
Batisse, Sylvia, *Gallardon, France*
Bayar, Mikail, *Le Coteau, France*
Beard, Thomas Whitbread, *Eastbourne, East Sussex*
Belahlou, Fatima, *Nimes, France*
Blanchard, Alain, *Paris, France*
Boemo, Julien, *Lorraine, France*
Brukås, Silje, *Bergen, Norway*
Buldanlioglu, Gulgun, *Istanbul, Turkey*
Bullmore, Elizabeth, *Birmingham, West Midlands*
Burden, Maxwell Jasper, *Birmingham, West Midlands*
Carriere, Elle Laurence, *Montreal, Quebec, Canada*
Chamberlain-Adams, Jemima Prudence, *London*
Chang Cheng-Yi, *Taichung City, Taiwan, R.O. China*
Chang Tsui Ping, *New Taipei City, Taiwan*
Chang Yu Chen, *Kaohsiung City, Taiwan*
Charanas, Georgios, *Athens, Greece*
Chen Hsiu-Man, *New Taipei City, Taiwan, R.O. China*
Chen Ming-Hsueh, *I Lan Hsien, Taiwan, R.O. China*
Chen Muyu, *Guilin, Guangxi, P.R. China*
Chen Qiao, *Beijing City, P.R. China*
Chen Qingying, *Xiamen, Fujian, P.R. China*
Chen Ruoxi, *Changsha, Hunan, P.R. China*
Chen Zhi Sang, *Beijing, P.R. China*
Chen Zhu, *Beijing, P.R. China*
Chen Fei, *Guangzhou, Guangdong, P.R. China*
Cheng Tzu Shan, *New Taipei City, Taiwan, R.O. China*
Cheng Yi Jing, *New Taipei City, Taiwan*
Cheng Xiaochuan, *Wuhan, Hubei, P.R. China*
Cheung Hoi Fun, *Homantin, Hong Kong*
Chiu Ti, *New Taipei City, Taiwan, R.O. China*
Chong Yim Mui, Cristy, *Tseung Kwan O, Hong Kong*
Chou Yu Chu, *Taichung City, Taiwan*
Cisamolo, Marie-Cecile, *Geneva, Switzerland*
Cohen, Jason, *East Barnet, Hertfordshire*
Cornelius, Victoria, *London*
Courrance, Maxence, *Aix-en-Provence, France*
Craig, Deborah Susan, *Sundbyberg, Sweden*
Dai Jun, *Kunshan, Jiangsu, P.R. China*
Dai Xinru, *Wuhan, Hubei, P.R. China*
De Bourgues, Ayena Julia, *Oron-la-Ville, Switzerland*
De Zoysa Jayatilleke, Liyana Gracelyn, *Colombo, Sri Lanka*
Deijen, Stephanie Elisabeth, *Amsterdam, The Netherlands*
Delaye, Aline, *Singapore, Singapore*
Desmortiers, Patricia, *Paris, France*
Dharmadasa, Etsushi, *NagoyaCity, Aichi, Japan*
Dong Shujun, *Beijing, P.R. China*
Dong Xinyu, *Xiamen, Fujian, P.R. China*
Duffy, Alexander, *Sutton Coldfield, West Midlands*
Earl, Jeremy, *Kettering, Northamptonshire*
Emanuelli, Odile, *Ivry-sur-Seine, France*
Fan Deng, *Guilin, Guangxi, P.R. China*
Fan Hing Wan, *Hung Hom, Hong Kong*
Fan Mingyue, *Shanghai, P.R. China*
Fang Liqun, *Beijing City, P.R. China*
Fang Xia, *Guangzhou, Guangdong, P.R. China*
Fang Yuyu, *Hangzhou, Zhejiang, P.R. China*
Fateeva, Tatiana, *Cannes, France*
Fauquet, Richard, *Courbevoie, France*
Fong Lap Kit, *Yuen Long, Hong Kong*
Foxwell, Kim, *Twickenham, Middlesex*
Francey, Jacob Colin, *London*
Fukuda, Noriko, *Tokyo, Japan*
Fung Hoi Ching, *Yuen Long, Hong Kong*
Gandhi, Hemang, *Mumbai, India*
Gangloff, Juliette, *Fos, France*
Gauthier, Diane, *Montreal, Quebec, Canada*
Giacobetti, Tom, *Carouge, Switzerland*
Girardet, Marine, *Paris, France*
Gong Qingxu, *Dalian, Liaoning, P.R. China*
Gong Hancheng, *Wuhan City, Hubei, P.R. China*
Gozlan, Esther, *Paris, France*
Gui Fu, *Guilin, Guangxi, P.R. China*
Guo Zheng, *Wuhu, Anhui, P.R. China*
Guy, Angharad, *London*
Gyde, John Mark Andrew, *Abingdon, Oxfordshire*
Hall, Claire-Louise, *Newcastle-upon-Tyne, Tyne and Wear*
Han Hou, *Beijing, P.R. China*
Han Jiayang, *Beijing, P.R. China*
Han Jie, *Nanchang City, Jiangxi, P.R. China*
Hantamanirisoa, Christiane, *Antananarivo, Madagascar*
Hao Haiyan, *Zhanjiang City. Guangdong, P.R. China*
He Chin Ju, *Kaohsiung City, Taiwan, R.O. China*
He Jiao, *Guiyang, Guizhou, P.R. China*
Heath, Caitlin Rose, *Montreal, Quebec, Canada*

Hein Naing Oo, *Yangon, Myanmar*
Hergott, Laurianne, *Obernai, France*
Higgo, Emma Grace, *Hindhead, Surrey*
Hnin Wutyi Soe, *Yangon, Myanmar*
Ho Wingyan Joyce, *Brooklyn, New York, USA*
Hou Yancheng, *Wuhan, Hubei, P.R. China*
Htaik, Hay Man Than, *Yangon, Myanmar*
Hu Aning, *Guilin, Guangxi, P.R. China*
Huang Li-Lien, *New Taipei City, Taiwan, R.O. China*
Huang Lingxi, *Guilin, Guangxi, P.R. China*
Huang Sipei, *Ezhou, Hubei, P.R. China*
Huang Ying, *Beijing, P.R. China*
Huang Yue, *Suzhou, Jiangsu, P.R. China*
Hui Xue, *Beijing, P.R. China*
Hung Tzu Chun, *Hsinchu City, Taiwan, R.O. China*
Hung Hoo, *Tsuen Wan, Hong Kong*
Huo Xiaobing, *Shijiazhuang, Hebei, P.R. China*
Jia Qiong, *Dalian, Liaoning, P.R. China*
Jiang Dong, *Beijing, P.R. China*
Jiang Haiyan, *Shanghai, P.R. China*
Jiang Xiaowen, *Shanghai, P.R. China*
Jiang Xueqin, *Shanghai, P.R. China*
Juo Shiou Fang, *Taichung City, Taiwan*
Kadigamuwa, Nethmin Kasun, *Kandy, Sri Lanka*
Kagan, Thierry, *Neuilly-sur-Seine, France*
Katsurada, Yusuke, *Tokyo, Japan*
Knuckey, Samantha Una, *Prestbury, Cheshire*
Korcia, Sandrine Bettane, *Marseille, France*
Lassau, Clothilde, *Cartigny, Switzerland*
Law, Suang See, *Singapore, Singapore*
Layton, Janina Sarah, *London*
Leclerc, Thibault, *Gland, Switzerland*
Leduc, Gabrielle-Ann, *Rouyn-Noranda, Quebec, Canada*
Lee, Ji-Eun, *Montreal, Quebec, Canada*
Lee Kun Tai, *Kaohsiung City, Taiwan, R.O. China*
Legros, Maria S., *New York, New York, USA*
Leung Man Shu, Elsa, *Mid Levels, Hong Kong*
Lewis, Rhiannon, *Birmingham, West Midlands*
Lhuaamporn, Thanapong, *Bangkok, Thailand*
Li Rong, *Beijing, P.R. China*
Li Shanshan, *Beijing, P.R. China*
Li Shiu Chin, *New Taipei City, Taiwan*
Li Wen, *Beijing, P.R. China*
Li Wenzhuo, *Wuhai, Hubei, P.R. China*
Li Yikun, *Guilin, Guangxi, P.R. China*
Li Zhen, *Guilin, Guangxi, P.R. China*
Li Zhenjia, *Beijing, P.R. China*
Liang Dongkang, *Wuhan, Hubei, P.R. China*
Liang Ning, *Beijing, P.R. China*
Liang Chaoying, *Wuhan, Hubei, P.R. China*
Liechti, Rupa, *Elstree, Hertfordshire*
Lin Yi Ping, *Taoyuan City, Taiwan*
Lin Yu-Jie, *New Taipei City, Taiwan, R.O. China*
Ling Tung-Wei, *Taipei City, Taiwan, R.O. China*
Liu Cheng Fang, *Kaosiung City, Taiwan, R.O. China*
Liu Jia Hong, *Bangkok, Thailand*
Liu Jing, *Beijing, P.R. China*
Liu Kaichao, *Beijing, P.R. China*
Liu Lu, *Beijing, P.R. China*
Liu Lu, *Tongling, Anhui, P.R. China*
Liu Na, *Shanghai, P.R. China*
Liu Xiaofeng, *Chengdu, Sichuan, P.R. China*
Liu Ying, *Shanghai, P.R. China*
Liu Yingying, *Beijing, P.R. China*
Liu Yuli, *Shaoyang, Hunan, P.R. China*
Liu Zhao Li, *Beijing, P.R. China*
Liu Xuanchen, *Zhoushan, Zhejiang, P.R. China*
Long Songyun, *Guilin, Guangxi, P.R. China*
Luan Dongqi, *Beijing, P.R. China*
Luk Ka Wa, *Wongtai Sin, Hong Kong*
Luo Jinglang, *Beijing, P.R. China*
Luo Yuxin, *Nanjing, Jiangsu, P.R. China*
Lusher, Lila, *Whangarei, Northland, New Zealand*
Ma Chunao, *Beijing, P.R. China*
Ma Jing, *Beijing, P.R. China*
Ma Suk Fong Cecilia, *Shatin, Hong Kong*
Mak Ka Wai, *Wong Tai Sin, Hong Kong*
Martin Uludag, Nina Maelle Lawin, *Paris, France*
Martinez, Anaël, *Le Camnet, France*
May, Eric, *Verbier, Switzerland*
Meidong Zhu, *Guilin, Guangxi, P.R. China*
Meng Yuchen, *Beijing, P.R. China*
Meoni, Annabella, *Montreal, Quebec, Canada*
Miller, Mona, *Portland, Oregon, USA*
Ming Zeng, *Guilin, Guangxi, P.R. China*
Mingyue Chen, *Guilin, Guangxi, P.R. China*
Moe Kyaw, *Fishkill, New York, USA*
Mohamadou, Abdou, *Antananarivo, Madagascar*
Mohammed, Osama Salman Taqi, *Manama, Bahrain*
Morris, Charlene Sarah, *Watlington, Oxfordshire*
Mouralian, Nicole, *Laval, Quebec, Canada*
Nacht, Coralie, *Vich, Switzerland*
Nassi, David, *Norwalk, Connecticut, USA*
Nayak, Asha, *Egham, Surrey*
Nenzen, Charlotte Kristina, *London*
Odake, Shoko, *Tokyo, Japan*
Okubo, Emi, *Sagamihara City, Kanagawa, Japan*
Okuda, Ayako, *Tokyo, Japan*
Oomatsu, Akira, *Tokyo, Japan*
Paiwand, Abdul Rahim, *Edmonton, Alberta, Canada*
Parkin, Charlotte Hannah, *Caterham, Surrey*
Peng Mingqiang, *Guilin, Guangxi, P.R. China*
Pentelow, Irene, *Shrewsbury, Shropshire*
Pimentel Paranhos, Patricia, *London*
Polly, Teresa, *Knoxville, Tennessee, USA*
Porter, Grace, *Stone, Staffordshire*
Praill, Gregory, *Hockley, Essex*
Price, Amy, *South Darenth, Kent*
Qin Qiaohong, *Guilin, Guangxi, P.R. China*
Qiu Chen, *Wuhan, Hubei, P.R. China*
Qiu Ze Hong, *Xiamen, Fujian, P.R. China*
Rabetokotany, Andrimandimby Lantomanantsoa, *Antananarivo, Madagascar*
Redjem, Sihame Brioua, *Nanterre, France*
Richard, Genevieve, *Brossard, Quebec, Canada*
Rol, Emmanuelle, *Marseille, France*
Ryan, Veronica, *London*
Saito, Mari, *Tokyo, Japan*

Sarson, Gregory Carl, *Toowong, Queensland, Australia*
Scott, Louisa, *London*
Senaratne, Yoshinee, *Nugegoda, Sri Lanka*
Senior, Lauren J., *Leeds, West Yorkshire*
Shen Jiamin, *Guilin, Guangxi, P.R. China*
Shen Rongrong, *Beijing, P.R. China*
Shen Shuo, *Macheng, Hubei, P.R. China*
Sheriff, Fatima, *La Roche-Guyon, France*
Shi Shupeng, *Foshan, Guangdong, P.R. China*
Shi Ruoyu, *Wulumuqi, Xinjiang, P.R. China*
Smith, Kerry-Kate, *London*
Steffens, Hounaida, *Nanterre, France*
Su Yung Chu, *Kaohsiung City, Taiwan, R.O. China*
Su Yung-Han, *Taipei City, Taiwan, R.O. China*
Sun Haoyang, *Beijing, P.R. China*
Sun Xiaoyu, *Beijing, P.R. China*
Sun Ziwei, *Fuzhou, Fujian, P.R. China*
Synnott, Suzie, *Outremont, Quebec, Canada*
Sze Ching Man Suki, *Shatin, Hong Kong*
Tang Chung Fu, *Homantin, Hong Kong*
Tang Jiani, *Wuxi, Jiangsu, P.R. China*
Tang Tiankai, *Ningbo, Zhejiang, P.R. China*
Testill, Emma, *Cannock, Staffordshire*
Thiel, Gunyasiree, *London*
Tint, Yin Moe, *Yangon, Myanmar*
Tung Jen-Hao, *Taichung City, Taiwan, R.O. China*
Uchida, Yoshiaki, *Tokyo, Japan*
Velickaite, Akvile, *London*
Venville, Sarah, *Auckland, New Zealand*
Verchere, David, *Toulouse, France*
Wang Chuan, *Zixing, Hunan, P.R. China*
Wang, Dan, *Beijing, P.R. China*
Wang Guohua, *Weifang, Shandong, P.R. China*
Wang Han, *Beijing, P.R. China*
Wang Jiafen, *Shanghai, P.R. China*
Wang Kailin, *Beijing, P.R. China*
Wang Kang, *Beijing, P.R. China*
Wang Lei, *Beijing, P.R. China*
Wang Meng, *Nanchang, Jiangxi, P.R. China*
Wang Shuang, *Guilin, Guangxi, P.R. China*
Wang Yifei, *Hegang, Heilongjiang, P.R. China*
Wang Yiying, *Beijing, P.R. China*
Wang Yu Qi, *Guiyang, Guizhou, P.R. China*
Wang Zhilin, *Shenzhen, Guangdong, P.R. China*
Wang Xiaoyun, *Wulumuqi, Xinjiang, P.R. China*
Wang Zhe, *Nanyang, Henan, P.R. China*
Weng Ruizhi, *Beijing, P.R. China*
Weng Yahui, *Zhengzhou, Henan, P.R. China*
Whittington, Flora, *St Helier, Jersey, Channel Islands*
Wilkinson, Damien Keith, *Danesfort, Co. Kilkenny, R.O. Ireland*
Wong, Hiu Moon, *Homantin, Hong Kong*
Wong Yu Ting, *Tai Po, Hong Kong*
Woodman, Jonathan Andrew, *Harrogate, North Yorkshire*
Wright, William, *London*
Wu Chia Jung, *Kaohsiung City, Taiwan, R.O. China*
Wu Hsin-Yi, *New Taipei City, Taiwan, R.O. China*
Wu Mengnan, *Longyan, Fujian, P.R. China*
Wu Wenjie, *Foshan, Guangdong, P.R. China*
Xiaorong, Jiang, *Guilin, Guangxi, P.R. China*
Xie Qiongxia, *Shanghai, P.R. China*
Xin Wen, *Beijing, P.R. China*
Xing Chen, *Beijing, P.R. China*
Xu Cendi, *Beijing, P.R. China*
Xu Lingxiao, *Beijing, P.R. China*
Xu Qinzi, *Beijing, P.R. China*
Xu Yanfei, *Guilin, Guangxi, P.R. China*
Xue Jie, *Shatin, Hong Kong*
Xue Zixuan, *Shanghai, P.R. China*
Yang Chen-Yu, *Taipei City, Taiwan, R.O. China*
Yang Hsiao-Chu, *Taipei City, Taiwan, R.O. China*
Yang Huey-Wenn, *Taipei City, Taiwan, R.O. China*
Yang Xiao, *Beijing, P.R. China*
Yang Xin, *Guilin, Guangxi, P.R. China*
Yang Xue-Chang, *New Taipei City, Taiwan, R.O. China*
Yang Yang, *Guilin, Guangxi, P.R. China*
Yang Yi-En, *Taipei City, Taiwan, R.O. China*
Yang Yong, *Ningbo, P.R. China*
Yang Yuling, *Beijing, P.R. China*
Yang Yunjing, *Montreal, Quebec, Canada*
Yang Yuyue, *Beijing, P.R. China*
Yao Jing, *Fuzhou, Fujian, P.R. China*
Yazawa, Emiko, *Woodside, New York, USA*
Ye Hanqi, *Guilin, Guangxi, P.R. China*
Ye Shan, *Shanghai, P.R. China*
Ye Nan, *Leqing, Zhejiang, P.R. China*
Yi Nannan, *Beijing, P.R. China*
Yiying Su, *Guilin, Guangxi, P.R. China*
Yoong Li Min, Rachel, *Birmingham, West Midlands*
Young, Nicola Hester, *Bristol*
Yu Xidan, *Longyan, Fujian, P.R. China*
Yuan Rui Feng, *Shenzhen, Guangdong, P.R. China*
Yuan Wei, *Guilin, Guangxi, P.R. China*
Yuan Jingjing, *Shangqiu, Henan, P.R. China*
Yung Hoi Yan, *Central, Hong Kong*
Zeng Xin, *Wuhan, Hubei, P.R. China*
Zerhouni, Yousra Abdou, *Montreal, Quebec, Canada*
Zhai Mengqi, *Beijing, P.R. China*
Zhai Chun, *Wulumuqi, Xinjiang, P.R. China*
Zhang Guifang, *Beijing, P.R. China*
Zhang Lei, *Beijing, P.R. China*
Zhang Lijuan, *Wuhan, Hubei, P.R. China*
Zhang Lingjie, *Beijing, P.R. China*
Zhang, Mingxi, *Chongqing, P.R. China*
Zhang, Sirong, *Guilin, Guangxi, P.R. China*
Zhang, Ting, *Montreal, Quebec, Canada*
Zhang Weiming, *Qinhuangdao, Hebei, P.R. China*
Zhang Xiao, *Shanghai, P.R. China*
Zhang Yan, *Guangzhou, Guangdong, P.R. China*
Zhao Chengcheng, *Wuhan, Hubei, P.R. China*
Zhao Siyi, *Beijing, P.R. China*
Zhao Xiaoxia, *Weihai City, Shangdong, P.R. China*
Zhao Yi, *Beijing, P.R. China*
Zhen Wang, *Guilin, Guangxi, P.R. China*
Zheng, Bingyu, *Beijing, P.R. China*
Zheng, Qiong, *Wenling, Zhejiang, P.R. China*
Zhong, Anna Hua, *Yau Ma Tei, Hong Kong*
Zhou, Fangyuan, *Guiding, Guizhou, P.R. China*

Zhu, Xiaofei, *Shanghai, P.R. China*
Zhu, Yuenan, *Hangzhou, Zhejiang, P.R. China*
Zou, Ran, *Beijing, P.R. China*

Foundation Certificate in Gemmology

Qualified

Abbassi, Matin, *Highgate, London*
Achermann, Katharina, *Nidwalden, Switzerland*
Acil, Cecilia Deniz, *Jarfalla, Sweden*
Aiken, Juliette, *London*
Allen, Pixie, *Birmingham, West Midlands*
Alonso-Perez, Raquel, *Arlington, Massachusetts, USA*
Aranguiz Romero, Claudia Carola, *Villars-sur-Glâne, Switzerland*
Armengaud, Anne Florence, *Paris, France*
Aron-Brunetiere, Patricia, *Raray, France*
Arrive, Raphael, *Annecy, France*
Ashri, Atul, *Reading, Berkshire*
Atack, Philip, *Coventry, West Midlands*
Aung, Thet Oo, *Yangon, Myanmar*
Aung, Thet Tun, *Yangon, Myanmar*
Auramornrat, Tanothai, *Bangkok, Thailand*
Baghdadi, Abeer, *Jeddah, Saudi Arabia*
Bai Wei, *Beijing, P.R. China*
Bailey, Elizabeth, *Burnaston, Derbyshire*
Balmer, Isabel, *Derby, Derbyshire*
Banasiak, Edyta, *Putnam Valley, New York, USA*
Bayar, Mikail, *Le Coteau, France*
Beauséjour, Joanie, *Saint-Armand, Quebec, Canada*
Bejarano Prieto, Fernando Jose, *Lima, Peru*
Benfield, Emma, *Winchester, Hampshire*
Bensimon, Laurent, *Neuilly-sur-Seine, France*
Bernardo, Fabio, *Bologna, Italy*
Bhattarai, Amikar, *Yangon, Myanmar*
Birch, Ritsuko, *Telford, Shropshire*
Bloomfield, Katie, *Harrogate, North Yorkshire*
Boatwright, Sally, *Ely, Cambridgeshire*
Bockenmeyer, Ingrid, *Sucy-en-Brie, France*
Boyce, Georgina Elizabeth, *London*
Bradley, Joanna Maria, *Sheffield, South Yorkshire*
Brady, Aoife Elizabeth, *London*
Bryant, Amanda, *Chiswick, London*
Bullock, Emily, *Birmingham, West Midlands*
Buridard, Ambre, *Paris, France*
Burton, Amy Louise, *London*
Cai Yiming, *Beijing, P.R. China*
Cai, Jinge, *Shatin, Hong Kong*
Cani, Sandra, *London*
Cao Yunyu, *Beijing, P.R. China*
Carson, Claire, *Southend-on-Sea, Essex*
Cevallos, Pamela, *New York, New York, USA*
Challal, Sabrina, *London*
Chan Ching Ching, Hilary, *Shatin, Hong Kong*
Chan Ching Wai, *Tsuen Wan, Hong Kong*
Chan Kam, *Tsuen Wan, Hong Kong*
Chan Kin Wai, *Kowloon, Hong Kong*
Chan Lai Yi, *Ho Man Tin, Hong Kong*
Chan Wing Kit, *Yuen Long, Hong Kong*
Chan Yan Yan, *Kwun Tong, Hong Kong*
Chan Yuen Lam, Lucia, *Lam Tin, Hong Kong*
Chan, Sheung Ki, *Tin Shui Wai, Hong Kong*
Chang Hsiang-Ting, *New Taipei City, Taiwan, R.O. China*
Chang Pi Yu, *New Taipei City, Taiwan, R.O. China*
Chang Siwen, *Beijing, P.R. China*
Chang Su-Ying, *Taichung, Taiwan, R.O. China*
Chang Tsui Ping, *New Taipei City, Taiwan, R.O. China*
Chang Xing, *Shanghai, P.R. China*
Chang Yu Chen, *Kaohsiung City, Taiwan, R.O. China*
Chao Chien-Chiang, *Taichung, Taiwan, R.O. China*
Chauveron, Alain, *Bordeaux, France*
Chedid, Karine, *Paris, France*
Chen Chen, *Shanghai, P.R. China*
Chen Feng Chieh, *Kaohsiung, Taiwan, R.O. China*
Chen Hung-Ju, *New Taipei City, Taiwan, R.O. China*
Chen Lin-En, *New Taipei City, Taiwan*
Chen Muyu, *Guilin, Guangxi, P.R. China*
Chen Po Kai, *Kaohsiung City, Taiwan, R.O. China*
Chen Wei Hua, *Shenzhen, Guangdong, P.R. China*
Chen Wei-Ting, *Taipei City, Taiwan, R.O. China*
Chen Yanran, *Beijing, P.R. China*
Chen Yuxin, *Beijing, P.R. China*
Chen Yuxin, *Guilin, Guangxi, P.R. China*
Chen Zhiying, *Linhai, Zhejing, P.R. China*
Cheng Hin Wah, *Aberdeen, Hong Kong*
Cheng Yi Jing, *New Taipei City, Taiwan, R.O. China*
Cheung Chi Man, *Yuen Long, Hong Kong*
Cheung Shuk Ting, *Tsing Yi, Hong Kong*
Cheung Yan Kit, *Shatin, Hong Kong*
Cheung Yin Ting, *Kowloon, Hong Kong*
Chiesura, Marco, *Genova, Italy*
Chiu Ti, *New Taipei City, Taiwan, R.O. China*
Chou Yu Chu, *Taichung City, Taiwan, R.O. China*
Chow Sze Kam, *Tuen Mun, Hong Kong*
Chow Wai Yin, *Central, Hong Kong*
Chu, Jiyuan, *Hangzhou, P.R. China*
Chuang Hsin Ying, *Taipei City, Taiwan, R.O. China*
Chung Yueh Chi, *Kaohsiung City, Taiwan, R.O. China*
Clarke, Lucy, *London*
Clohessy-Brown, Amber, *Birmingham, West Midlands*
Collin-Randoux, Héloïse, *Garches, France*
Cousins, Julian, *Faversham, Kent*
Cupillard, Bruno, *Besancon, France*
Cutmore, Joanne, *Faringdon, Oxfordshire*
Dai, Jialin, *Sanmenxia, Henan, P.R. China*
Davis, Ruth, *Edinburgh*
De-Leuw, Lara, *Derby, Deryshire*
Deng Xia, *Shanghai, P.R. China*
Deng Yufei, *Suzhou, Jiangsu, P.R. China*
Dennison, Rebecca, *London*
Detroyat, Stanislas, *Bangkok, Thailand*
Dewanarayana, Amalsha Chiran, *Harrow, Middlesex*
Dharmasiri, Anuruddha, *Colombo, Sri Lanka*
Dhunna, Divjot Singh, *Punjab, India*
Dieu de Bellefontaine, Mary, *Billericay, Essex*

Dong Lingxu, *Guangzhou, Guangdong, P.R. China*
Doyle, Robert Charles, *Laval, Quebec, Canada*
Duandao, Rungrawee, *Bangkok, Thailand*
Durand, Jennifer Margaret, *Burton On Trent, Staffordshire*
Dzikowski, Tashia, *Basel-Stadt, Switzerland*
Easen, Grace, *Chelmsford, Essex*
Eerdmans-Lindenbergh, Idzarda, *Rotterdam, The Netherlands*
Eichler, Alexandre, *Limoges, France*
Eriksson, Sandra, *Lannavaara, Sweden*
Faber, Lily, *London*
Fang Hsing Wen, *Siluo Township, Yunlin, Taiwan, R.O. China*
Farrow, Rachel May, *Saffron Walden, Essex*
Fateeva, Tatiana, *Yangon, Myanmar*
Feng Ye, *Shanghai, P.R. China*
Flynn, Inez, *Dublin, R.O. Ireland*
Fok Ka Lin, *Chai Wan, Hong Kong*
Fors, Linda, *Kiruna, Sweden*
Francis, Amanda-Louise, *Blackheath, London*
Fu Yizhu, *Beijing, P.R. China*
Fujii, Yuko, *Tokyo, Japan*
Fung Chun Yan, *Kwun Tong, Hong Kong*
Gangloff, Juliette, *Fos, France*
Gao Fang, *Beijing, P.R. China*
Gao Yue, *Shanghai, P.R. China*
Garcia-Carballido, Carmen, *Tarves, Aberdeenshire*
Garcia-Marriott, Sonya, *London*
Garrett, Kathryn, *Worcester Park, Surrey*
Gensini, Graziano, *Genoa, Italy*
Giacobetti, Tom, *Carouge, Switzerland*
Gillings, Marc, *Birmingham, West Midlands*
Girardin, Philippe, *Drummondville, Quebec, Canada*
Godwyn, Jo, *Glasgow*
Gorringe, Oliver, *Redhill, Surrey*
Gozlan, Esther, *Paris, France*
Green, Jennifer Lauren, *Sutton, Surrey*
Grenyer, Neil, *Melbourne, Derbyshire*
Gu Weifeng, *Shanghai, P.R. China*
Guay, Richard, *Saint-Justin, Quebec, Canada*
Guibelin, Laetitia, *Morteau, France*
Guo Fengyun, *Hefei, Anhui, P.R. China*
Guo Han, *Ruili, Yunnan, P.R. China*
Guo Jinmei, *San Po Kang, Hong Kong*
Guo Yuchao, *Beijing, P.R. China*
Guo Zehang, *Shantou, Guangdong, P.R. China*
Haddad, Zena, *London*
Hamdaoui, Mustapha, *Choisy-le-Roi, France*
Hamel, Jean Francois, *Montreux, Switzerland*
Han Dongdong, *Beijing, P.R. China*
Han Dongmei, *Shenzhen , Guangdong, P.R. China*
Han Xue, *Beijing, P.R. China*
Hanaki Yu, *Beppu City, Oita, Japan*
Hann, Janet, *Bromley, Kent*
Hantamanirisoa, Christiane, *Antananarivo, Madagascar*
Hao Yun, *Beijing, P.R. China*
Harb, Rawan Jalal, *London*
He Huizhen, *Shanghai, P.R. China*
He Tianshu, *Beijing, P.R. China*
He, Min, *Shanghai, P.R. China*
Heath, Caitlin Rose, *Montreal, Quebec, Canada*
Hendrix-Hollstein, Anja, *Aerdenhout, The Netherlands*
Henkel, Thomas, *Montreal, Quebec, Canada*
Herbin, Thomas, *Lésigny, France*
Herries, Jane Denise, *Castle Douglas, Kirkcudbrightshire, Scotland*
Hirao, Keiko, *Osaka City, Osaka, Japan*
Hirayama, Naoka, *Tokyo, Japan*
Ho Ka Mei, *Mei Foo Sun Chuen, Hong Kong*
Hoffman Bermejo, Nova, *Stockholm, Sweden*
Hong Qibo, *Shanghai, P.R. China*
Hood, James Scott, *Knoxville, Tennessee, USA*
Hou Juncan, *Beijing, P.R. China*
Hou Yun Tien, *Kaohsiung City, Taiwan, R.O. China*
Hsu Ting-Yu, *Taipei City, Taiwan, R.O. China*
Htut, Phyo Win, *Yangon, Myanmar*
Hu Aning, *Guilin, Guangxi, P.R. China*
Hu Wai Ping, *Tin Shui Wai, Hong Kong*
Hu Zhe, *Beijing, P.R. China*
Huang Baoyi, *Westbury, New York, USA*
Huang Dong-He, *Kao-Xung City, Taiwan, R.O. China*
Huang Han, *Dazhou, Sichuan, P.R. China*
Huang Hongchuan, *Jinhua, Zhejiang, P.R. China*
Huang Jun, *Shanghai, P.R. China*
Huang Mianzhi, *Rheinland-Pfalz, Germany*
Huang Saifeng, *Shanghai, P.R. China*
Huang Shana, *Guilin, Guangxi, P.R. China*
Huang Yuanxin, *Guangzhou, Guangdong, P.R. China*
Huang Yuzhang, *Guilin, Guangxi, P.R. China*
Hung Erh-Nu, *New Taipei City, Taiwan, R.O. China*
Hung Shih-Tsung, *Kaohsiung City, Taiwan, R.O. China*
Ichikawa, Yurie, *Chuo-Ku Tokyo, Japan*
Iezaki, Kei, *Nishi, Tokyo, Japan*
Irwin, Emma, *Yangon, Myanmar*
Isaak, Sameul Ivan, *Lannavaara, Sweden*
Izzard, Georgina Sara, *Stansted, Essex*
Jacmain, Irina, *Noisy Le Sec, France*
Jao, Andy, *Taipei City, Taiwan, R.O. China*
Jayarathne, Ruwini, *Moratuwa, Sri Lanka*
Ji Bin, *Rizhao, Shandong, P.R. China*
Jia Ru, *Beijing, P.R. China*
Jiang Chao, *Shanghai, P.R. China*
Jiang Chenglei, *Beijing, P.R. China*
Jiang Haijing, *Sai Ying Pun, Hong Kong*
Jing Jie, *Hebei Province, P.R. China*
Jogia, Sonal, *Harrow, Middlesex*
Joubert, Kerryn, *London*
Ju Qiulin, *Shanghai, P.R. China*
Juo Shiou Fang, *Taichung City, Taiwan, R.O. China*
Kakati, Sushmita, *West Byfleet, Surrey*
Kang, Mibeom, *Yokkaichi City, Mie, Japan*
Kao Wei Chen, *New Taipei City, Taiwan, R.O. China*
Karadjia, Heydar, *Antananarivo, Madagascar*
Kariche, Yanis Chelbi, *Neuilly-sur-Seine, France*
Karlsson, Fredrik, *Stockholm, Sweden*

Katsakiori, Konstantina, *Nea Smyrni, Greece*
Ke Ding, *Beijing, P.R. China*
Kei Man Lai, *Tseung Kwan O, Hong Kong*
Kenouche, Naguib, *Neullly-sur-Seine, France*
Kercher, Jason Robert, *Norwich, Norfolk*
Ketcher, Alyce, *Wellington, Somerset*
Keung Ka Yee, *Tin Shui Wai, Hong Kong*
Khaing, Kay Thi, *Yangon, Myanmar*
Khine Thu, May, *Yangon, Myanmar*
Khoo Shoew Peng, Penny, *Yuen Long, Hong Kong*
Khoudian, Christina, *Colchester, Essex*
Khowpong, Charuwan, *Bangkok, Thailand*
King, Rachel Eloise, *Edinburgh*
King, Rosanna, *Athy, County Kildare, R.O. Ireland*
Kingan, Saffron Jemima Irons, *Auckland, New Zealand*
Kinoshita, Takako, *Tokyo, Japan*
Klumb, Alexander, *Baden-Württemberg, Germany*
Knight Bruce, Vita, *London*
Knight, Naomi Rose, *Stockwell, London*
Knowles-Cutler, Laura, *Westerham, Kent*
Kolye, Ekaterina, *St Moritz, Switzerland*
Kong Yu, *Shanghhai, P.R. China*
Kotkis, Olga Ella, *Nizhniy, Novgorod, Russia*
Krishnamurti, Anjani, *London*
Kuan Chao Wen, *Keelung City, Taiwan, R.O. China*
Kuo Chia-Ying, *New Taipei City, Taiwan, R.O. China*
Kwan Chi Fai, *Cheung Sha Wan, Hong Kong*
Kwok Tung, Zoe, *Mid-levels, Hong Kong*
Kwong Chin-Ting, *Chai Wan, Hong Kong*
Kwong Yui-Cho, *Chai Wan, Hong Kong*
Kyi, Nan Khine Thazin, *Yangon, Myanmar*
Lafler, Renata, *Harriman, Tennessee, USA*
Lai Kwok Hung, *Tsing Yi, Hong Kong*
Lai Xiangxiang, *Beijing, P.R. China*
Lam Hang Suen, *Lai Chi Kok, Hong Kong*
Lam Hoi Ki, *Kowloon, Hong Kong*
Lam Shuk Yi, *Kowloon, Hong Kong*
Lam Siu Man, *Tsing Yi, Hong Kong*
Lansley, Juliette Elizabeth, *Heathfield, East Sussex*
Lau Fung Shan, *Tuen Mun, Hong Kong*
Lau Ka Wai, *Lam Tin, Hong Kong*
Lau Kam Wo, *Fanling, Hong Kong*
Lau Nga Ling, *Tuen Mum, Hong Kong*
Lau Sin Wah, *Mongkok, Hong Kong*
Lavoie Ste-Marie, Bénédicte, *Montreal, Quebec, Canada*
Le Roux, Liezel, *Singapore, Singapore*
Lecouvey Mayoraz, Andrea, *Bras, France*
Leduc, Gabrielle-Ann, *Rouyn-Noranda, Quebec, Canada*
Lee, Shao-Chun, *Douliu City, Yunlin, Taiwan, R.O. China*
Lei Yu, *Causeway Bay, Hong Kong*
Leigh-Pemberton, Robert, *London*
Lem, Renske, *The Hague, The Netherlands*
Lemon, Victoria, *Glasgow*
Leong, Aliana, *Macau S.A.R., P.R. China*
Leung Car Ni, *Quarry Bay, Hong Kong*
Leung Ching Han, Estella, *Sheung Shui, Hong Kong*
Leung Ho Shuen, *Lamma Island, Hong Kong*
Leung Pui Po, *Tseung Kwan O, Hong Kong*
Leung Wai Yee Jouie, *Tai Po, Hong Kong*
Levenez, Orianne, *La Forêt Fouesnant, France*
Lhuaamporn, Thanapong, *Bangkok, Thailand*
Li Chia Hung, *New Taipei City, Taiwan, R.O. China*
Li Dianhui, *Beijing, P.R. China*
Li Dongyang, *Beijing, P.R. China*
Li Fengyi, *Beijing, P.R. China*
Li Jinjun, *Guilin, Guangxi, P.R. China*
Li Kam Ping, *Tseung Kwan O, Hong Kong*
Li Lai Bun Anita, *Fanling, Hong Kong*
Li Qian, *Beijing, P.R. China*
Li Qidi, *Beijing, P.R. China*
Li Ruoxi, *Beijing, P.R. China*
Li Shiu Chin, *New Taipei City, Taiwan, R.O. China*
Li Wai Yu, *Colombo, Sri Lanka*
Li Wenpeng, *Beijing, P.R. China*
Li Yaguang, *Beijing, P.R. China*
Li Yingjiang, *Beijing, P.R. China*
Li Yu-Ting, *Ping-Dong Xien, Taiwan, R.O. China*
Li Zhuchenzi, *Shanghai, P.R. China*
Li, Chi Ho, *Tin Shui Wai, Hong Kong*
Liang Huan, *Beijing, P.R. China*
Liang Ping, *Shanghai, P.R. China*
Liang Xi, *Shenzhen, Guangdong, P.R. China*
Liao Guoping, *Beijing, P.R. China*
Lim Sai Kit, *Yau Ma Tei, Hong Kong*
Lin Chang Te, *New Taipei City, Taiwan, R.O. China*
Lin Chenlu, *Beijing, P.R. China*
Lin Jun-Yu, *Ping-Dong Xien, Taiwan, R.O. China*
Lin Meng-Yao, *Taichung, Taiwan, R.O. China*
Lin Sandar, *Yangon, Myanmar*
Lin Sheng Che, *Taipei City, Taiwan, R.O. China*
Lin Yi Ping, *Taoyuan City, Taiwan, R.O. China*
Lin Ying, *Guilin, Guangxi, P.R. China*
Lin Yu Cheng, *New Taipei City, Taiwan, R.O. China*
Lin Zhi Yi, *Kowloon, Hong Kong*
Lisurenko, Marina, *Aberdeen*
Liu Baitong, *Shengyang City, Liaoning, P.R. China*
Liu Gaoli, *Beijing, P.R. China*
Liu Hong Lin, *Kaohsiung City, Taiwan, R.O. China*
Liu Jiao, *Guilin, Guangxi, P.R. China*
Liu Jinhua, *Shanghai, P.R. China*
Liu Xiang, *Beijing, P.R. China*
Liu Xiaoli, *Shanghai, P.R. China*
Liu Yu-Chun, *Taipei City, Taiwan, R.O. China*
Lo Ying-Ting, *Shetou Township, Taiwan, R.O. China*
Logan, Amy, *Birmingham, West Midlands*
Lognay, Lauriane, *Brossard, Quebec, Canada*
Longhurst, Stephanie, *Blandford Forum, Dorset*
Loyd, Tabitha Launa, *London*
Lu Hanyu, *Taizhou City, Jiangsu, P.R. China*
Lu Hao Teng, *Kaohsiung City, Taiwan, R.O. China*
Lu Juwei, *Shanghai, P.R. China*
Lu Li, *Shanghai, P.R. China*
Lu Wan-Yu, *New Taipei City, Taiwan, R.O. China*
Lu Yina, *Hangzhou, Zhejiang, P.R. China*

Luete, Peggy, *Neuilly-Plaisance, France*
Lui Wing-Tak, *New Taipei City, Taiwan, R.O. China*
Luo, Dan, *Shanghai, P.R. China*
Ma Hongjing, *Beijing, P.R. China*
Ma Shuangyi, *Beijing, P.R. China*
Ma Yu, *Hangzhou, Zhejiang, P.R. China*
Mackie, Annabel, *London*
Mali, Batoure, *Antananarivo, Madagascar*
Man Koon Ho, *Ma Wan, Hong Kong*
Manustrong, Areeya, *Bangkok, Thailand*
Marquis, Sophie Jessica Annabelle, *Torteval, Guernsey, Channel Islands*
Martin Uludag, Nina Maelle Lawin, *Paris, France*
Martinez, Anaël, *Le Camnet, France*
Mattice, Gabriel, *Oceanside, California, USA*
Maung, Win Nandar, *Yangon, Myanmar*
McEvilly, Bernadette, *Dublin, R.O. Ireland*
Meteleva, Elena, *Yangon, Myanmar*
Michel, Paulina, *Vienna, Austria*
Mirza, Hishaam James, *Parnell, Auckland, New Zealand*
Moe, Kyi Soe, *Yangon, Myanmar*
Moghe, Devika, *Surat, India*
Mohamadou, Abdou, *Antananarivo, Madagascar*
Mohamed Hilmy, Mohamed Fahmy, *Harrow, Middlesex*
Mohideen, Noorul Asma, *Colombo, Sri Lanka*
Morando, Giacomo, *Genoa, Italy*
Morgan, Rachel, *Horsham, West Sussex*
Moya, Lucille, *Saint Georges D'Oléron, France*
Mu Jia, *Beijing, P.R. China*
Muskin, Sarah, *London*
Nagai, Takeo, *Osaka, Japan*
Nakata, Miyuki, *Osaka, Japan*
Ndriana, Christian, *Marseille, France*
Ng Wai Chung, *Ma Wan, Hong Kong*
Ng Wing-Lam, *Chai Wan, Hong Kong*
Ng, Yat Wa, *Tseung Kwan O, Hong Kong*
Ng-Pooresatien, Nattida, *Bangkok, Thailand*
Nicolas, Jonathan, *Muntinlupa City, Philippines*
Ning Zhenhua, *Beijing, P.R. China*
Niu Xiaoxue, *Beijing, P.R. China*
Nosel, Joyce, *Villejuif, France*
O'Sullivan, Ryan, *Nottingham, Nottinghamshire*
Olm, Mark C., *Tucson, Arizona, USA*
Ou Minhui, *Beijing, P.R. China*
Ourny, Olivier, *Neuchâtel, Switzerland*
Packeerally, Aqeelah, *Wattala, Sri Lanka*
Paiwand, Abdul Rahim, *Edmonton, Alberta, Canada*
Palthey, Katherine, *Grasse, France*
Pan Jingwen, *Beijing, P.R. China*
Pan Xin, *Lanzhou City, Gansu, P.R. China*
Pao Tracia, *Taipei City, Taiwan, R.O. China*
Pardoe, Jennifer, *Birmingham, West Midlands*
Paul-Kessel, Antje, *Laren, The Netherlands*
Paw, Naw Lah May, *Yangon, Myanmar*
Peng, Jingcheng, *Beijing, P.R. China*
Peng, Kuo-Chen, *Zhutian Township, Pingtung, Taiwan, R.O. China*
Perera, Yasasi, *Sri Jayawardenapura, Sri Lanka*
Perren, Simon Grantley Dean, *Seven Hills, Queensland, Australia*
Petit, Fabienne, *Versailles, France*
Picello, Fabio, *Mondovi, Cuneo, Italy*
Pickering, Zoe, *Melton Mowbray, Leicestershire*
Pimentel Paranhos, Patricia, *London*
Pong Kwai Fong, Maggie, *Ma On Shan, Hong Kong*
Poon Tsz Kwan, *Sheung Shui, Hong Kong*
Psimouli, Eleftheria, *Kypseli, Greece*
Pu Zhenxiao, *Shanghai, P.R. China*
Qian Wenni, *Shanghai, P.R. China*
Qin Yongda, *Beijing, P.R. China*
Qu Hongting, *Beijing, P.R. China*
Qu Yi, *Qingdao, Shandong, P.R. China*
Rasolonjatovo, Georges Gina, *Antananarivo, Madagascar*
Rastogi, Kushagra, *Uttar Pradesh, India*
Ren, Manfei, *Tokyo, Japan*
Rice, Jennifer, *Hull, East Yorkshire*
Rix, Tuperna, *Nuussuaq, Greenland*
Rochelet, Géraldine, *Paris, France*
Rong Ting, *Beijing, P.R. China*
Rong Xue Qin, *Colombo, Sri Lanka*
Ruan Chentao, *Beijing, P.R. China*
Rytel, Miroslawa, *Staten Island, New York, USA*
San Kyi, Nyein Pyae Sone, *Southwark, London*
Sandar, Aye, *Yangon, Myanmar*
Santana da Silva, Dillyene Deenysser, *Malakoff, France*
Saralapova, Assia, *Nice, France*
Sasaki, Mina, *Yokohama, Kanagawa, Japan*
Satou, Naoto, *Saitama-City, Saitama, Japan*
Schintu, Emanuele, *Bologna, Italy*
Senaratne, Yoshinee, *Nugegoda, Sri Lanka*
Seneca, Laurent, *Roquebrune Carnoles, France*
Shen Yiming, *Shanghai, P.R. China*
Sheriff, Fatima, *La Roche-Guyon, France*
Shih Yu Hong, *Taipei City, Taiwan, R.O. China*
Shishido, Michiko, *Yokohama City, Kanagawa, Japan*
Simard, Camille, *Voinsles, France*
Sit Shan Na, *Tseung Kwan O, Hong Kong*
Smith, Rachel Jane, *Portsmouth, Hampshire*
So Shuk Man, *Shatin, Hong Kong*
Somsa-Ard, Nanthaporn, *Bangkok, Thailand*
Song Liwen, *Central, Hong Kong*
Song Peiming, *Beijing, P.R. China*
Song Qingzhuo, *Shanghai, P.R. China*
Song Wanying, *Beijing, P.R. China*
Song Yihua, *Beijing, P.R. China*
Song Ying, *Shanghai, P.R. China*
Stadlin, Sonja Andrea, *Baar, Zug, Switzerland*
Stammegna, Delphine, *Marseille, France*
Stephenson, Lee-Ann, *Welwyn Garden City, Hertfordshire*
Stonley, Fiona, *Birmingham, West Midlands*
Sudprasert, Patharaphum, *Bangkok, Thailand*
Suma, Hanna, *Henlow, Bedfordshire*
Sun Jie, *Qingdao, P.R. China*

Sun Jilan, *Zhejiang, P.R. China*
Sun Jing, *Tianjin, P.R. China*
Sun Mengdi, *Zaozhuang, P.R. China*
Sun Yuxin, *Beijing, P.R. China*
Sun, Weishi, *London*
Sunga, Mary Josephine Feliciano, *Clifton, New Jersey, USA*
Szarota, Artur, *Brentford, London*
Sze Hoi Lee, *Lam Tin, Hong Kong*
Tai Yuen Kong, *Cheung Chau, Hong Kong*
Taiclet, Alexia, *Paris, France*
Takagi, Asako, *Kanagawa-Ken, Japan*
Tang Yongfang, *Weihai, P.R. China*
Tang, Heidi Hoi Yee, *Birmingham, West Midlands*
Taylor, Victoria, *Montreal, Quebec, Canada*
Teh De, Jack, *Kowloon, Hong Kong*
Thomas, Isaac Matthew David, *Bristol*
Thorsson, Karin Bianca, *Stockholm, Sweden*
Tian Jiang, *Beijing, P.R. China*
Tjong Lee Ping, *Tsing Yi, Hong Kong*
To Hok Fong, *Ngau Tau Kok, Hong Kong*
To Yui Sang, *Tsuen Wan, Hong Kong*
Tobin, Rachel, *London,*
Toche, Claire, *Aubagne, France*
Tom, Graham, *London*
Triki, Alexandre, *Emerainville, France*
Tsai Pei Ju, *Yuanchang, Yunlin, Taiwan, R.O. China*
Tsai Tzu-Yin, *New Taipei City, Taiwan, R.O. China*
Tsang Hon Man, *Tseung Kwan O, Hong Kong*
Tsang King Yam, *Tin Shui Wai, Hong Kong*
Tsang Man, Judy, *Siu Sai Wan, Hong Kong*
Tse Chui Lin, *Yuen Long, Hong Kong*
Tsui King Yin, *Tsing Yi, Hong Kong*
Tyumentseva, Ekaterina, *London*
Van Den Donk, Marieke, *Haarlem, The Netherlands*
Van Leeuwen, Suzanne, *Aalsmeer, The Netherlands*
Vendrell, Christopher, *New York, New York, USA*
Venn, Andrea, *Beavercreek, Ohio, USA*
Verchere, David, *Toulouse, France*
Vicente, Elisabeth, *Paris, France*
Villaret, Christine, *Paris, France*
Wai Saw Min, *Yangon, Myanmar*
Wainer, Stephane, *Singapore, Singapore*
Walker, Gloria, *Southall, Middlesex*
Walker, Patrick John C., *Southall, Middlesex*
Wang Bing, *Beijing, P.R. China*
Wang Chia Li, *New Taipei City, Taiwan, R.O. China*
Wang Han, *Shanghai, P.R. China*
Wang Hue-Mei, *Taichung, Taiwan, R.O. China*
Wang Kai, *Beijing, P.R. China*
Wang Qi, *Huangdao, Qingdao, P.R. China*
Wang Tian Xin, *Tiu Keng Leng, Hong Kong*
Wang Tsung-Min, *Shanghai, P.R. China*
Wang Weiwei, *Beijing, P.R. China*
Wang Xiazhe, *Shanghai, P.R. China*
Wang Xueqing, *Beijing, P.R. China*
Wang Yajue, *Beijing, P.R. China*
Wang Yanqiong, *Shanghai, P.R. China*
Wang Yinan, *Beijing, P.R. China*
Wang Zitong, *Guangzhou, P.R. China*
Weber, Laurence, *Geneva, Switzerland*
Weeramong Khonlert, Vararut, *Bangkok, Thailand*
Wei Chang Hsi, *Taipei City, Taiwan, R.O. China*
Wei Jiarong, *Hebei Province, P.R. China*
Wei Jinchao, *Beijing, P.R. China*
Welford-Ranson, Daisy, *Windsor, Berkshire*
Weng Chi Tang, *New Taipei City, Taiwan, R.O. China*
Weng Yihai, *Shanghai, P.R. China*
Weng, Mei Han, *Taipei City, Taiwan, R.O. China*
Whittaker, Nicola, *London,*
Win Than Than, *Yangon, Myanmar*
Wong Ho Yin, *Tai Po, Hong Kong*
Wong Hoi Ting, *Tai Po, Hong Kong*
Wong Ka Yan, *Tuen Mum, Hong Kong*
Wong Shing Yan, Sarita, *Shatin, Hong Kong*
Wong Wai Ki, Vikki, *Shatin, Hong Kong*
Wootton, Ashley Gowan, *Great Dunmow, Essex*
Wu Cheng Lung, *New Taipei City, Taiwan, R.O. China*
Wu Chia Jung, *New Taipei City, Taiwan, R.O. China*
Wu Chien Chi, *New Taipei City, Taiwan, R.O. China*
Wu Hsin-Yi, *New Taipei City, Taiwan, R.O. China*
Wu Jeng Long, *Kaohsiung City, Taiwan, R.O. China*
Wu Ruolin, *Beijing, P.R. China*
Wu Shuai, *Beijing, P.R. China*
Wu Yu Chan, *Shenzhen, P.R. China*
Wyrley-Birch, Frederick John, *Hexham, Northumberland*
Xi Nanxia, *Qu Zhou City, Zhejiang, P.R. China*
Xia Mingqi, *Qingzhou City, Shandong, P.R. China*
Xiang Shihui, *Shanghai, P.R. China*
Xie Ziyun, *Beijing, P.R. China*
Xin Meiying, *Dalian City, Liaoning, P.R. China*
Xing Chen, *London*
Xiong Jaikai, *Sheung Wan, Hong Kong*
Xu Fan, *Shanghai, P.R. China*
Xu Jie, *Suzhou, Jiangsu, P.R. China*
Xu Ting, *Shanghai, P.R. China*
Xu Weixuan, *Beijing, P.R. China*
Xu Yan, *Shanghai, P.R. China*
Xu Zihao, *Beijing, P.R. China*
Xue Ru, *Shijiazhuang City, Hebei, P.R. China*
Xue Wenyu, *Shanghai, P.R. China*
Xue Zixuan, *Shanghai, P.R. China*
Yam Man Hung, *Tseung Kwan O, Hong Kong*
Yan Qiuli, *Beijing, P.R. China*
Yang Huey-Wenn, *Taipei City, Taiwan, R.O. China*
Yang Jia-Song, *Guanyin, Taoyuan, Taiwan, R.O. China*
Yang Qin, *Hangzhou, P.R. China*
Yang Wancheng, *Beijing, P.R. China*
Yang Xin, *Guilin, Guangxi, P.R. China*
Yang Yi, *Jinan, Shandong, P.R. China*
Yang Yujiao, *Beijing, P.R. China*
Yang Yunjing, *Montreal, Quebec, Canada*
Ye Hanqi, *Guilin, Guangxi, P.R. China*
Ye Lin, *Beijing, P.R. China*
Yeh Shu Fen, *Kaohsiung City, Taiwan, R.O. China*
Yeung Siau Fung, *New York, New York, USA*

Yeung Woon Ying, Maggie, *Tsing Yi, Hong Kong*
Yin Shihui, *Ningbo City, Zhejiang, P.R. China*
Yin Zhenzhu, *Poissy, France*
Yip Kar Men, *Wan Chai, Hong Kong*
Yoda, Yuko, *Tokyo, Japan*
Yu Ka Man, *Kwai Chung, Hong Kong*
Yu Shin Yang, *Taipei City, Taiwan, R.O. China*
Yu Tzu Fang, *Zhudong, Hsinchu, Taiwan, R.O. China*
Yu Yinglei, *Beijing, P.R. China*
Yuan Hang, *Shanghai, P.R. China*
Yuen, Angel, *Tsuen Wan, Hong Kong*
Yung Yat Kwok, *Yuen Long, Hong Kong*
Zhang Chen, *Shanghai, P.R. China*
Zhang Jie, *Beijing, P.R. China*
Zhang Liang, *Bedford, Bedfordshire*
Zhang Linxue, *Guilin, Guangxi, P.R. China*
Zhang Luqing, *Shenyang City, Liaoning, P.R. China*
Zhang Mei, *Beijing, P.R. China*
Zhang Min Yu, *Shenzhen, Guangdong, P.R. China*
Zhang Shuo, *Beijing, P.R. China*
Zhang Sirong, *Guilin, Guangxi, P.R. China*
Zhang Yan, *Guangzhou, Guangdong, P.R. China*
Zhang Yanling, *Shanghai, P.R. China*
Zhang Yi, *Shanghai, P.R. China*
Zhang Yixuan, *Beijing, P.R. China*
Zhang Yu, *London*
Zhang Zhizheng, *Beijing, P.R. China*
Zhao Wei, *Guilin, Guangxi, P.R. China*
Zhao Xinyi, *Beijing, P.R. China*
Zhao Yanhong, *Shanghai, P.R. China*
Zhao Yuan, *Shanghai, P.R. China*
Zheng Chenyu, *Nagoya City, Aichi, Japan*
Zheng Shuyuan, *Beijing, P.R. China*
Zhong Yuanyuan, *Beijing, P.R. China*
Zhou Baojie, *Dongying City, Shandong, P.R. China*
Zhou Hui, *London*
Zhou Meng, *Beijing, P.R. China*
Zhou Quan, *Beijing, P.R. China*
Zhou Yurui, *Tianjin, P.R. China*
Zhou Zihan, *Beijing, P.R. China*
Zhou Ziyang, *Guangzhou, P.R. China*
Zhu Qianwen, *Shanghai, P.R. China*
Zhu Shichao, *Guilin, Guangxi, P.R. China*
Zhu Yuanhua, *Shanghai, P.R. China*
Zhu Yun You, *Taoyuan City, Taiwan, R.O. China*
Zhu Zihui, *Beijing, P.R. China*
Zhuang Shao Wei, *Qingdao. Shandong Province, P.R. China*
Zwick, Annette, *London*

Diamond Diploma Examination

Qualified with Distinction

Ashri, Atul, *Reading, Berkshire*
Beard, Thomas Whitbread, *Eastbourne, East Sussex*
Chan Hiu Ching, *Shatin, Hong Kong*
Cheer, Peter Richard, *Somerton, Somerset*
Lai Ka Man, *Mayfair, London*
Leung Ying, Evie, *Tsing Yi, Hong Kong*
Li Hiu Ying, *Chai Wan, Hong Kong*
Lineker-Mobberley, Maryanne, *Bridgnorth, Shropshire*
Molon, Valentina, *Varese, Italy*
Moorhead, Lisa, *London*
Newson, John Frederick, *Calne, Wiltshire*
Perry, Fran, *Biggleswade, Bedfordshire*
Ruddie, Elaine, *London*
Saleem, Melanie, *Manchester, Greater Manchester*
Sandum, Mark Antony, *Bexleyheath, Kent*
Shaw, Stephanie Anne, *London*
Williams, Kathryn Ann Jenevora, *Dover, Kent*
Wyer, William, *Wilmslow, Cheshire*
Yiu King Ting, Eric, *Kowloon, Hong Kong*

Qualified with Merit

Boyce, Georgina Elizabeth, *London*
Chu Pui Suen, *Sham Shui, Hong Kong*
Foxwell, Kim, *Twickenham, Middlesex*
Fritz, Eric, *Tucson, Arizona, USA*
Fung Hang Shun Jessica, *Tai Po, Hong Kong*
Gonzalez, Olga, *New York, USA*
Harries, Rebecca, *Long Ditton, Surrey*
Jiang Haijing, *Sai Ying Pun, Hong Kong*
Le, Wai Hang, *Lai Chi Kok, Hong Kong*
Lo Hau Yin, *Kowloon, Hong Kong*
Lo On Ki, *Tsuen Wan, Hong Kong*
Marshall, Georgia Black, *Meopham, Kent,*
Nash-Wilson, Jake, *Bristol*
Rexworthy, Simon Ramsay, *Market Drayton, Shropshire*
Shek Sze Wan, *Tuen Mun, Hong Kong*
Spencer, Sally Jane, *Didcot, Oxfordshire*
Steele, Sarah, *York, Yorkshire*
Tang Tiankai, *Ningbo, Zhejiang, P.R. China*
Velickaite, Akvile, *London*
Walker, Susan, *Elwood, Victoria, Australia*
Wu Weiran, *Beijing, P.R. China*
Yip Pui Sze, *Tai Po, Hong Kong*

Qualfied

Ball, Gareth, *Letterkenny, County Donegal, R.O. Ireland*
Bowkett, Alexandra, *Stroud, Gloucestershire*
Bullmore, Elizabeth Mary, *Birmingham, West Midlands*
Callan, George, *London*
Chan Im Fan, *Central, Hong Kong*
Chan Ka Ling, *Tin Shui Wai, Hong Kong*
Chan Lap Yee, *Shueng Shui, Hong Kong*
Chan Nga Fong, *Macau, P.R. China*
Chan Tak Wai, *Shatin, Hong Kong*
Chan Wai Chi Chilly, *Tin Shui Wai, Hong Kong*
Chau Kam Chi, *Kowloon, Hong Kong*
Cheang Chi Ioi, *Macau, P.R. China*
Chen Xiao Qin, *Kwai Chung, Hong Kong*
Cheng Hei Lam, *Tai Po, Hong Kong*
Cheng Oi Lam, *Yuen Long, Hong Kong*
Cheng Wai Ching, *Kowloon, Hong Kong*

Cheng Wai Lei, *Sai Wan, Hong Kong*
Cheung Wing Yee, *Tsing Yi, Hong Kong*
Chiu Ka Man, *Kwun Tong, Hong Kong*
Cho, Sze Man, *Kwun Tong, Hong Kong*
Chui Chun Hin, *Shatin, Hong Kong*
Donnelly (nee Smith), Yvonne Louise, *Prescot, Merseyside*
Fong Hoi Yip, William, *Kowloon, Hong Kong*
Friar, Harry, *Romford, Essex*
Fu Haitao, *Beijing, P.R. China*
Fu Xinli, *Beijing, P.R. China*
Gill, Harinder, *Southall, Middlesex*
Gogarty, Madeleine, *Wimbledon, London*
Heltzel, Christopher, *Kilkenny, County Kilkenny, R.O. Ireland*
Ho Pak Ngai, *Shatin, Hong Kong*
Jogia, Sonal, *Harrow, Middlesex*
Ketcher, Alyce Janet, *Wellington, Somerset*
Kolator, Barbara, *London*
Kuang Chuyi, *Beijing, P.R. China*
Kwong Tak Chiu, *Tung Chung, Hong Kong*
Kwong Wai Fan, *Tin Shui Wai, Hong Kong*
Kwong San Fong Cathy, *Kowloon, Hong Kong*
Lam Pui Yu, Carol, *Ma On Shan, Hong Kong*
Lam Yin Han Neona, *To Kwa Wan, Hong Kong*
Lam Wai Ting, *Quarry Bay, Hong Kong*
Lau Kin Yip, *Ma On Shan, Hong Kong*
Lau Wai Kin, *Shatin, Hong Kong*
Lee Kwun San, *Shatin, Hong Kong*
Lee Po Yan, *Lam Tin, Hong Kong*
Leicester, Keith, *St Helens, Merseyside*
Li Dongyang, *Beijing, P.R. China*
Li Man Wah Irine, *Tseung Kwan O, Hong Kong*
Li Wenzhuo, *Wuhan, Hubei, P.R. China*
Li Yin Hu, *Hung Ham, Hong Kong*
Liu Man Leong, Vincent, *Kowloon, Hong Kong*
Milo, Nathan Nicholas, *London*
Minns, Russell James, *Northampton*
Ng Kwok Hung, *Mongkok, Hong Kong*
Ng Wing Man, *Tsuen Wan, Hong Kong*
Ng Wing Sze, *Sheung Shui, Hong Kong*
Niu Tianju, *London*
Poon Ka Ben, *Yuen Long, Hong Kong*
Rashid, Attif, *Northampton, Northamptonshire*
Ross, Yvonne, *Grangecon, County Wicklow, R.O. Ireland*
Saban, Makarim, *Taipo, Hong Kong*
Schindler, Leo Joseph Peter, *Kingston-upon-Thames, Surrey*
Spicer, Paul, *Hove, East Sussex*
Sze Cheung, *Tung Chung, Hong Kong*
Tai Pui Man, *Yuen Long, Hong Kong*
Tam Ka Hey, *Tuen Mun, Hong Kong*
Tam Ka Ming, *Shatin, Hong Kong*
Tam Suk Han, Sara, *Ma On Shan, Hong Kong*
Taylor, Elizabeth Anne, *Midhurst, West Sussex*
Ting Evon, *Tsuen Wan, Hong Kong*
Tse Cheuk Kwan, *Yuen Long, Hong Kong*
Tse Lai Kwan, *Kowloon, Hong Kong*
Tso Hau Yee, Michelle, *Causeway Bay, Hong Kong*
Vildiridi, Lilian Venetia, *Knightsbridge, London*
Wan, Jinghan, *Beijing, P.R. China*
Wang Yizhu, *Beijing, P.R. China*
Wehrly, Richard, *Strandhill, Co. Sligo, R.O. Ireland*
Wong Ching Lan, Teresa, *Tuen Mun, Hong Kong*
Wong Hon Lam, Donald, *Kowloon, Hong Kong*
Wong Kwan Wai Alison, *Kennedy Town, Hong Kong*
Wong Kwong Mei Ice, *Kowloon, Hong Kong*
Wong Po Yin, *Tseung Kwan O, Hong Kong*
Wong Sin Yan, *Sai Wan Ho, Hong Kong*
Wong, William, *Kowloon, Hong Kong*
Wong Yee Fan, Angela, *Chai Wan, Hong Kong*
Wong Kay Yee, *Tseung Kwan O, Hong Kong*
Wormack, Michael, *London*
Wu Yee Lee, *Tuen Mun, Hong Kong*
Xie Zhuohong, *Beijing, P.R. China*
Yang Dong Wen, *Kowloon, Hong Kong*
Yang Ning Ning, *Kowloon, Hong Kong*
Yau Chor Suet, *Shatin, Hong Kong*
Yeung Yuen Man, *Shatin, Hong Kong*
Yiu Yan Fong, Winnie, *Wan Chai, Hong Kong*
Zhang Zhizheng, *Beijing, P.R. China*

OBITUARIES

Roger Leon Merk died on 3 November 2015. Roger was one of a kind, an exceptional man, husband and friend. No tragedies stopped his zeal to live his life to the fullest. He lost his father at 6, his grandfather at 10, and his mother at 17. His Aunt Myrtle took him in and created a loving, caring home in San Diego, and helped him to become the educated man he was. Her husband Chuck got him interested in gems and minerals. He took gemmology to another level; he became an icon, educator, collector and mentor, with a particular passion for jade.

Tragedy struck when his heart failed at a young age. He was lucky enough to receive a heart transplant that gave him another 20 years.

Roger organized the annual Sinkankas Symposia (13 in all) in honour of John Sinkankas. These themed events were held at the Gemological Institute of America campus in Carlsbad, California, USA, and were co-sponsored by the San Diego Mineral & Gem Society.

Roger is survived by a wealth of family and friends, his wife, this aunt, another aunt, his brothers, sister, and cousins.

Myrtle PeterSchieck

Douglas Brill FGA (D.1987), Halifax, West Yorkshire, died on 2 August 2015.

Ann P. Sabina Stenson FGA, Ottawa, Ontario, Canada, died recently.

Shine Bright

Celebrating 20 Years of Opening the World of Jewelry and Gemstones to Everyone!

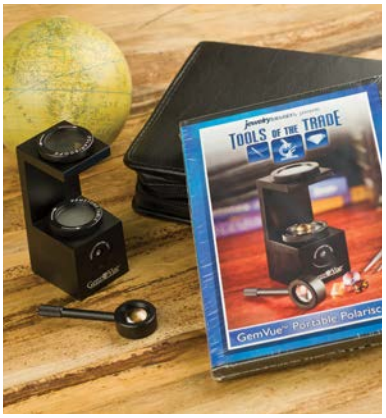

As the largest retailer of loose gemstones in the world, Jewelry Television is committed to offering more of the naturally beautiful treasures that our customers adore.

Education, Expertise & Entertainment

We take pride in our longstanding commitment to education. With programs like our web-based GEM-A course and our on-air Jewel School® series, our partnerships bring industry luminaries straight into the homes of jewelry and gemstone aficionados everywhere.

Educational videos, professional tools of the trade, plus live programming with knowledgeable hosts place Jewelry Television and jtv.com at the forefront of a dynamic learning and shopping environment.

Into the Future

At the heart of our vision is a continuing quest to deliver the rarest of gemstones, plus educational resources and world-class gemstone authorities to our customers. We believe this is the ultimate way to enlighten, inform and entertain, as we take flight into our next decade.

20 yrs
jewelry television®

JTV Your Way

To order call +1 800-619-3000 or visit jtv.com

Learning Opportunities

CONFERENCES AND SEMINARS

3rd Annual Jewelry History Series
26–27 January 2016
Miami Beach, Florida, USA
www.originalmiamibeachantiqueshow.com/show/jewelry-series

45th ACE IT Annual Winter Education Conference
31 January–1 February 2016
Tucson, Arizona, USA
www.najaappraisers.com/html/conferences.html

AGTA Tucson GemFair 2016
2–7 February 2016
Tucson, Arizona, USA
www.agta.org/tradeshows/gft-seminars.html
Note: Includes a seminar programme.

Pueblo Gem & Mineral Show Lecture Series
2 and 5 February 2016
Tucson, Arizona, USA
www.pueblogemshow.com/show-events.aspx

AGA Cutting Edge Conference
3 February 2016
Tucson, Arizona, USA
http://accreditedgemologists.org/currevent.php

Tucson Gem and Mineral Show
11–14 February 2016
Tucson, Arizona, USA
www.tgms.org
Note: Includes a seminar programme.

PDAC International Convention, Trade Show & Investors Exchange
6–9 March 2016
Toronto, Ontario, Canada
www.pdac.ca/convention
Session of interest: Diamonds in Southern Africa: Back to the Beginning

Hasselt Diamond Workshop 2016
9–11 March 2016
Hasselt, Belgium
www.uhasselt.be/sbdd

The Open Forum on Sustainability & Responsible Sourcing in the Jewelry Industry
10–13 March 2016
New York, New York, USA
www.jewelryindustrysummit.com

Amberif—International Fair of Amber, Jewellery and Gemstones
16–19 March 2016
Gdansk, Poland
www.amberif.amberexpo.pl/title,SEMINAR,pid,1284.html
Note: Includes a seminar programme.

AGS Conclave
13–16 April 2016
Washington DC, USA
www.americangemsociety.org/conclave2016

Swiss Gemmological Society Conference
17–19 April 2016
Magglingen, Switzerland
www.gemmologie.ch

Arusha Gem Fair
19–21 April 2016
Arusha, Tanzania
www.arushagemshow.com
Note: Includes a seminar programme.

Scottish Gemmological Association Conference 2016
29 April–2 May 2016
Peebles, Scotland
www.scottishgemmology.org/conference

2nd Mediterranean Gemmological and Jewellery Conference
7–9 May 2016
Valencia, Spain
www.gemconference.com

30th Annual Santa Fe Symposium
15–18 May 2016
Albuquerque, New Mexico, USA
www.santafesymposium.org

SNAG^{neXt}
19–21 May 2016
Asheville, North Carolina, USA
www.snagmetalsmith.org/events/snagnext

10th International Conference on New Diamond and Nano Carbons
22–26 May 2016
Xi'an, China
http://ndnc2016.xjtu.edu.cn

Compiled by Georgina Brown and Brendan Laurs

Northwest Jewelry Conference
12–14 August 2016
Seattle, Washington, USA
www.northwestjewelryconference.com

46th ACE IT Annual Mid-Year Education Conference
13–16 August 2016
Newport Beach, California, USA
www.najaappraisers.com/html/conferences.html

2016 International Appraisers Conference
11–14 September 2016
Boca Raton, Florida, USA
www.appraisers.org/Education/conferences

IRV Loughborough Conference
17–19 September 2016
Loughborough, UK
www.jewelleryvaluers.org/Loughborough-Conference

EXHIBITS

Europe

Celts: Art and Identity
Until 31 January 2016
British Museum, London
www.britishmuseum.org/whats_on/exhibitions/celts.aspx

Urartian Jewellery Collection
Until 31 January 2016
Rezan Has Museum, Istanbul, Turkey
www.rhm.org.tr/en/event/rezan-has-museum-urartian-jewellery-collection

Brilliant! – Jewellery – Photograph – Sound
Until 31 January 2016
The National Museum of Finland, Helsinki, Finland
www.kansallismuseo.fi/en/nationalmuseum/exhibitions/temporary#brilliant_jewelry

Fitting and Befitting—Fibulae and Brooches
Until 21 February 2016
Schmuckmuseum, Pforzheim, Germany
www.schmuckmuseum.de/flash/SMP_en.html

Bejewelled Treasures: The Al Thani Collection
Until 28 March 2016
Victoria and Albert Museum, London
www.vam.ac.uk/content/exhibitions/exhibition-bejewelled-treasures-the-al-thani-collection

Take it Personally [Jewellery and Adornment]
Until 1 June 2016
Museum of Cultural History, Oslo, Norway
www.khm.uio.no/english/visit-us/historical-museum/temporary-exhibitions/2015/this-is-personal.html

Open Space—Mind Maps. Positions in Contemporary Jewellery
11 March 2016–15 May 2016
Nationalmuseum Design, Stockholm, Sweden
www.nationalmuseum.se/sv/English-startpage/Exhibitions/Upcoming-Exhibitions

A Motley Crew—New Pieces from the Collection
18 March 2016–12 June 2016
http://www.museumspass.com/en/Museums2/Pforzheim/Schmuckmuseum-Pforzheim/A-Motley-Crew

Heavenly Bodies—The Sun, Moon and Stars in Jewellery
8 July–30 October 2016
Schmuckmuseum, Pforzheim, Germany
www.schmuckmuseum.de/flash/SMP_en.html

Elements: From Actinium to Zirconium
Until 26 February 2017
Ulster Museum, Belfast, Northern Ireland
http://nmni.com/um/What-s-on/Current-Exhibitions/Elements---From-Actinium-to-Zirconium

North America

The Glassell Collections of African, Indonesian and Pre-Columbian Gold
Until 30 January 2016
Museum of Fine Arts, Houston, Texas, USA
www.mfah.org/art/collections/Glassell-Gold-Collections

Turquoise, Water, Sky: The Stone and Its Meaning
Until 2 May 2016
Museum of Indian Arts & Culture, Santa Fe, New Mexico, USA
www.indianartsandculture.org/current?&eventID=1989

A Passion for Jade: The Heber Bishop Collection
Until 19 June 2016
The Metropolitan Museum of Art, New York, New York, USA
www.metmuseum.org/exhibitions/listings/2015/passion-for-jade

Variations on a Theme: 25 Years of Design from the AJDC
Until July 2016
Gemological Institute of America, Carlsbad, California, USA
www.gia.edu/gia-museum-variations-theme-25-years-design-AJDC

Thunderbirds: Jewelry of the Santo Domingo Pueblo
Until 5 September 2016
Abby Aldrich Rockefeller Folk Art Museum, Williamsburg, Virginia, USA
www.colonialwilliamsburg.com/do/art-museums/rockefeller-museum/thunderbirds-jewelry

Fabergé from the Matilda Geddings Gray Foundation Collection
Until 27 November 2016
The Metropolitan Museum of Art, New York, New York, USA
www.metmuseum.org/exhibitions/listings/2011/faberge

Glitterati. Portraits & Jewelry from Colonial Latin America
Until 27 November 2016
Denver Art Museum, Denver, Colorado, USA
www.denverartmuseum.org/exhibitions/glitterati

Arts of Islamic Lands: Selections from The al-Sabah Collection, Kuwait
Until 29 January 2017
Museum of Fine Arts, Houston, Texas, USA
www.mfah.org/exhibitions/arts-islamic-lands-selections-al-sabah-collection-

Gold and the Gods: Jewels of Ancient Nubia
Until 14 May 2017
Museum of Fine Arts, Boston, Massachusetts, USA
www.mfa.org/exhibitions/gold-and-gods

City of Silver and Gold: From Tiffany to Cartier
Ongoing
Newark Museum, New Jersey, USA
www.newarkmuseum.org/SilverAndGold.html

Fabergé: From a Snowflake to an Iceberg
Ongoing
Houston Museum of Natural Science, Texas, USA
www.hmns.org/exhibits/special-exhibitions/faberge-a-brilliant-vision

Gemstone Carvings
Ongoing
Houston Museum of Natural Science, Texas, USA
www.hmns.org/exhibits/special-exhibitions/gemstone-carvings

Gilded New York
Ongoing
Museum of the City of New York, New York, USA
www.mcny.org/content/gilded-new-york

Jewelry, from Pearls to Platinum to Plastic
Ongoing
Newark Museum, New Jersey, USA
www.newarkmuseum.org/jewelry

Mightier than the Sword: The Allure, Beauty and Enduring Power of Beads
Ongoing
Yale Peabody Museum of Natural History, Yale University, New Haven, Connecticut, USA
http://peabody.yale.edu/exhibits/mightier-sword-allure-beauty-and-enduring-power-beads

Australia

Opals
Until 14 February 2016
South Australian Museum, Adelaide, South Australia
www.samuseum.sa.gov.au/explore/exhibitions/opals

A Fine Possession: Jewellery and Identity
Until 22 May 2016
Powerhouse Museum, Sydney, New South Wales, Australia
www.powerhousemuseum.com/exhibitions/jewellery

OTHER EDUCATIONAL OPPORTUNITIES

Gem-A Workshops and Courses
Gem-A, London
www.gem-a.com/education/course-prices-and-dates.aspx

Lectures with The Society of Jewellery Historians
Burlington House, London, UK
www.societyofjewelleryhistorians.ac.uk/current_lectures

23 February 2016
Jo Whalley—A Journey to India: The Jewellers' Art Revealed

26 April 2016
Henriette Lidchi—Navajo and Pueblo Jewellery of the American Southwest

28 June 2016
Neil Wilkin—Bronze Age Bodily Adornment: How was It Made and Worn

27 September 2016
Galina Korneva—The Grand Duchess Maria Pavlovna's Contacts with Paris Jewellers and her Collection of Treasures

New Media

Tourmaline—Fascinating Crystals with Fantastic Inner Worlds

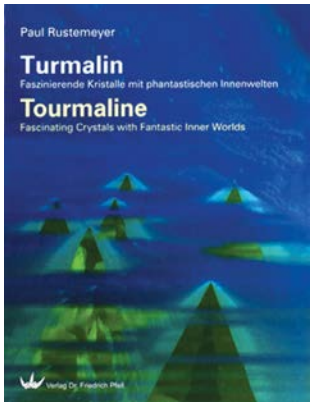

By Paul Rustemeyer, 2015. Verlag Dr. Friedrich Pfeil, Munich, Germany, 272 pages, illus., ISBN 978-3899371949, www.pfeil-verlag.de/06geol/e4_94.php (in English and German). €59.80 hardcover.

In the preface of this impressive book, the author states: "The observer might become meditatively immersed in the tourmaline paintings and may go on imaginative trips into the new landscapes." Indeed the photographs in this book (many of which resemble beautiful paintings) certainly transport the reader to another world—the colourful patterns seen in slices of tourmaline.

The book is printed on high-quality paper, is beautifully designed and laid-out, and the reproduction quality of the photos is excellent. Many of the tourmaline crystals are shown before they were sliced and are accompanied by photographs of the resulting slices (or series of slices). Selected full-page enlargements of some of the more spectacular portions of the slices further reveal amazing colours and patterns that would mostly go unseen without magnification. A black background is used on every page not containing a full-page photo, allowing the images to truly 'pop'. The limited amount of text (always appearing on left-hand pages) is well written and easy to understand for non-specialists. Different font colours are used for English (yellow) and German (white), making it easy for the reader to find their preferred language.

The author has arranged the sections of the book according to the main cause of the dominant patterns shown by the slices:

- 'From Black Crystals to TurmalinArt' presents a series of examples that reveal the inner beauty of black tourmaline crystals when thin sections of them are prepared perpendicular (and in some cases, parallel) to the c-axis. The author explains how he saws the crystals into slices and polishes one side before mounting them on glass slides for final grinding and polishing until the optimal colour appearance is displayed (typically only 0.1–0.01 mm in thickness).
- 'The Structure of Tourmalines' briefly reviews the crystal structure of the mineral to help put the geometric patterns seen in slices into context. Also included are photos of crystal specimens showing myriad variations in colour and morphology.
- 'The Color Palette of the Tourmalines' illustrates the tremendous variety of colours seen in faceted gemstones and in crystals. Simplified explanations of the causes of colour are provided.
- 'The Growth of Tourmaline Crystals' contains many attractive diagrams and photos of tourmaline specimens to illustrate their crystallization process in granitic pegmatites. (Tourmaline formation in metamorphic rocks is not covered.)
- 'The Structures of Crystal Forms' provides an excellent correlation between the various crystal faces and the patterns seen in slices cut perpendicular to the c-axis.
- 'Rim Structures' focuses on features seen within the concentrically zoned portions of slices, which correspond to prism faces.
- 'Oriented Overgrowth' displays the complex mosaic structures seen in slices when a crystal is overgrown by a series of needles and tubes parallel to the c-axis. Also shown are features attributed to skeletal overgrowths.
- 'Delta Structures' portrays a specific type of triangular zoning in tourmaline slices that corresponds to the localized growth of steeper pyramidal faces. The resulting features are particularly reminiscent of landscapes, especially when they are influenced by dislocations in the crystal.
- 'Trigonal Dislocations' provides examples of the complex patterns that result when defects in the lattice of a growing crystal propagate as dislocations.
- 'Division into Parallel Aggregates' shows interesting mosaic networks that result when a growing crystal gradually or abruptly changes into an aggregate structure that is oriented parallel to the c-axis.
- 'The Healing of Broken Tourmalines' records periods of regrowth in 'bent' and broken crystals, including the formation of parallel tubes that may create chatoyancy in cabochons.
- 'Naturally Corroded Tourmaline Crystals' depicts geometrical etch pits and hillocks

resulting from post-grown dissolution, beautifully revealed in photomicrographs taken in reflected light.
- 'Healing of Corroded Tourmalines' shows the results of further crystal growth (often by tourmaline of a different colour) after a period of dissolution.
- 'Healed Corrosion of Cavities' displays some particularly abstract patterns that are produced when irregular areas of dissolution that penetrated deep within a crystal are filled-in by subsequent tourmaline growth.

At the conclusion of the book, the author provides a brief bibliography of tourmaline monographs (with a full listing of tourmaline literature supplied at http://www.pfeil-verlag.de/ef1.html), as well as an index.

While it is easy to become pleasurably absorbed in the richness of the photography, the scientific value of this book should not be overlooked. Through the use of helpful diagrams and photographic comparisons of crystals before and after slicing, as well as neatly arranged series of slices that were obtained from the same crystal, the reader comes away with a much better understanding of the complex crystal growth history of tourmaline.

This reviewer noted only a few very minor errors in the text: p. 42 indicates that the blue colour of Paraíba tourmaline is due to 4% copper, while much lower amounts of Cu are typical (i.e. ~0.5–2 wt.% CuO); p. 44 gives the location of Sweet Home mine rhodochrosite crystals as Utah, rather than Colorado; p. 160 mentions earthquakes as the cause of broken tourmalines that subsequently undergo regrowth in pegmatite pockets, but such breakage is commonly ascribed to pocket rupture due to fluid overpressure; and throughout the book verdelite (green tourmaline) is referred to as 'verdilithe'. In addition, a table-of-contents page would have been helpful for navigating the book.

It is rare to encounter such an effective and inspirational melding of art and science applying to any mineral. This book is sure to please tourmaline aficionados, and also will appeal to many mineralogists, gemmologists, photographers and those who appreciate the beauty of the natural world.

Brendan M. Laurs

Fei Cui Jade—A Stone & a Culture

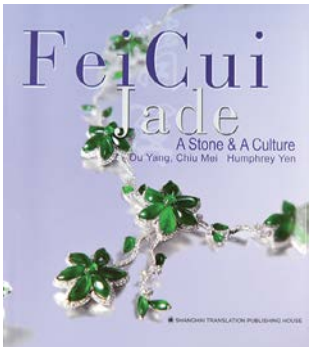

By Chiu Mei Ou Yang and Humphrey Yen, 2015. Shanghai Translation Publishing House, Shanghai, China, 248 pages, illus., ISBN 978-7532764716. HK$480.00.

It is rare in the marketplace to see a comprehensive book on jadeite that is written in English. Both authors have over 30 years of expertise studying jadeite, and they present their information from a Chinese and a gemstone professional point of view.

The reader soon learns that in China what we call *jadeite* is referred to as *fei cui*. This term is said to come from the Chinese name for the kingfisher, as its feathers are so beautiful. The authors repeat the term *fei cui jade* hundreds of times in the book, and this reviewer found this a bit redundant, although it is understandable that the authors wish to promote the terminology used by the Chinese. Many countries have colloquial names for various gem materials. For instance, colourless topaz is often called *gouttes d'eau* in Brazil, alluding to the appearance of drops of water.

The book is well laid out, and includes the following chapters:

1. The Concept and Definition of Jade
2. The Occurrence of Deposits of Fei Cui Jade
3. Color and Other Important Factors in the Valuation of Fei Cui Jade
4. The Varieties of Fei Cui Jade
5. Classification of Rough Fei Cui Jade
6. The Processing Techniques and Classification of Finished Fei Cui Jade Products
7. Jade-like Minerals and Simulants
8. Artificial Treatments of Fei Cui Jade and Their Identification
9. Valuation of Fei Cui Jade
10. The Trending in Marketing of Fei Cui Jade

Each chapter contains a variety of interesting facts and explanations, and many of these will be unfamiliar to most Westerners. For instance, Chapter 3 starts with (1) why jadeite comes in so many colours, and then points out the differences between (2) the primary colouring elements Fe, Cr and Mn, and the secondary colours caused by oxidation and decomposition, and ends with (3) the 'base' or 'fabric' of fei cui jade. This reviewer has not seen such a compilation discussed previously. The authors further provide a classification of six 'bases', and the most amusing is "4) Cooked lotus root: Translucent color like the cooked lotus root used in Chinese cuisine usually with a slight pink or purple color. A cooked lotus root base is not considered very good."

The book contains approximately 380 colour photographs, illustrations and diagrams. The first

10 full-page colour photos are excellent, and in this reviewer's opinion they alone are probably worth the price of the book. Also present are several tasteful advertisements (full-page size and in colour) that are not terribly distracting.

When gem collectors and dealers consider the market value of coloured stones, a comparison with jadeite yields an interesting perspective. The jade market changed in 2006 when the Burmese government brought the first Chinese dealers into the auctions, and jadeite sales went from millions to billions of dollars within a few short years. By comparison, a recent emerald auction held by Gemfields generated US$40 million and made international headlines. When this is compared to the ~US$2.04 billion generated by a recent Burmese jade auction, one realizes this is 50 times the size of that emerald headline. There have been many billion-dollar-plus auctions of Burmese jadeite (see www.palagems.com/gem_news_burma_stats.php), making it the most important coloured stone in terms of sales during the past decade.

William Larson

OTHER BOOK TITLES*

Coloured Stones

Amazonite: Mineralogy, Crystal Chemistry and Typomorphism
By Mikhail Ostrooumov, 2015. Elsevier Science Publishing Co., Amsterdam, The Netherlands, 228 pages, ISBN 978-0128037218. £73.00 softcover.

Bursztyn i Forma—Amber and Form
By Anna Sobecka, 2015. International Amber Association, Gdańsk, Poland, 56 pages, ISBN 978-8391289495 (in English and Polish). Free download from www.amber.org.pl/index.php/download_file/view/448.

***Jade*, 3rd edn.**
By Fred and Charlotte Ward, 2015. Gem Book Publishers, Malibu, California, ISBN 978-1887651172. US$19.95 softcover.

Krása Drahokamu—Európsky Drahý Opál z Dubníka. Edition EurOpal—The Beauty of the Gem
By Peter Semrád, 2015. Granit, Prague, Czech Republic, 224 pages. ISBN 978-8072960972 (in English and Czech). €60 hardcover.

Lapis Lazzuli—Magia del Blu
By G. C. Parodi, 2015. Sillabe, Livorno, Italy, 391 pages, ISBN 978-8883477980 (in Italian). €35 softcover.

Turquoise, Water, Sky: Meaning and Beauty in Southwest Native Arts
By Maxine E. McBrinn and Ross E. Altshuler, 2015. Museum of New Mexico Press, Albuquerque, New Mexico, USA, 172 pages, ISBN 978-0890136041. US$29.95 softcover.

Diamonds

All About Diamonds
By Lana Frank, 2015. Self-published by AuthorHouse, 72 pages, ISBN 978-1504952620. US$30.99 hardcover, $24.99 softcover, or $3.99 Kindle edition.

Clarity, Cut, and Culture: The Many Meanings of Diamonds
By Susan Falls, 2014. NYU Press, New York, New York, USA, 224 pages, ISBN 978-1479879908. US$24.00 softcover.

Gem Localities

České a Moraveské Vltavíny. Czech and Moravian Moldavite
By Radek Hanus et al., 2015. Granit, Prague, Czech Republic, 128 pages, ISBN 978-8072960941 (in Czech). €19 hardcover.

***Rockhounding Montana: A Guide to 100 of Montana's Best Rockhounding Sites*, 3rd edn.**
By Montana Hodges, 2015. FalconGuides, Guilford, Connecticut, USA, ISBN 978-0762781621. US$18.95 softcover.

General Reference

Crystallization and Science of Crystals
Ed. by Sharon Levine, 2015. NY Research Press, New York, New York, USA, 342 pages, ISBN 978-1632381033. US$145.00 hardcover.

Drawings of Mineral Masterpieces
By Eberhard Equit, 2015. Eberhard Equit Verlag, Germany, 350 pages, ISBN 978-3000504242. US$450.00 hardcover (linen with slipcase).

Introducing Mineralogy
By John Mason, 2015. Dunedin Academic Press, Edinburgh, 128 pages, ISBN 978-1780460284. £14.99 softcover.

Latest in Crystal Growth
Ed. by Sharon Levine, 2015. NY Research Press, New York, New York, USA, 432 pages, ISBN 978-1632384386. US$160.00 hardcover.

***Minerals and Their Localities*, 3rd edn.**
By Jan H. Bernard and Jaroslav Hyršl, 2015. Granit,

* Compiled by Georgina Brown and Brendan Laurs

Prague, Czech Republic, 920 pages, ISBN 978-8072960989. €120 hardcover.

The Munich Show / Mineralientage München: Theme Book Precious Stones
Ed. by The Munich Show, 2016. Wachholtz Verlag, Hamburg, Germany, ISBN 978-3529054617. £25.67 hardcover.

Rocks, Gems, and Minerals
By Garret Romaine, 2015. FalconGuides, Guilford, Connecticut, USA, ISBN 978-1493009060. US$14.95 softcover.

Understanding Minerals and Crystals
By Terence McCarthy and Bruce Cairncross, Penguin Random House South Africa, Parklands, South Africa, 304 pages, ISBN 978-1431700844. US$20.95 softcover.

Instruments and Techniques

Infrared Spectroscopy of Minerals and Related Compounds
By Nikita V. Chukanov and Alexandr D. Chervonnyi, 2015. Springer Science+Business Media, Berlin, Germany, 732 pages, ISBN 978-3319253473. £178.00 hardcover.

***Modern Luminescence Spectroscopy of Minerals and Materials*, 2nd edn.**
By Michael Gaft, Renata Reisfeld and Gerard Panczer, 2015. Springer Science+Business Media, Berlin, Germany, 606 pages, ISBN 978-3319247632. £126.50 hardcover.

Jewellery and *Objets d'Art*

Bejewelled: Treasures of the Al Thani Collection
By Susan Stronge, 2015. V&A Publishing, London, 176 pages, ISBN 978-1851778577. £25.00 hardcover.

Everything You Need to Know about the Crown Jewels
By Joanne Hayle, 2015. Self-published, 144 pages, ISBN 978-1519538697. £6.99 softcover.

The Guy Ladrière Collection of Gems and Rings
By Diana Scarisbrick, 2015. Philip Wilson Publishers, London, 320 pages, ISBN 978-1781300398. £40.00 hardcover.

If these Jewels could Talk
By Beth Bernstein, 2015. Antique Collector's Club, Suffolk, 256 pages, ISBN 978-1851498079. £50.00 hardcover.

Indian Folk Jewellery: Designs and Techniques
By Waltraud Ganguly, 2015. B.R. Publishing Corporation, Delhi, India, 128 pages, ISBN 978-9350502129. US$100.00 hardcover.

Jewellery 1970–2015: Bollmann Collection
By Karl Bollmann, 2015. Arnoldsche Art Publishers, Stuttgart, Germany, 144 pages, ISBN 978-3897904286 (in English and German). £25.00 hardcover.

Jewels of Miriam Haskell
By Deanne Farneti Cera, 2015. Antique Collector's Club, Suffolk, 208 pages, ISBN 978-1851496983. £35.00 hardcover.

The Lost Treasure of Leicestershire
By Jim Wright, 2015. Self-published, 11 pages, ASIN B017TBC5F0. £0.99 Kindle edition.

Not Too Precious
By Elizabeth Goring and Gregory Parsons, 2015. Ruthin Craft Centre, Ruthin, Wales, 76 pages, ISBN 978-1905865123. £18.00 hardcover.

Le Pitture delle Antichità di Ercolano nelle Gemme del XVIII e XIX Secolo. The Paintings of the Antichità di Ercolano in 18th and 19th Century Gem-Carving
By Gabriela Tassinari, 2015. Associazione Internazionale Amici di Pompei, Naples, Italy, 162 pages (in Italian and English). €24.50.

Precious Materials in Asian History: Essays on Turquoise, Amber, Ivory, Diamond and Gold
By Berthold Laufer, 2016. Orchid Press, Bangkok, Thailand, 275 pages, ISBN 978-9745241091. US$45.00 softcover.

A Rothschild Renaissance: Treasures from the Waddesdon Bequest
By Dora Thornton, 2015. British Museum Press, London, 288 pages, ISBN 978-1851497843. £30.00 hardcover.

Schmuckmuseum Pforzheim: Museum Guide
By Cornelie Holzach, 2015. Arnoldsche Art Publishers, Stuttgart, Germany, 170 pages, ISBN 978-3897904439 (in English and German). £13.00 softcover.

Stoned: Jewelry, Obsession, and How Desire Shapes the World
By Aja Raden, 2015. Ecco Press, New York, New York, USA, 368 pages, ISBN 978-0062334695. US$27.99 hardcover.

Take This Ring: Medieval and Renaissance Rings from the Griffin Collection
By Sandra Hindman, 2015. Brepols, Turnhout, Belgium, 236 pages, ISBN 978-0991517251. €40.00 softcover.

Töchter der Steppe, Söhne des Windes: Gold und Silber der Turkmenen
By Jürgen Wasim Frembgen, 2015. Hirmer Verlag, Munich, Germany, 148 pages (in German). €29.90 softcover.


ANNUAL SPRING
SALE
1ST – 12TH February 2016
Monday – Friday, 9.30am – 5pm
MARCUS MCCALLUM FGA
PRECIOUS STONES, BEADS & PEARLS
A wide range of precious and semi-precious stones,
beads and freshwater pearls, personally selected
from around the world.
Unusual stones a speciality.
ROOM 27-31, NEW HOUSE
67-68 HATTON GARDEN, LONDON EC1N 8JY
TELEPHONE: +44(0)20 7405 2169
FACSIMILE: +44(0)20 7405 9385
email:info@marcusmccallum.com
www.marcusmccallum.com

Literature of Interest

Coloured Stones

Application of spectroscopic methods in mineralogical and gemmological research of gem tourmalines. P. Bačík, J. Fridrichová, J. Štubňa and P. Antal, *Acta Geologica Slovaca,* **7**(1), 2015, 1–9, www.geopaleo.fns.uniba.sk/ageos/articles/bytea.php?path=bacik_et_al&vol=7&iss=1.*

Chemical composition, mineral component and microstructure of light-colored jadeitite with different values of relative density. R. Liang, W.M. Chen, Z.F. Zhang, Y. Liu, Y. Ma, Y. Lan and T.J. Lu, *Journal of Gems & Gemmology,* **17**(3), 2015, 19–29 (in Chinese with English abstract).

Comparative analysis of familiar red gems in terms of colorimetry. L.L. Dong and E.D. Zu, *Bulletin of the Chinese Ceramic Society,* **34**(6), 2015, 1720–1724 (in Chinese with English abstract).

Kristallchemie und Farbe von Granaten kommerzieller Edelsteinvorkommen [Crystal chemistry and color of garnets from commercial gemstone deposits]. T. Lind, *Gemmologie: Zeitschrift der Deutschen Gemmologischen Gesellschaft,* **64**(1/2), 2015, 1–41 (in German with English abstract).

Origin determination of dolomite-related white nephrite through iterative-binary linear discriminant analysis. Z. Luo, M. Yang and A.H. Shen, *Gems & Gemology*, **51**(3), 2015, 300–311, http://dx.doi.org/10.5741/gems.51.3.300.*

A study of the radioactive level of rough jadeites. H. Ou Yang and Z. Zhang, *Acta Petrologica et Mineralogica*, **33**(2), 2014, 74–76 (in Chinese with English abstract).

Diamonds

Analysis on potentiality of diamond mine prospecting in Henan Province. G. Hou, M. Li, C. Wu, Y. Xu, X. Pang and Y. Zhi, *Journal of Gems & Gemmology*, **16**(6), 2014, 1–5 (in Chinese with English abstract).

The Aurora Collection: An excursion into the world of fancy color diamonds. T. Hainschwang and F. Notari, *InColor*, **29**, 2015, 30–35.

Botswana: African diamond giant. E.A. Laniado, *World Diamond Magazine,* **5**, 2015, 78–80, www.worlddiamondmark.org/sites/default/files/wdmmagazineissue5.pdf.*

Cleaving the Halqeh-ye-Nur diamonds: A dynamic fracture analysis. C. Atkinson, P.M. Martineau, R.U. Khan, J.E. Field, D. Fisher, N.M. Davies, J.V. Samartseva, S.J. Putterman and J.R. Hird, *Philosophical Transactions A,* **373**(2038), 2015, article 20140270 (11 pages), http://dx.doi.org/10.1098/rsta.2014.0270.*

Comparison of luminescence lifetimes from natural and laboratory irradiated diamonds. S. Eaton-Magaña, *Diamond and Related Materials,* **58**, 2015, 94–102, http://dx.doi.org/10.1016/j.diamond.2015.06.007.

Letšeng's unique diamond proposition. R. Shor, R. Weldon, A.J.A. Janse, C.M. Breeding and S.B. Shirey, *Gems & Gemology*, **51**(3), 2015, 280–299, http://dx.doi.org/10.5741/gems.51.3.280.*

Letters—Natural diamonds mistakenly identified as NPD synthetic diamonds. T. Hainschwang, F. Notari and E. Fritsch (with reply by K.S. Moe and P. Johnson), *Gems & Gemology*, **51**(3), 2015, 331–333, www.gia.edu/gems-gemology.*

The need for the SI3 grade. M. Sevdermish and G. Borenstein, *World Diamond Magazine,* **5**, 2015, 44–45, www.worlddiamondmark.org/sites/default/files/wdmmagazineissue5.pdf.*

Pink color in type I diamonds: Is deformation twinning the cause? D. Howell, D. Fisher, S. Piazolo, W.L. Griffin and S.J. Sibley, *American Mineralogist,* **100**(7), 2015, 1518–1527, http://dx.doi.org/10.2138/am-2015-5044.

Review of lithospheric diamonds and their mineral inclusions. X. Zhao, G. Shi and J. Zhang, *Advances in Earth Science,* **30**(3), 2015, 310–322 (in Chinese with English abstract).

Use of spectroscopic methods for determination of diamond origin and treatment. J. Fridrichová, P. Bačík, R. Škoda and P. Antal, *Acta Geologica Slovaca,* **7**(1), 2015, 11–18, www.geopaleo.fns.uniba.sk/ageos/articles/bytea.php?path=fridrichova_et_al&vol=7&iss=1.*

Gem Localities

The best grossular garnets from the Jeffrey mine, Asbestos, Quebec. M. Amabili, D. Trinchillo and R. Tyson, *Mineralogical Record,* **46**(6), 2015, 817–834.

Colombian trapiche emeralds: Recent advances in understanding their formation. I. Pignatelli, G. Giuliani, D. Ohnenstetter, G. Agrosì, S. Mathieu, C. Morlot and Y. Branquet, *Gems & Gemology*,

Compiled by Brendan Laurs

* Article freely available for download, as of press time

51(3), 2015, 222–259, http://dx.doi.org/10.5741/gems.51.3.222.*

Gemstone silica veins in Kremenjača volcanic rocks (Serbia). L. Kurešević and S. Dević, *Geologica Macedonica*, **28**(1), 2014, 33–38, http://js.ugd.edu.mk/index.php/GEOLMAC/article/download/852/822.*

L'améthyste de Boudi, au Maroc [Amethyst from Boudi, Morocco]. V. De Barros, C. Soberka, A. El Harfi, F. Troilo and S. Mouaddib, *Revue de Gemmologie,* **193**, 2015, 6–12 (in French).

De nouveaux rubis à Madagascar [New rubies from Madagascar]. R.W. Hughes, W. Manorotkul and B. Hughes, *Revue de Gemmologie,* **193**, 2015, 13–20 (in French).

Rare gem mineral deposits from Brazil - Part 3. M. Luiz de Sá Carneiro Chaves, J. Karfunkel, L.A. Gomes da Silveira, R. Scholz, K. Krambrock, C.H. Dias and D.B. Hoover, *Australian Gemmologist*, **25**(10), 2015, 346–353.

Silica veins in Gaj-Lazine locality (central Serbia) as gemstone [*sic*]. L. Kurešević and S. Dević, *Geologica Macedonica*, **28**(2), 2014, 185–192, http://js.ugd.edu.mk/index.php/GEOLMAC/article/download/925/863.*

Tracking emeralds from the Musakashi area of Zambia. V. Pardieu, S. Detroyat, S. Sangsawong and S. Saeseaw, *InColor*, **29**, 2015, 18–25.

True North Gems Greenland mining - The final lap. A. Fagan, *InColor*, **29**, 2015, 36–49.

An unusual color-change almandine from Fazenda Rodolita, Tocantins State, Brazil. D.B. Hoover, J. Karfunkel, K. Krambrock and A. Fonseca Fernandes, *Australian Gemmologist*, **25**(10), 2015, 337–345.

Instruments

Design and renovation on light source system of gem microscope. R. Liao, X. Li, Z. Liu and S. Xu, *Journal of G ems & Gemmology*, **16**(4), 2014, 61–69 (in Chinese with English abstract).

Report on high intensity LED fibre optic light. T. Linton, A.C. Paul and A. Smallwood, *Australian Gemmologist*, **25**(10), 2015, 358–360.

Miscellaneous

Considerations when pricing gemstones based on lab reports. C. Lule, *GemGuide*, **34**(5), 2015, 3–6.

Does price dispersion increase with quality? Evidence from the online diamond market. F.-C. Wolff, *Applied Economics,* **47**(55), 2015, 5996–6009, http://dx.doi.org/10.1080/00036846.2015.1061645.

Healing images. Gems and medicine. V. Dasen, *Oxford Journal of Archaeology*, **33**(2), 2014, 177–191, http://dx.doi.org/10.1111/ojoa.12033.

The mineral collection of the Natural History Museum in Vienna. V.M.F. Hammer, *Mineralogical Record,* **46**(6), 2015, 863–884.

Online diamond ring sales fraud. S.C. Edwards, *Australian Gemmologist*, **25**(10), 2015, 361–363.

The roughness on polished gemstone surfaces. A.V. Nadur, R.A.S. Gütller, S.S. Carmo and H. Kahn, in F. Dong, Ed., *Proceedings of the 11th International Congress for Applied Mineralogy*, Springer, Cham, Switzerland, 2015, 233–239, http://dx.doi.org/10.1007/978-3-319-13948-7_24.

Shine bright like a diamond: A hedonic model of grading and pricing an experience good. J.A. Lee, S.B. Caudill and F.G. Mixon, *Applied Economics,* **46**(16), 2014, 1829–1838, http://dx.doi.org/10.1080/00036846.2014.884707.

News Press

Beyond green jade. D. Au, *New York Times*, 13 May 2015, www.nytimes.com/2015/05/14/fashion/beyond-green-jade.html.*

Changes are reshaping the world's diamond market. J. Ewing, *New York Times*, 13 May 2015, www.nytimes.com/2015/05/14/fashion/reshaping-the-worlds-diamond-market.html.*

Gemfields targets prospects in Colombia. M. van Wyngaardt, *Mining Weekly*, 10 September 2015, www.miningweekly.com/article/gemfields-targets-prospects-in-colombia-2015-09-10.*

Has technology killed the jewelry industry? B. Shah, *Pacific Standard*, 7 January 2015, www.psmag.com/nature-and-technology/tech-killed-jewelry-industry-97335.*

Lab-grown diamonds set to fill projected deficit as mined production declines. Z. Mavuso, *Mining Weekly*, 18 September 2015, www.miningweekly.com/article/lab-grown-diamonds-set-to-fill-projected-deficit-as-mined-production-declines-2015-09-18.*

Myanmar's $40 billion jade trade labelled 'biggest natural resource heist' in modern history. K. Long, ABC Australia, 22 October 2015, www.abc.net.au/news/2015-10-23/myanmar-jade-trade-biggest-heist-in-modern-history/6880144.*

Organic Gems

Historical survey of the internal use of unprocessed amber. C.J. Duffin, *Acta Medico-Historica Adriatica,* **13**(1), 2015, 41–74, http://hrcak.srce.hr/file/209650.*

Research of characteristics of coral composition and structure (1). L. Feng, H. Lu and Q. Zhang, *Superhard Material Engineering,* **26**(2), 2014, 50–54 (in Chinese with English abstract).

Research of characteristics of coral composition and structure (2). L. Feng, H. Lu and Q. Zhang, *Superhard Material Engineering,* **26**(3), 2014, 55–59 (in Chinese with English abstract).

Pearls

Development of cultured pearl circles and shape after initial graft and second nucleus insertion in the black-lipped pearl oyster *Pinctada margaritifera*. C.-L. Ky, J. Demmer, M. Sham-Koua and P. Cabral, *Journal of Shellfish Research,* **34**(2), 2015, 319–328, http://dx.doi.org/10.2983/035.034.0214.

Grading and pricing Japanese and Chinese cultured pearls. R.B. Drucker, *GemGuide,* **34**(6), 2015, 10–11.

Synthetics and Simulants

HPHT synthesis and crystalline quality of large high-quality (001) and (111) diamond crystals. H. Sumiya, K. Harano and K. Tamasaku, *Diamond and Related Materials,* **58**, 2015, 221–225, http://dx.doi.org/10.1016/j.diamond.2015.08.006.

Identification characteristics of gem-grade natural glass. L. Wang, D.M. Zhu, J.Y. Sun, A.P. Hu and F. Zhang, *Journal of Gems & Gemmology*, **17**(3), 2015, 43–47 (in Chinese with English abstract).

Large colorless HPHT-grown synthetic gem diamonds from New Diamond Technology, Russia. U.F.S. D'Haenens-Johansson, A. Katrusha, K.S. Moe, P. Johnson and W. Wang, *Gems & Gemology*, **51**(3), 2015, 260–279, http://dx.doi.org/10.5741/gems.51.3.260.*

Treatments

Analysis and modification of blue sapphires from Rwanda by ion beam techniques. D. Bootkul, C. Chaiwai, U. Tippawan, B. Wanthanachaisaeng and S. Intarasiri, *Nuclear Instruments and Methods in Physics Research Section B: Beam Interactions with Materials and Atoms,* **365**(Part A), 2015, 288–293, http://dx.doi.org/10.1016/j.nimb.2015.07.029.

Color in topaz produced by electron irradiation. A. Yookong and W. Wongkokua, *Proceedings Book—The 41st Congress on Science and Technology of Thailand (STT41)*, Nakhon Ratchasima, Thailand, 6–8 November 2015, 78–82, www.scisoc.or.th/stt41/images/stt41/download/Proceedings%20Book.pdf.*

Compilations

***G&G* Micro-World.** Cleavage in pink diamond • Rough diamond with green cleavage surface • Gahnite inclusions in cat's-eye heliodor • Trapiche pezzottaite • Modified Rheinberg illumination • Melt inclusions in Montana sapphires • Molybdenite in topaz. *Gems & Gemology*, **51**(3), 2015, 324–330, www.gia.edu/gems-gemology.*

Gem News International. Large star emerald • Faceted red rutile • 'Star and cross' quartz from Brazil • 'Olive' green serpentine cabochon • Petrified wood from Thailand and Myanmar • Coated rock crystal imitation of ruby • Cubic zirconia as peridot imitation • Coral inclusions in plastic • Hydrogrossular imitating jadeite • Impregnated and dyed turquoise • Tino Hammid obituary. *Gems & Gemology*, **51**(3), 2015, 334–345, www.gia.edu/gems-gemology.*

Lab Notes. Graining in pink diamond • Yellow HPHT-treated rough diamond • Color-zoned emerald • Orange faceted eosphorite • Large faceted hibonite • Dyed and natural green jadeite • Coated kornerupine beads • Assembled cultured blister pearl • Large abalone pearls • Irradiated green-blue CVD synthetic diamonds • Polished topaz imitating diamond rough. *Gems & Gemology*, **51**(3), 2015, 312–322, www.gia.edu/gems-gemology.*

Conference Proceedings

13th Swiss Geoscience Meeting 2015. Basel, Switzerland, 21 November 2015, 122–135, http://geoscience-meeting.ch/sgm2015/downloads.*

Geosudeste 2015—14º Simpósio de Geologia do Sudeste, 8º Simpósio do Cretáceo do Brasil, VI Simpósio Nacional de Ensino e História de Ciências da Terra. Campos do Jordão, Brasil, 26–29 October 2015, 242–263, http://geosudeste.com.br/anais/ANAIS-GEOSUDESTE-2015-completo.pdf (in Portuguese).*

SLRI - GeM Symposium 2015. Synchrotron Technology for Gemology and Mineralogy Applications, The 41st Congress on Science and Technology of Thailand (STT41), Nakhon Ratchasima, Thailand, 6–8 November 2015, B147–B165, http://econference.sut.ac.th/stt41/web/downloads/Book%20of%20Abstract-1st%20Draft.pdf.*

43rd Annual Yellowknife Geoscience Forum. D. Irwin, P.X. Normandeau and S.D. Gervais, Northwest Territories Geological Survey, Yellowknife, Canada, 24–26 November 2015, www.nwtgeoscience.ca/sites/default/files/abstract_ykgsf_compilation_2015_nov_10_1.pdf.*

Index

Compiled by Carol M. Stockton

Volume 34
Numbers 1–8, 2014–2015

Notes on changes from prior subject indexes:
- Author names are no longer listed alphabetically by name within this index, but they continue to be shown in parentheses in this subject index.
- Book reviews and reviews of other media are now listed alphabetically by title under the single heading 'Book and other media reviews', instead of being individually listed throughout the Index.
- The Abstracts section of *The Journal* has been replaced by Literature of Interest.

C

D

J

T

Gem-A
THE GEMMOLOGICAL ASSOCIATION OF GREAT BRITAIN

BIRMINGHAM CITY University

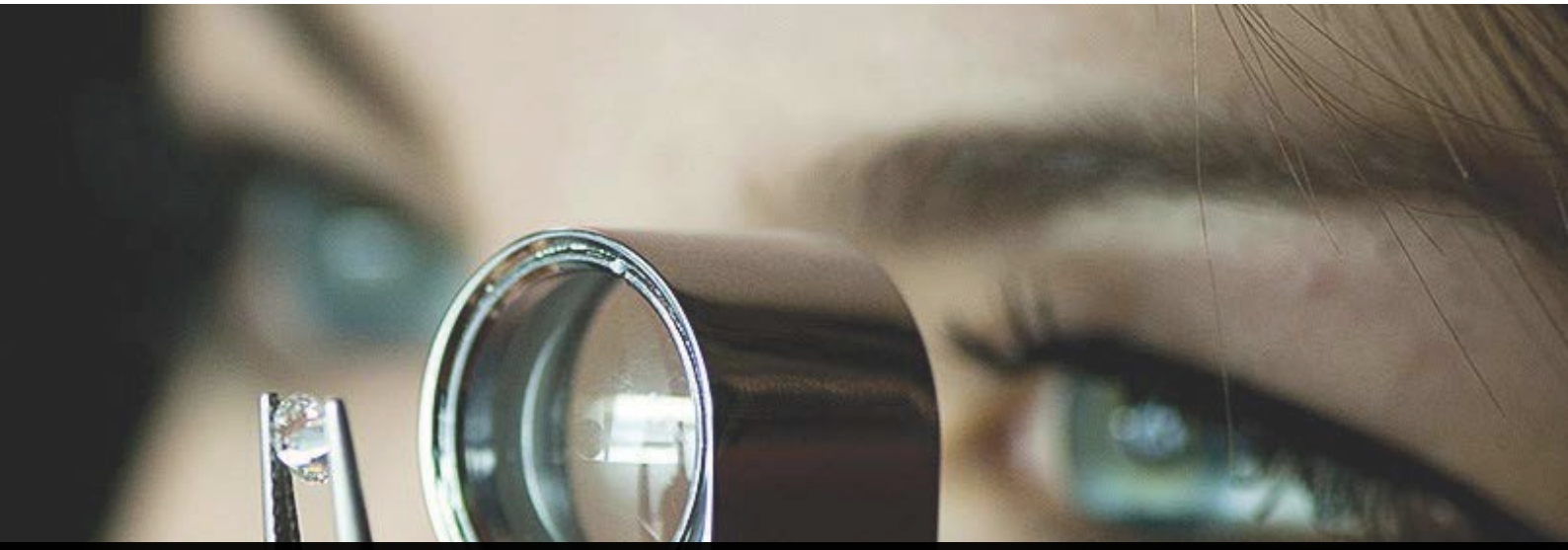

Turn your Diplomas into a degree

If you hold a **Gemmology** and **Diamond Diploma** and are a current Gem-A Member, you can now work towards a **BSc (Hons) in Gemmology and Jewellery Studies.** Offered by Birmingham School of Jewellery and taught at Gem-A's headquarters near Hatton Garden, this one-year top-up course covers advanced gemmology practice and theory (including advanced lab equipment), geology theory, advanced diamond grading and jewellery valuation.

This is a full time course (including lectures, lab classes and study time) starting in September 2016, course price £9,000. To apply for this course, sign up via UCAS (course code 73J9), or for more information contact **education@gem-a.com**.

Understanding Gems

Join us.

The Gemmological Association of Great Britain, 21 Ely Place, London, EC1N 6TD, UK. T: +44 (0)20 7404 3334 F: +44 (0)20 7404 8843.
Registered charity no. 1109555. A company limited by guarantee and registered in England No. 1945780. Registered Office: 3rd Floor, 1-4 Argyll Street, London W1F 7LD.

Little by little,
a little becomes a lot.
— Tanzanian proverb

Pala International

Palagems.com / Palaminerals.com
+1 800 854 1598 / +1 760 728 9121

Tanzanite, Merelani Hills, Tanzania • 21.79 ct • 16.8 x 16.0 x 1.05 mm
Photo: Mia Dixon